

**THE GENERATION AND CHARACTERIZATION OF AVIAN
REOVIRUS TEMPERATURE SENSITIVE MUTANTS**

By

Megan Kathleen Patrick

A Thesis
Submitted to the Faculty of Graduate Studies
in Partial Fulfillment of the Requirements
for the Degree of

Master of Science

Department of Medical Microbiology and Infectious Diseases
University of Manitoba
Winnipeg, Manitoba
Canada



National Library
of Canada

Acquisitions and
Bibliographic Services

395 Wellington Street
Ottawa ON K1A 0N4
Canada

Bibliothèque nationale
du Canada

Acquisitions et
services bibliographiques

395, rue Wellington
Ottawa ON K1A 0N4
Canada

Your file Votre référence

Our file Notre référence

The author has granted a non-exclusive licence allowing the National Library of Canada to reproduce, loan, distribute or sell copies of this thesis in microform, paper or electronic formats.

The author retains ownership of the copyright in this thesis. Neither the thesis nor substantial extracts from it may be printed or otherwise reproduced without the author's permission.

L'auteur a accordé une licence non exclusive permettant à la Bibliothèque nationale du Canada de reproduire, prêter, distribuer ou vendre des copies de cette thèse sous la forme de microfiche/film, de reproduction sur papier ou sur format électronique.

L'auteur conserve la propriété du droit d'auteur qui protège cette thèse. Ni la thèse ni des extraits substantiels de celle-ci ne doivent être imprimés ou autrement reproduits sans son autorisation.

0-612-57570-5

Canada

**THE UNIVERSITY OF MANITOBA
FACULTY OF GRADUATE STUDIES

COPYRIGHT PERMISSION PAGE**

The Generation and Characterization of Avian Reovirus Temperature Sensitive Mutants

BY

Megan Kathleen Patrick

**A Thesis/Practicum submitted to the Faculty of Graduate Studies of The University
of Manitoba in partial fulfillment of the requirements of the degree**

of

Master of Science

MEGAN KATHLEEN PATRICK ©2001

Permission has been granted to the Library of The University of Manitoba to lend or sell copies of this thesis/practicum, to the National Library of Canada to microfilm this thesis and to lend or sell copies of the film, and to Dissertations Abstracts International to publish an abstract of this thesis/practicum.

The author reserves other publication rights, and neither this thesis/practicum nor extensive extracts from it may be printed or otherwise reproduced without the author's written permission.

TABLE OF CONTENTS

TABLE OF CONTENTS	I
ACKNOWLEDGEMENTS	VI
LIST OF FIGURES	VII
LIST OF TABLES	VIII
LIST OF ABBREVIATIONS	IX
ABSTRACT	1
1. INTRODUCTION	3
1.1 Avian reovirus: background and general characteristics	3
1.2 Virus structure	4
1.3 Lifecycle of avian reovirus	9
1.3.1 Virus attachment and entry	9
1.3.2 Replication	9
1.3.3 Assembly	12
1.3.4 Syncytia formation	12
1.4 Temperature sensitive mutants	13
1.5 Exploitation of the segmented genome	15
1.5.1 Reassortment	15
1.5.2 Genetic recombination	20
1.5.3 Reassortant mapping	21
1.6 Objectives of the research programme	22
2. MATERIALS AND METHODS	24

2.1 Stock cells and viruses	24
2.2 Viral manipulation	24
2.2.1 Viral plaque assay	25
2.2.2 Viral passage	25
2.2.3 Plaque purification	25
2.2.4 Concentration of viral stocks	26
2.3 Chemical mutagenesis and plaque purification of <i>ts</i> clones	26
2.4 Determination of temperature sensitivity	27
2.4.1 Efficiency of plating (EOP) assay	27
2.4.2 Efficiency of lysis (EOL) assay	28
2.5 Recombination assay	29
2.5.1 Standard <i>Reoviridae</i> recombination formula	29
2.5.2 Recombination index (RI) formula	29
2.5.3 Novel EOP recombination formula	29
2.6 Reassortant mapping	30
2.6.1 Generation of reassortants	30
2.6.2 Isolation of viral double stranded RNA (dsRNA)	30
2.6.3 Identification of reassortants by SDS-PAGE	31
2.7 Identification of total viral double stranded RNA (dsRNA) production	31
2.7.1 Infection and $^{32}\text{PO}_4^{-3}$ labeling of viral dsRNA	32
2.7.2 Cytoplasmic extraction of radiolabeled viral dsRNA	32
2.7.3 Labeled viral dsRNA resolved by SDS-PAGE	32
2.8 Electron Microscopy	32

2.8.1	Thin section transmission electron microscopy	33
2.8.2	Proportions of viral and sub-viral particles	33
2.9	Determination of the ARV 138 and <i>tsA12</i> mutant S2 gene sequence	34
2.9.1	Preparation of viral template	34
2.9.2	Design of primers specific for the S2 gene segment	35
2.9.3	Reverse transcription polymerase chain reaction (RT-PCR)	35
2.9.4	Amplification of S2 gene and cDNA purification	38
2.9.5	Cycle sequencing	38
3.	RESULTS	40
3.1	Generation and identification of avian reovirus (ARV) temperature sensitive (<i>ts</i>) mutants	40
3.1.1	Generation of ARV <i>ts</i> mutants	40
3.1.2	Identification of ARV <i>ts</i> mutants	42
3.1.2.1	Isolation of ARV <i>ts</i> mutants and initial EOP screening	42
3.1.2.2	Efficiency of lysis assay	44
3.2	Genetic recombination analysis of the panel of ARV <i>ts</i> mutants	48
3.2.1	Recombination analysis: standard <i>Reoviridae</i> recombination formula	48
3.2.2	Recombination analysis: recombination index (RI) formula	52
3.2.3	Recombination analysis: novel EOP recombination formula	53
3.2.4	Organization of ARV <i>ts</i> mutants into recombination groups	57
3.3	Total dsRNA synthesis of ARV <i>ts</i> mutants	58
3.4	Efficiency of plating profile of ARV <i>ts</i> mutants	62
3.5	Reassortant mapping of selected ARV <i>ts</i> mutant clones	65

3.5.1	Reassortant mapping of <i>tsA12</i>	65
3.5.2	Reassortant mapping of <i>tsD46</i>	68
3.6	Electron microscopic analysis of <i>tsA12</i> and <i>tsD46</i>	72
3.6.1	Analysis of <i>tsA12</i>	72
3.6.1.1	Viral and sub-viral particle counts for <i>tsA12</i> infections	72
3.6.1.2	Thin section electron microscopy analysis of <i>tsA12</i> infected cells	76
3.6.2	Analysis of <i>tsD46</i>	79
3.6.2.1	Viral and sub-viral particle counts for <i>tsD46</i> infections	79
3.6.2.2	Thin section electron microscopy of <i>tsD46</i>	80
3.7	The S2 gene sequence as determined for ARV 138 and <i>tsA12</i>	80
3.7.1	Identification of the <i>tsA12</i> mutation	80
3.7.2	Secondary structure prediction	81
4.	DISCUSSION	86
4.1	Chemical mutagenesis	86
4.2	Efficiency of lysis assay and efficiency of plating assay	87
4.3	Organization of ARV <i>ts</i> mutants through genetic recombination analysis	88
4.4	The <i>tsA12</i> mutant and recombination group A summary	92
4.4.1	Morphology of <i>tsA12</i>	93
4.4.2	Secondary structure predictions for the <i>tsA12</i> σ A protein	95
4.4.3	Biological role of σ A in dsRNA production	96
4.5	The <i>tsD46</i> mutant and recombination group D	99
4.5.1	Electron microscopic analysis of <i>tsD46</i>	100

4.5.2 Biological role of λ B in dsRNA production	101
4.6 Recombination groups B, C, E, F, G and ungrouped mutants dsRNA production	101
4.7 Future directions	102
5. REFERENCES	104

Acknowledgements

I would like to acknowledge, and sincerely thank, my supervisor Dr. Kevin Coombs. Over the last several years, Kevin has been my teacher, my mentor, and a true friend. I am grateful for the support and guidance he has offered and the patience he has shown in all aspects of my life. Kevin is truly an exceptional supervisor, and I am fortunate for the opportunity to have been a part of his lab.

A special thanks to Dr. Fred Aoki who first employed me as a summer student in the department, and peaked my interest in the field of virology.

I would like to thank all the past and present members of the Coombs' Structural Virology group that I have known: Israel Mendez, Magdalena Swanson, Tammy Stuart, Laura Hermann, Paul Hazelton, Natalie Keirstead, Amanda Everton, and Wanhong Xu. I am extremely thankful for their encouragement, aid and advice over the years. Most importantly, I am grateful for their friendship that I will always cherish.

I would also like to thank Dr. Paul Hazelton for his assistance with the electron microscopy work. I greatly appreciated his guidance and patience.

Thank you to my committee members, Dr. Neil Simonsen and Dr. Mike Butler, whose valuable advice, challenge, and encouragement were greatly appreciated.

LIST OF FIGURES

1. ARV genotype, protein profile, and predicted structure	5
2. Components of the avian reovirus double shelled capsid and various morphological states of the virus	8
3. Mixed infection and production of reassortant progeny	16
4. ARV 138, ARV 176, and reassortant electropherotypes resolved by SDS-polyacrylamide gel electrophoresis	18
5. The ARV 138 S2 cDNA sequence and designed primers	36
6. Survival curves of ARV 138 and ARV 176 after chemical mutagenesis	41
7. Efficiency of lysis (EOL) plates at permissive and restrictive temperatures	45
8. Total dsRNA production at non-permissive temperature	60
9. Efficiency of plating profiles for <i>ts</i> mutants that belong to recombination groups A-G	63
10. Electropherotypes of ARV 138, ARV 176, <i>tsD46</i> , and reassortants produced from a <i>tsD46</i> x ARV 176 mixed infection	70
11. Graphical representation of the proportions of viral and sub-viral particles for ARV 138, <i>tsA12</i> , and <i>tsD46</i> at permissive and non-permissive temperature	74
12. Thin section electron micrographs of ARV 138 and <i>tsA12</i> infected cells at permissive and non-permissive temperature	77
13. Predicted secondary structure of ARV 138 σ A protein	82
14. Proposed conformational change in the <i>tsA12</i> σ A protein	97

LIST OF TABLES

1. Efficiency of plating (EOP) values of isolated ARV 138 <i>ts</i> mutants	43
2. Organization of ARV 138 <i>ts</i> mutants into recombination groups	50
3. ARV 138 <i>ts</i> mutants that cannot be placed into defined groups	54
4. Reassortant mapping of <i>tsA12</i>	67
5. Reassortant mapping of <i>tsD46</i>	69
6. Viral and sub-viral particle counting of ARV 138, <i>tsA12</i> , and <i>tsD46</i> at permissive and non-permissive temperature	73
7. Predicted secondary structure changes in <i>tsA12</i> σ A protein	85

LIST OF ABBREVIATIONS

- (-) RNA: negative sense ribonucleic acid**
(+) RNA: plus sense ribonucleic acid
ARV: avian reovirus
BRV: baboon reovirus
BSA: bovine serum albumin
cDNA: copy deoxyribonucleic acid
CPE: cytopathic effect
dATP: deoxyadenosine triphosphate
dCTP: deoxycytosine triphosphate
dGTP: deoxyguanosine triphosphate
DMSO: dimethyl sulfoxide
dsRNA: double stranded ribonucleic acid
DTT: dithiothreitol
dTTP: deoxythymidine triphosphate
EOL: efficiency of lysis
EOP: efficiency of plating
ISVP: intermediate subviral particle
MOI: multiplicity of infection
mRNA: messenger ribonucleic acid
MRV: mammalian reovirus
NBV: nelson bay reovirus
PBS/EDTA: phosphate buffered saline/ethylenediamine tetraacetate
PBS: phosphate buffered saline
PCR: polymerase chain reaction
PFU: plaque forming unit
PI: post-infection
P_x: passage (x = passage number)
RdRp: RNA dependent RNA polymerase

RI: recombination index

RNA: ribonucleic acid

Rnasin: RNase inhibitor

RT: reverse transcription/transcriptase

SC-Mg buffer: sodium cacodylate- magnesium chloride buffer

SDS-PAGE: sodium dodecyl sulfate polyacrylamide gel electrophoresis

ssRNA: single stranded ribonucleic acid

TBE buffer: tris/ boric acid/ EDTA buffer

***ts*:** temperature sensitive

***ts*⁺:** non-temperature sensitive

ABSTRACT

Currently, little is known about the genetic and biological functions of avian reovirus (ARV), an atypical member of the family *Reoviridae* and the prototype of all non-enveloped syncytia-inducing viruses. In this study, we created temperature sensitive (*ts*) mutants by chemical mutagenesis of ARV strain 138. We developed a novel efficiency of lysis (EOL) technique to screen for temperature sensitivity and used the classical efficiency of plating (EOP) assay to identify 17 ARV *ts* mutants. Pairwise mixed infection of these mutants and evaluation of recombinant progeny *ts* status led to their organization into 7 recombination groups. This indicates that these new groups of ARV mutants represent the majority of the ARV genome. To phenotypically characterize each mutant and localize the effects of the *ts* lesion within the viral lifecycle, the ability to synthesize double stranded RNA (dsRNA) at permissive (33.5°C) and non-permissive temperature (39.5°C) was analyzed. Recombination groups A, D, E, F, and G failed to produce dsRNA 39.5°C, and indicated their mutations inhibit a stage prior to or during replication or genome packaging. In contrast, recombination groups B and C were capable of dsRNA synthesis at both temperatures, and suggested the effects of their *ts* lesions exist in the capsid assembly process or virus release. The temperature sensitive lesions in two mutants were mapped by the reassortant assay and were identified within the S2 and L2 gene segment for recombination groups A (prototype *ts*A12) and D (prototype *ts*D46), respectively. Morphological analysis of *ts*A12 indicated an accumulation of cores and incomplete outer shell particles at non-permissive temperature.

The *tsA12* S2 gene segment (σ A major core protein) was sequenced and suggested that a single amino acid change (proline₁₅₈ to leucine₁₅₈) is responsible for the *ts* phenotype.

Unlike *tsA12*, the assembly defect of *tsD46* is characterized by a decrease in all viral and sub-viral particles at non-permissive temperature. The *tsD46* *ts* mutation resides within the presumed RNA dependent RNA polymerase protein, λ B, and may be responsible for the poor growth phenotype at restrictive temperature.

1. INTRODUCTION

1.1 Avian reovirus: background and general characteristics.

Avian reovirus (ARV) infects a variety of avian species worldwide (Jordan and Pattison, 1996). ARV infections, spread through fecal contaminated food and water sources (Jordan and Pattison, 1996), are responsible for considerable economic losses in commercial breeding operations (Herenda and Franco, 1996). Immature infected birds commonly develop tenosynovitis (viral arthritis), a condition that cripples those affected and causes a general lack of performance, such as diminished weight gains and poor feed conversion rates, and leads to a reduced marketability of the bird (Calnek *et al.*, 1997).

Avian reovirus is a member of the orthoreovirus genus in the family *Reoviridae*. The orthoreoviruses are divided into 3 subgroups: mammalian reovirus (MRV) species (subgroup 1), avian reovirus and nelson bay reovirus (NBV) species (subgroup 2), and baboon reovirus (BRV) (subgroup 3). In comparison to MRV, the prototypic member of the genus, little is known about ARV (Van Regenmortel *et al.*, 2000). To date, investigations have identified structural and molecular similarities between ARV and MRV. ARV is a non-enveloped, icosahedral particle (70-80 nm diameter) with two protein capsid layers (inner shell or core and the outer shell). The virion carries 10 linear double stranded RNA (dsRNA) gene segments that encode 11 proteins (Sheng Yin *et al.*, 2000; Shmulevitz and Duncan, 2000). The genome migrates to 3 size classes by SDS-polyacrylamide gel electrophoresis (SDS-PAGE): 3 large segments (L1, L2, L3), 3 medium sized segments (M1, M2, M3), and 4 small segments (S1, S2, S3, S4). Nine of

the gene segments are monocistronic and encode a single different protein (7 structural: λ A, λ B, λ C, μ A, μ B, σ A, σ B; 2 non-structural: μ NS, σ NS), while the S1 gene segment encodes a structural protein (σ C) and non-structural protein (p10) (Figure 1) (Martinez-Costas *et al.*, 1997; Shmulevitz and Duncan, 2000). Important differences between ARV and MRV interactions with their host cells have been reported, such as ARV's lack of hemagglutination and the ability of ARV to induce syncytium (Martinez-Costas *et al.*, 1997). ARV infected cells promote fusion with adjacent cells (syncytia formation), unlike mammalian reoviruses. All non-enveloped viruses capable of inducing syncytia belong to the *Reoviridae* family, where ARV serves as the prototypic fusogenic virus. A novel 10 kDa ARV protein (p10) induces this fusion and proteins with similar function and important conserved motifs were identified in NBV and BRV (Shmulevitz and Duncan, 2000).

1.2 Virus structure.

The structure of avian reovirus is largely unknown; however, the model presented in Figure 1 (Duncan, 1996; Van Regenmortel *et al.*, 2000) is constructed based on ARV and MRV protein distribution similarities and correlation to the MRV crystal structure (Reinisch *et al.*, 2000). Although the morphology of ARV has not been confirmed, crude structural analyses have identified only small differences from MRV (Van Regenmortel *et al.*, 2000). The avian reovirus capsid consists of two concentric protein layers, similar to other members of the *Reoviridae*. The capsid is assembled from the 8 viral structural proteins, whereas the viral non-structural proteins (μ NS, σ NS, p10) are not included in

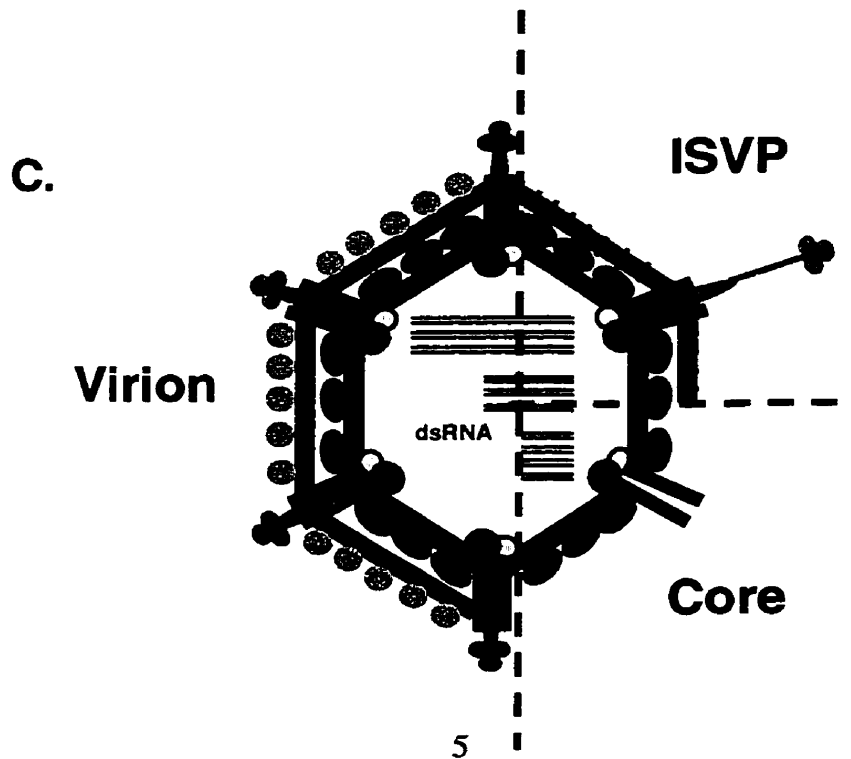
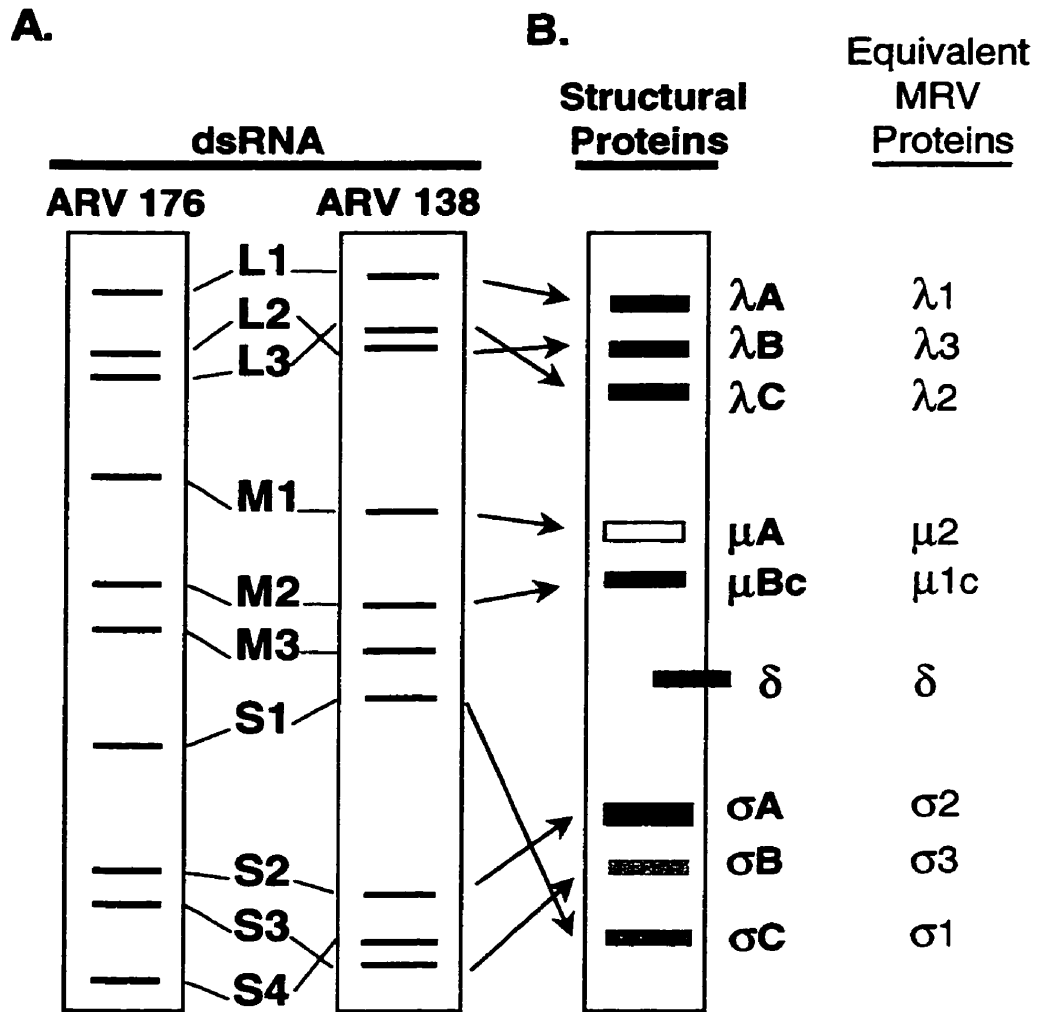


Figure 1. ARV genotype, protein profile, and predicted structure. **A.** The 10 dsRNA gene segments of ARV 138 and ARV 176 and their unique electropherotypes (gene segment mobilities) are presented as seen by SDS-polyacrylamide gel electrophoresis (SDS-PAGE). **B.** The ARV structural proteins encoded by these gene segments are shown as resolved by SDS-PAGE. Cleavage of μ Bc during entry generates the δ protein of the ISVP. To indicate that δ is not a structural protein within the mature virion, it is shown off center within the gel. The equivalent mammalian reovirus structural proteins are listed adjacent to the ARV protein profile. **C.** The predicted location of the structural proteins (color coded for reference to the protein profile) are depicted in the cartoon particle that is sectioned into the three sequential stages of viral uncoating: the virion, intermediate sub-viral particle (ISVP), and core.

the mature virion. The inner capsid or core forms a complete icosahedral particle with spikes (λC) that protrude from the 12 vertices (Figure 1). The outer shell (Figure 1) condenses onto the pre-assembled core, and forms an incomplete protein layer of T=13 symmetry (assumed based on similarity to MRV outer shell structure; Van Regenmortel *et al.*, 2000). The core (Figure 1 and 2) is comprised of 5 structural proteins (λA , λB , λC , μA , σA). λA and σA are the major core proteins while the λC pentamers (spikes) and λB and μA minor internal proteins are associated only at the vertices (Martinez Costas *et al.*, 1995; 1997). The outer shell (Figure 1 and 2) consists of μB , μBc , σB , and 12 σC trimers at each vertex (Theophilus *et al.*, 1995). μB is an uncleaved precursor of major structural protein μBc and is present in minor amounts relative to its cleavage product (Duncan, 1996). The λC protein of the inner capsid transverses the outer layer and is exposed at the surface of the virion (Martinez Costas *et al.*, 1997). The virus is found to exist in 4 morphological states: virion, ISVP, core, and top component (Figure 1 and 2). The mature virion consists of the inner and outer capsid layers as mentioned above. The virion is proteolytically processed (in vitro or during infection) such that σB is degraded, μBc is cleaved, and σC extends to give rise to an intermediate subviral particle (ISVP). ISVP loss of σC and the μBc cleavage product produces the core, the final uncoated form found within the host cytoplasm. The fourth structure, top component, is a defective particle produced during infection that retains the double capsid but lacks the dsRNA genome. Thus, top component particles acquired their name due to their low buoyant density in cesium chloride compared to mature virus.

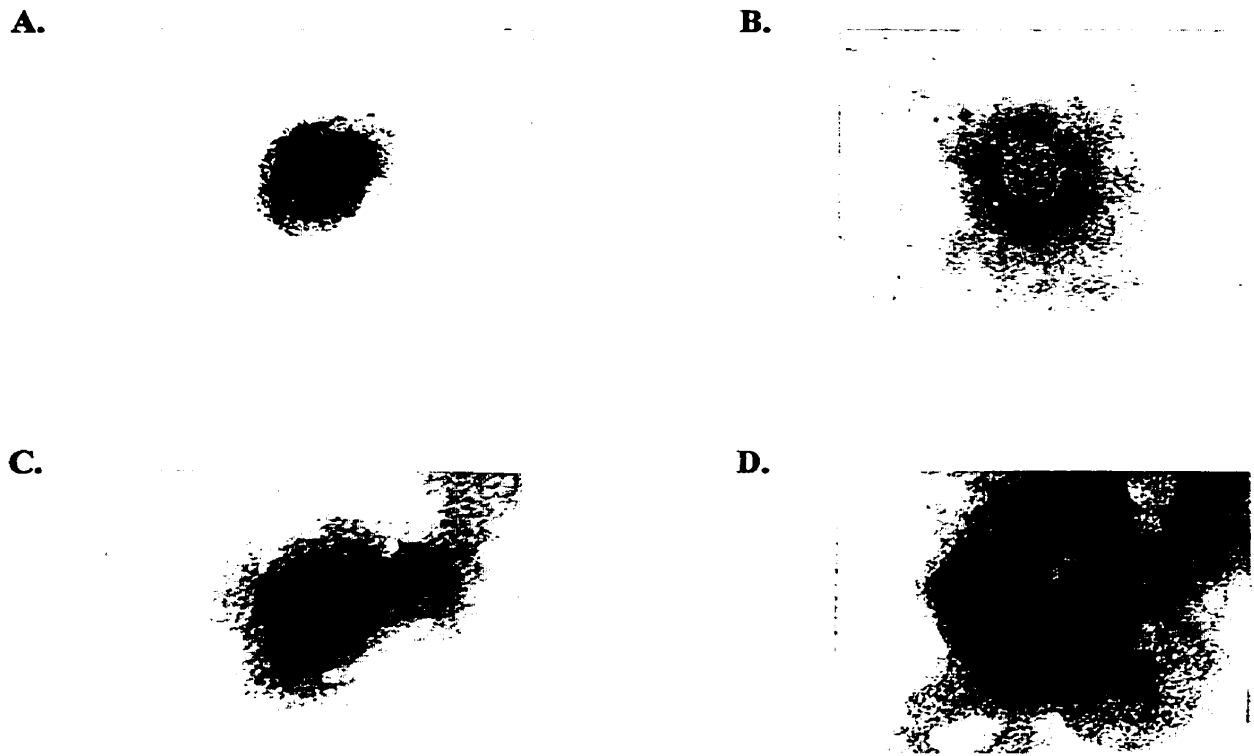


Figure 2. Components of the avian reovirus double shelled capsid and various morphological states of the virus. ARV 138 infected cell lysates were prepared and pelleted onto formvar coated 400 mesh grids and stained with phosphotungsten acid as described in Materials and Methods, section 2.7.2. Viral and sub-viral particles were visualized in a Philips model 201 electron microscope and photographs were taken. All prints are at a final magnification of 200, 000x. **A.** Virion: the mature virion consists of 10 segments of dsRNA encased by a double layered protein capsid, similar to other members of the family *Reoviridae*. **B.** The core: the inner capsid layer of the virion. **C.** Outer shell: the outer protein layer that adds onto the core structure to complete the capsid structure. **D.** Top component: a defective viral particle produced during infection that is composed of the double protein shell but lacks the dsRNA genome.

1.3 Lifecycle of avian reovirus.

1.3.1 Virus attachment and entry.

Attachment of the mature virion to the target cell, mediated by the σ C cell attachment protein, facilitates entry via the receptor mediated endocytosis pathway (Theophilus *et al.*, 1995). The acidic endosomal environment is required to process ARV outer capsid proteins during entry and leads to the production of the ISVP. As the conversion to the ISVP occurs, σ C is extended and σ B is lost (Sheng Yin *et al.*, 2000). Cleavage of the major outer capsid protein μ Bc into δ exposes hydrophobic residues that promote interaction with the endosomal membrane and entry into the cytoplasm (Duncan, 1996). Unlike MRV entry, a delayed, independent cleavage event of μ Bc occurs and gives rise to δ' . The functional significance the two μ Bc cleavage specificities is unknown and δ' may reflect an intermediate entry step or a byproduct of an unproductive entry pathway (Duncan, 1996). The ISVP is processed further (μ Bc/ δ and σ C loss) and results in the production of the transcriptionally active core particle within the host cytoplasm (Martinez-Costas *et al.*, 1997). Production of an ISVP prior to host cell attachment allows the virus to bypass receptor mediated endocytosis entry and fuse directly with the cell membrane (Duncan, 1996). Group and serotype specific antibodies target the σ B major outer capsid protein and the cell attachment protein (σ C) respectively, and inhibit viral infection (Sheng Yin *et al.*, 2000; Theophilus *et al.*, 1995).

1.3.2 Replication.

To date, ARV replication has not been described, in contrast to the extensively characterized MRV replication strategy. Similarities between ARV and MRV intravirion

protein distributions and functions suggest they may possess a common replication cycle. The uncoating of reoviruses is incomplete and the core represents the final entry product. This core particle is transcriptionally active and carries all enzymes for transcription of (+) sense messenger RNAs (mRNA). Collectively, RNA dependent RNA polymerase (RdRp), helicase, and RNA triphosphatase activities are found within the polymerase (MRV λ 3) and its cofactor (MRV μ 2). Based on correlation to MRV and stoichiometric analyses the predicted equivalent ARV proteins are λ B and μ A, respectively (Van Regenmortel *et al.*, 2000). The MRV λ 2 and ARV λ C proteins possess guanylyltransferase and methyltransferase activity and catalyze the addition of a 5' methylated cap to mRNA transcripts (Martinez-Costas *et al.*, 1995).

The mammalian reovirus replication cycle occurs in three stages: primary transcription, secondary transcription, and encapsidation. Primary transcription from the parental (-)RNA template produces 5' capped mRNAs. Transcripts are extruded from the core through channels within MRV λ 2 spikes (ARV equivalent: λ C) and enter the cytoplasm for translation by host translational machinery. Four genes are transcribed (MRV: L1, M3, S3, S4) and the early proteins they encode (MRV: λ 3, μ NS, σ NS, σ 3 respectively) function to stimulate primary transcription from all 10 template (-)RNAs. These 5' capped mRNAs are translated or, later in the replication cycle, act as template for the synthesis of the dsRNA genome. A single copy of each (+)RNA strand is assorted into a transcriptase/assortment complex where synthesis of the complementary (-)strand occurs. Conserved nucleotide sequences on the 10 RNA segments allow discrimination of viral RNA from host RNA. Avian reovirus S-class gene segments contain conserved

terminal 5'-GCUAA--//--UCAUC-3' sequences (read, by convention, from the (+)RNA sequence) (Sheng Yin *et al.*, 2000) and suggests they may function as the virus-host RNA recognition signals. However, identification of conserved motifs within the ARV M and L-class gene sequences is required. Individual mammalian reovirus RNA species also possess segment specific signals that allow the assortment complex to sequester all 10 different RNA species. The MRV σ NS protein binds single stranded RNA (ssRNA) and may function in assortment of gene segments. Similarly, the homologous ARV non-structural protein (σ NS) binds ssRNA in a sequence independent manner (Chiu *et al.*, 1997; Sheng Yin *et al.*, 2000; Yin *et al.*, 1998) but its role in RNA assortment is unknown. The mammalian reovirus non-structural protein μ NS binds ssRNA and associates with the cell cytoskeleton and may also have a role in genome packaging (Van Regenmortel *et al.*, 2000). The function of ARV μ NS has not been described. Secondary transcription results in the production of uncapped viral mRNAs from newly synthesized (-)RNA strand template. The majority of transcription occurs at this stage. Finally, structural proteins encapsidate the progeny dsRNA genomes to complete the replication cycle. These mature virions are arranged in paracrystalline arrays within non-membranous inclusion bodies in the cell cytoplasm (Van Regenmortel *et al.*, 2000).

Avian reoviruses have evolved a mechanism to evade an innate host antiviral response and promote survival. The σ A protein binds dsRNA in a sequence non-specific manner (Sheng Yin *et al.*, 2000) and its association with the viral genome segments prevents activation of host dsRNA dependent enzymes that inhibit protein synthesis (Martinez-Costas *et al.*, 2000). In contrast, the MRV σ 3 major outer capsid protein

(ARV equivalent: σB) prevents similar dsRNA induced mechanisms of host protein synthesis shut off (Imani and Jacobs, 1988).

1.3.3. Assembly.

To date, the avian reovirus assembly process has not been investigated. In contrast, studies that involve MRV temperature sensitive (*ts*) mutants have been used to delineate MRV assembly (Coombs, 1998). Encapsidation of viral dsRNA within the assortment complexes can be described in three sequential stages. The major core proteins $\lambda 1$ (ARV λA) and $\sigma 2$ (ARV σA) condense with the minor protein $\lambda 3$ (ARV λB) to form a primary core complex (Coombs, 1998; Hazelton, 1998). The addition of the pentameric spike protein $\lambda 2$ (ARV λC) and the cell attachment protein $\sigma 1$ (ARV σC) at each of the 12 vertices produces the complete core particle (Coombs, 1998). To complete assembly of the virion, the $\sigma 3$ (ARV σB) and $\mu 1/\mu 1c$ (ARV $\mu B/\mu Bc$) outer shell proteins complex together and then condense onto the core around the $\lambda 2$ spikes (Shing and Coombs, 1996). Assembly of MRV core and outer shell structures can occur independently of one another (Coombs *et al.*, 1994; Fields, 1971; Mutsuhisa and Joklik, 1974)

1.3.4 Syncytia formation

Prior to ARV release by host cell lysis, the infected cells develop into syncytia (10-12 hours post-infection), characteristic of orthoreovirus subgroup 2 (ARV, NBV) and 3 (BRV) (Shmulevitz and Duncan, 2000; Van Regenmortel *et al.*, 2000). Syncytia are large multinucleated cells produced from fusion of infected cells with adjacent cells. A novel 10 kDa non-structural protein (p10) first identified in avian reovirus is responsible

for this fusion event. Since the discovery of p10, non-structural fusogenic proteins have been identified in NBV (p10_{NBV}) and BRV (p15) and are collectively called FAST proteins (fusion associated small transmembrane proteins). The tricistronic S1 gene segment consists of one unexpressed open reading frame (ORF) and two functional ORFs, where the 1st ORF encodes p10 and the 2nd ORF encodes σ C (Shmulevitz and Duncan, 2000). Similarly, the equivalent MRV gene segment (S1) encodes the cell attachment protein (σ 1) and a non-structural protein (σ 1s). However, MRV σ 1s does not induce cell fusion. p10 is transported through the endoplasmic reticulum/golgi pathway and is inserted into the cell membrane as a type I integral transmembrane protein (Shmulevitz and Duncan, 2000) where it functions in cell-to-cell fusion and is not included in the mature virion structure. It is unknown if p10 acts independently to promote fusion or in conjunction with a host protein (Shmulevitz and Duncan, 2000). Syncytia formation is not essential for viral replication, release or pathogenesis but the rapid dissemination and increased rate of infection that results from cell-cell fusion is advantageous to the virus. In the final stages of infection ARV is released by cell lysis, typical of non-enveloped viruses (Duncan *et al.*, 1996).

1.4 Temperature sensitive (*ts*) mutants.

Conditionally lethal mutants have been extensively exploited to delineate many biologic processes in the field of virology (Black *et al.*, 1994; Carleton and Brown, 1996; Chen *et al.*, 1994; Compton *et al.*, 1990; Ericsson *et al.*, 1995; Millns *et al.*, 1994; Mitraki and King, 1992; Nagy *et al.*, 1995; Rixon *et al.*, 1992; Schwartzberg *et al.*, 1993; Shikova *et al.*, 1993; Wiskerchen and Muesing, 1995). Temperature sensitive (*ts*) mutant studies

have led to a more detailed understanding of protein function in attachment, entry, replication and assembly, intracellular communication, viral pathogenesis, and protein folding pathways in many viruses such as mammalian reovirus, rotavirus, orbivirus, poliovirus, and vaccinia virus (Coombs, 1998; Demasi and Traktman, 2000). In the *Reoviridae*, *ts* mutants have been generated by a variety of methods. The majority of MRV *ts* mutants were created by chemical mutagenesis (nitrous acid, nitrosoguanidine, proflavin, or 5-fluorouracil) of newly synthesized progeny dsRNA within infected cell cultures or mutagenesis of purified virions (Fields and Joklik, 1969; Ikegami and Gomatos, 1968). Serial passage of viruses at high multiplicity of infection or pseudorevertants rescued from persistent (non-lytic) *ts* mutant infections have also generated temperature sensitive mutants (Coombs, 1998). By definition, *ts* mutants are capable of infection, replication and release at permissive temperature whereas growth at non-permissive temperature results in an impaired or unproductive infection. Analysis of the mutant phenotype at non-permissive temperature in comparison to permissive temperature provides a link with gene and protein function relationships. In the *Reoviridae*, temperature sensitivity is characterized by the efficiency of plating (EOP) value, where viral titers at an elevated restrictive temperature are mathematically compared to titers at a lower permissive temperature (Fields and Joklik, 1969; Ramig, 1982). Theoretically, wild type virus grows well at both temperatures and has an EOP value of 1.0. In practice, wild type EOP values fluctuate randomly within a magnitude of 10 ($\log_{10}1$). *Ts* mutants are identified as having EOP values significantly less than 0.1 and to date, 58 MRV *ts* mutants (Coombs, 1998) and 31 simian rotavirus SA11 *ts* mutants (Ramig, 1982 and 1983) have been generated. Our investigation extended similar

studies to the more poorly understood avian reoviruses through the generation of the first genetically exploited panel of chemically derived ARV *ts* mutants.

1.5 Exploitation of the segmented genome.

1.5.1 Reassortment

Members of the *Reoviridae* possess a characteristic segmented linear dsRNA genome that migrates to 3 size classes on a SDS-polyacrylamide gel (Sharpe *et al.*, 1978; Van Regenmortel *et al.*, 2000). Different reovirus serotypes (of the same species) have unique dsRNA migration patterns, or viral electropherotypes, when resolved by electrophoresis (Sharpe *et al.*, 1978). For example, avian reovirus species serotypes ARV 138 and ARV 176 have unique electropherotypes as seen in Figure 1A. Mixed infections of host cells with different viral serotypes allows genetic mixing during gene segment assortment and produces reassortant progeny (viruses with hybrid genotypes) (Figure 3). The parental origin of the dsRNA segments can be identified by polyacrylamide gel electrophoresis (Figure 4). In the *Reoviridae*, reassortants result only from mixed infections within species limits and such hybrid progeny have been exploited in mammalian reovirus, rotavirus, and avian reovirus (Duncan, 1999; Nibert *et al.*, 1996; O'Hara *et al.*, submitted; Ramig, 1982 and 1983). If assortment of gene segments during mixed infection was a random event, 99.8% reassortant progeny would be expected (Figure 3). However, a total of 3-30% reassortant progeny are routinely produced. Nucleotide signals may direct preferential (non-random) reassortment of certain gene segments. Alternatively, random reassortment may occur where certain hybrid genotypes are less favorable and are undetected or a physical separation of inclusion bodies within

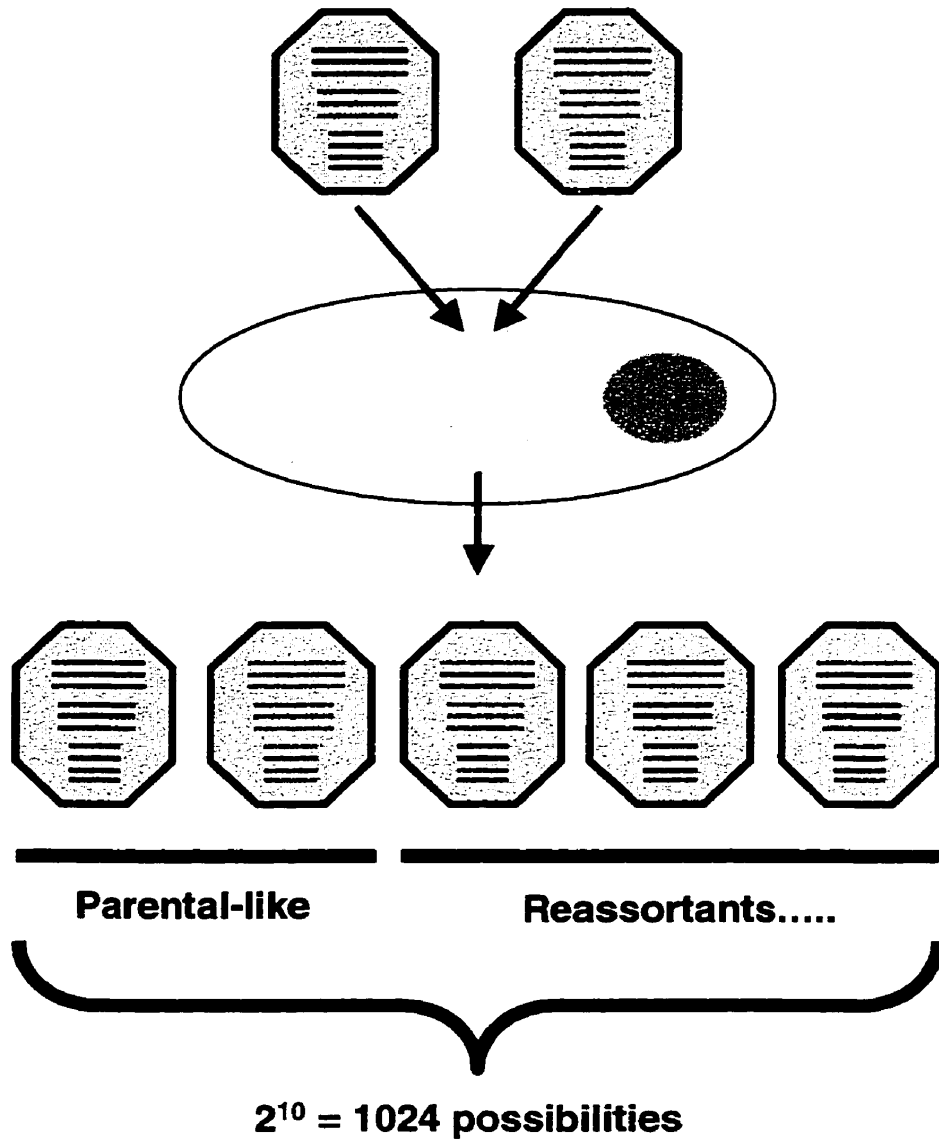


Figure 3: Mixed infection and production of reassortant progeny. Mixed infection with two different viral clones produces reassortants (progeny with hybrid genotypes) as progeny gene segments are mixed and acquired in the assortment stage of the viral lifecycle. If parents involved are of different serotypes (have unique electropherotypes) the origin of reassortant progeny gene segments can be identified by SDS-PAGE. Two unique sets of the 10 gene segments are involved in the assortment, and all 10 gene must be included in the progeny virions. Thus, if reassortment was a random process, we would expect $2^{10}=1024$ possible genotypes produced from the mixed infection. Two of the 1024 possibilities are parental like, while 99.8% of the progeny would be expected to have hybrid genotypes.

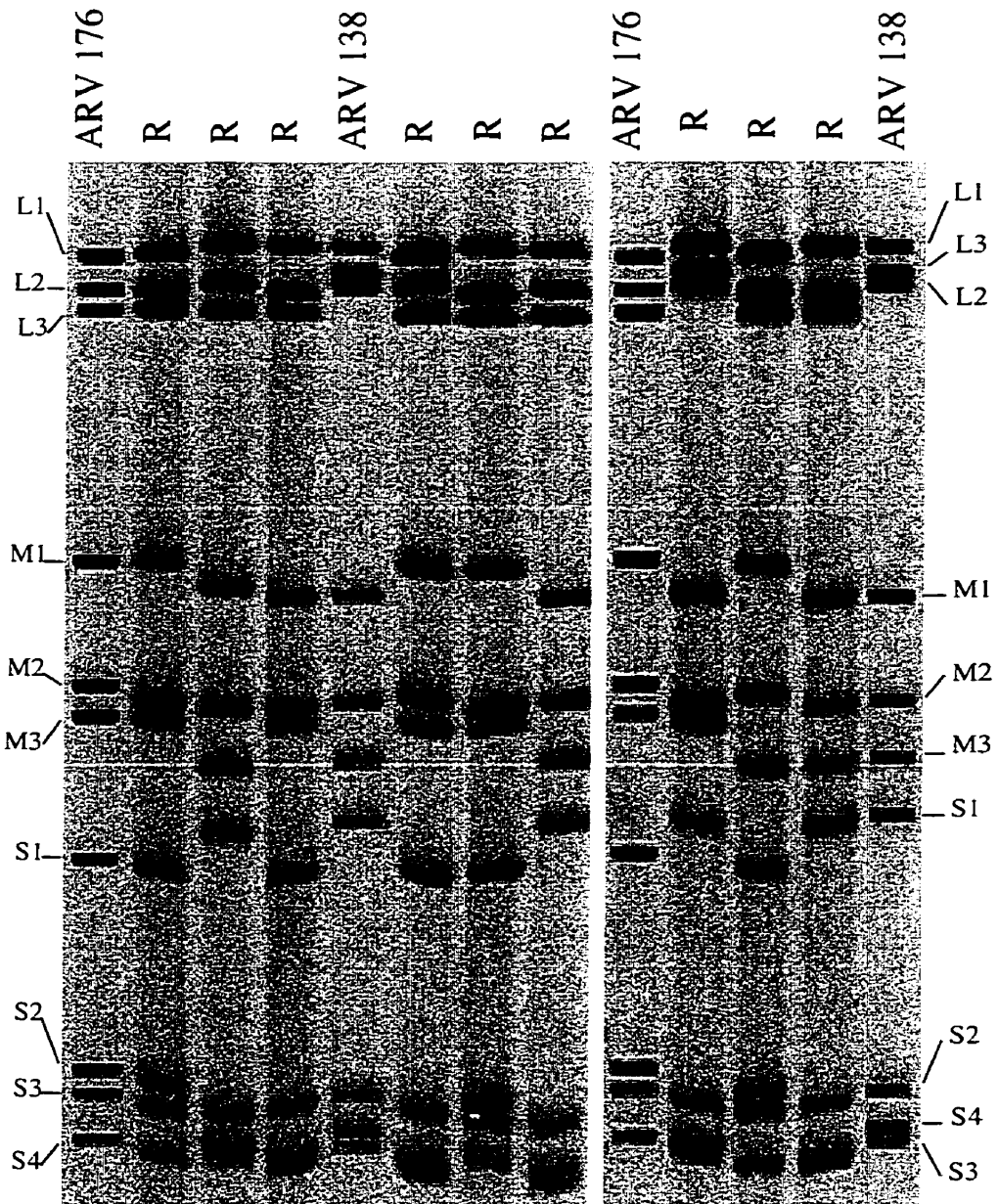


Figure 4. ARV 138, ARV 176, and reassortant electropherotypes resolved by SDS-polyacrylamide gel electrophoresis. ARV strain 138 and ARV strain 176 were subjected to mixed infection and reassortant (R) progeny were produced. The viral dsRNA was extracted and resolved by SDS-PAGE as detailed in Materials and Methods. RNA was electrophoresed in 12.5% gels for 67.5 hours, stained with ethidium bromide, and visualized and photographed under ultraviolet illumination. The electropherotypes of the parents and some of the reassortant progeny are shown. ARV 138 and ARV 176 represent different avian reovirus serotypes and have unique gene segment profiles. The parental origin of the reassortant gene segments can be identified by comparison to the parental genotypes. Gene segments are labeled along each side of the gel. The order of migration for ARV 138 and ARV 176 L2/L3 and S3/S4 gene segments are reversed with respect to each other.

the infected cell prevents complete mixing of progeny gene segments (Nibert *et al.*, 1996).

1.5.2 Genetic recombination.

The process of reassortment has been used to delineate many biological processes (O'Hara *et al.*, submitted; Ramig and Fields, 1983) and in the characterization of mammalian reovirus and rotavirus temperature sensitive mutants (Fields and Joklik, 1969; Ramig, 1982). Genetic recombination in viruses with segmented genomes (*Reoviridae*, *Orthomyxoviridae*) occurs through reassortment of individual gene segments rather than the classical means of strand breakage and rejoining (Ramig and Ward, 1991; Simpson and Hirst, 1968). MRV and rotavirus *ts* mutants have been organized into groups based on having their *ts* mutations in the same or different gene segments by genetic recombination analyses. In this approach, a host cell mixed infection with two different *ts* mutants that have *ts* mutations within the same gene segment would produce progeny that all retain the temperature sensitive phenotype. In contrast, a mixed infection of mutants whose *ts* lesions reside on different gene segments would produce a variety of reassortant progeny that contain both parental mutations, a single *ts* mutation, and no *ts* lesion. In MRV and rotavirus, recombination or the presence of wild-type-like progeny (lacking both parental *ts* mutations) has been assessed using a standard recombination formula:

$$\frac{(AB)_{NP} - (A+B)_{NP}}{(AB)_P} \times 100 \quad (\text{Fields and Joklik, 1969})$$

where mixed infection of host cells with parental viruses A and B produces progeny virions AB, and infections are carried out at non-permissive (NP) and permissive (P)

temperature (Coombs, 1998; Fields and Joklik, 1969; Ramig, 1982). The reported limits of recombination are variable where values <0%, <0.1%, or <0.2% indicate mutants belong to the same recombination group and values >1%, >2%, or 3% suggest mutants belong to different recombination groups (Coombs, 1998; Fields and Joklik, 1969; Ramig, 1982). An alternative formula has been used in bovine rotavirus *ts* mutant systems:

$$\text{Recombination Index (RI)} = \frac{(AB)_{NP}}{(A+B)_{NP}} \quad (\text{Greenberg } et al., 1981)$$

The RI formula does not account for growth at permissive temperature and may inaccurately assess recombination in mutants with moderate *ts* phenotypes. Genetic recombination experiments led to the organization of 58 MRV *ts* mutants into 8 recombination groups (Coombs, 1998), and 31 rotavirus *ts* mutants into 10 recombination groups (Ramig, 1982; 1983).

1.5.3 Reassortant mapping.

To identify the gene segment that harbors the *ts* lesion, reassortant mapping has been applied in mammalian reovirus (Ramig *et al.*, 1983) and rotavirus (Gombold and Ramig, 1987) *ts* mutant systems. This approach relies on the generation of reassortant progeny from mixed infections that involve a *ts* mutant clone and non-*ts* wild type virus of a different serotype (unique electropherotype). Reassortant electropherotypes and temperature sensitive status (EOP value) are determined. Those reassortants that retain temperature sensitivity are organized into one panel while reassortants that act non-*ts* are placed in a separate panel. Identified *ts* reassortants should all share a gene segment of mutant origin, while non-*ts* reassortants should share the corresponding gene segment of

wild type origin, and all other segments should be randomly assorted with respect to temperature sensitivity. This combination of results allows the gene segment associated with the *ts* phenotype to be identified and has been used extensively by many labs in MRV *ts* mutant studies (reviewed in Coombs, 1998).

1.6 Objectives of the research programme

As described in the previous sections, our knowledge of avian reovirus structure and lifecycle is limited and often based on correlation to the prototypic member of the *Reoviridae*, mammalian reovirus. However, important differences between ARV and MRV have been observed, such as the ability of ARV to induce cell-to-cell fusion and its lack of hemagglutination activity. Avian reovirus represents the prototype of all non-enveloped fusogenic viruses and possesses a novel protein (p10) responsible for syncytia formation. Such biologically relevant differences from MRV suggest analysis of avian reovirus is warranted, and may ultimately enhance our understanding of the *Reoviridae* family as a whole. Although many similarities to mammalian reovirus likely exist, it is hypothesized that some features of the ARV lifecycle are unique and result in the observed phenotypic differences. Furthermore, it is possible that other novel features of ARV exist that remain to be discovered. This study characterizes ARV protein function to attempt to enhance our knowledge of this virus and identify similarities and differences between ARV and mammalian reovirus.

Three decades ago, mammalian reovirus temperature sensitive mutants were first created, and the characterization of these clones and more recently isolated mutants has led to a more detailed understanding of the MRV lifecycle. This investigation extends

similar studies to the more poorly understood avian reoviruses through the generation of the first genetically exploited panel of chemically derived ARV *ts* mutants. These mutants were organized into recombination groups and the mutated gene segment was identified for some groups by reassortant analysis. The replication process of ARV has not yet been described. To localize ARV protein function in the stages prior to or during replication, or at the later stage of capsid assembly and release, the synthesis of viral dsRNA was examined for each mutant clone. To date, assembly of the avian reovirus capsid has not been investigated. Some *ts* mutants were morphologically characterized by thin section electron microscopy and particle count preparations to examine the ARV assembly process and confirm protein location within viral and sub-viral particles. For one *ts* mutant the precise protein alteration was identified and secondary structural changes were proposed. Examination and integration of the available biologic, morphologic, and protein sequence information has enhanced our understanding ARV protein function. Consequently, this panel of ARV *ts* mutants creates the tools necessary for ARV protein characterization and addresses some questions with respect to ARV biology. In addition, availability of these mutants will serve as a valuable resource to allow hypothesis generation and to pose additional questions about the biology of ARV and the *Reoviridae* as a whole.

2. MATERIALS AND METHODS

2.1 Stock cells and viruses. ARV strains 138 and 176 (Hieronymus, 1983; Duncan, 1998) are prototypic lab stocks and were passaged in the QM5 continuous quail cell line (kindly donated by Dr. R. Duncan of Dalhousie University, Halifax, Canada; Duncan, 1998). Cells were maintained in 1x Medium199 supplemented with 10% fetal calf serum (Gibco BRL), 10% tryptose phosphate broth (2% tryptone, 0.2% dextrose, 8.6mM NaCl, 1.8mM Na₂HPO₄), and 2 mM l-glutamine and grown in the presence of 5% CO₂ at 37°C. Confluent cell monolayers were routinely passaged by standard trypsinization procedures where media is removed, cells are washed with phosphate buffered saline/ethylenediamine tetraacetate (PBS/EDTA: 137mM NaCl, 0.3mM KCl, 0.8mM Na₂HPO₄, 0.1mM KH₂PO₄, 0.05mM EDTA) and 0.25% trypsin (source: porcine pancreas, Sigma) is added. The cells were incubated at 37°C for 5 minutes to allow the monolayer to detach and were then resuspended in the appropriate dilution volume of QM5 maintenance media. Stock QM5 cells were typically passaged twice weekly, and were split 1:6. Cells used for viral infections were incubated in the above media supplemented with 100U/ml penicillin, 100µg/ml streptomycin sulfate, and 1µg/ml amphotericin B (Coombs *et al.*, 1994).

2.2 Viral manipulation

2.2.1 Viral plaque assay. Serial dilutions of viral stocks were made in gel/saline (137 mM NaCl, 0.2 mM CaCl₂, 0.8 mM MgCl₂, 19 mM HBO₃, 0.1 mM Na₂B₄O₇, 0.3% [wt/vol] gelatin). Growth media was removed from sub-confluent QM5 monolayers in 6 well tissue culture dishes, diluted virus was added and adsorbed for 1 hour at room temperature with occasional rocking every 10 minutes to keep cells moist, then cells were overlaid with 1x Media199/1%agar. Dishes were incubated at the desired temperature and infected monolayers were fed and stained according to the following schedule. Plates incubated at 36°C or greater were fed with the Medium199/agar overlay on day 3 post infection (PI) and stained with 0.02% neutral red 5 days PI. Plates incubated at less than 36°C were fed on day 4 PI and stained 6 days PI. Plaques were generally counted 18 hr after the plates were stained and viral titer was calculated.

2.2.2 Viral passage. Maintenance media from sub-confluent QM5 monolayers was removed and the cells were infected with virus at a multiplicity of infection (MOI) less than 1 plaque forming unit (PFU)/cell. After 1 hour absorption at room temperature, fresh completed Medium199 was added. The infections were incubated at the appropriate temperature in the presence of 5% CO₂ until 90% cytopathic effect (CPE) was evident by light microscopy (generally, 3-4 days PI). Wild type viruses were grown at 37°C and mutant viruses were amplified at 33.5°C. Viral progeny were harvested by cell lysis induced by three cycles of freeze/thawing at -80°C and viruses were stored at 4 °C (for immediate use) or -80°C (for long term storage). Viruses were titered by plaque assay prior to use.

2.2.3 Plaque purification. To ensure clones originated from a single replicating virus and did not represent a mixed population of viruses, viral plaques were isolated and

picked. Samples were infected, overlaid and incubated as described earlier (section 2.2.1). Plaques were stained with 0.013% neutral red, incubated for 18 hours, and picked ($P_{0,\#1}$) using a sterile pasteur pipette. The viral/agar plugs were resuspended in 0.5ml QM5 maintenance media and placed at 4°C for 24 hours to allow viral diffusion into the media. $P_{0,\#1}$ stocks were used as the inoculum for an additional round of plaque purification ($P_{0,\#2}$). The double plaque purified stocks were amplified twice (P_1 , P_2) and harvested by freeze/thawing three times as described previously.

2.2.4 Concentration of viral stocks. Cellular debris from frozen/thawed viral stocks was pelleted at 1000rpm for 10 minutes in an IEC refrigerated floor centrifuge. The supernatant was collected, layered onto a 30% sucrose (in PBS) cushion and centrifuged in a Beckman SW28 rotor at 16,700 rpm for 1 hour to pellet virus. The pellet was resuspended in the desired minimal volume of QM5 maintenance media. Concentrated stocks were stored at -80°C and titered by plaque assay prior to use.

2.3 Chemical mutagenesis and plaque purification of *ts* clones. To generate *ts* mutants, sets of sub-confluent QM5 monolayers were infected with ARV 138 and ARV 176 at an MOI of 0.5-3 PFU/cell. After a 1 hour adsorption the infections were overlaid with media that contained 0.1-1000µg/ml nitrosoguanidine (N-methyl-N'-nitro-N-nitrosoguanidine) (Sigma-Aldrich), bromodeoxyuridine (5-bromo-2'-deoxyuridine) (Sigma-Aldrich), or proflavin (Sigma-Aldrich) and incubated at 37°C for 24 hours. Progeny virions were harvested by freeze thawing 3 times and titered to determine effects of the mutagen on virus replication and survival. The cell lysate from cultures that had been treated with 34µg/ml nitrosoguanidine showed approximately a 4% survival

compared to unmutagenized controls. The mutagenized ARV 138 stock that corresponded to this 4% survival rate was inoculated onto sub-confluent QM5 monolayers in P100 dishes, overlaid with Media199/agar and incubated for 8 days at 33.5°C (chosen as the permissive temperature for this study). Infections proceeded for 8 days PI to permit growth of the less viable mutagenized clones. Plates were lightly stained with 0.005% neutral red and returned to 33.5°C incubator (Fields, 1969). On day 9 plaques were identified by area and the plates were placed at 39.5°C (chosen as the non-permissive temperature for this study) for 2 days. Plaques that were identified at 33.5°C but failed to enlarge when placed at 39.5°C for 2 days were classified as potentially temperature sensitive (*ts*). These clones were picked with a sterile pasteur pipette and each picked sample was plaque purified again and amplified twice as described earlier.

2.4 Determination of temperature sensitivity.

2.4.1 Efficiency of plating (EOP) assay. Serial 1:10 dilutions of virus clones were infected into sub-confluent 6 well tissue culture plates in duplicate and incubated at 33.5°C and 39.5°C as described in section 2.2.1. Plaques were counted to obtain viral titer at the two temperatures and the EOP ratio was calculated to determine *ts* status by the following formula:

$$\text{EOP} = \frac{\text{Viral titer at non-permissive temperature}}{\text{Viral titer at permissive temperature}}$$

Unmutagenized non-*ts* virus grows equally well at both temperatures with a theoretical EOP value of 1.0. In practice, this value fluctuates randomly within a magnitude of 10.

Classically, *ts* mutants have EOP values more than 10-fold lower than that of unmutagenized parental virus EOP values (Coombs, 1998).

2.4.2 Efficiency of lysis (EOL) assay. Duplicate 96-well flat bottom plates with sub-confluent QM5 monolayers were infected with one 10 μ l aliquot of undiluted virus and aliquots (10 μ l) of 11 serial 1:3.16 ($\sim\sqrt{10}$) viral dilutions made in gel/saline. A total of 8 samples can be analyzed per pair of 96-well plates. After one hour adsorption the wells were overlaid with 95 μ l completed 1x Medium199. One plate of the pair was placed at 33.5°C and the other at 39.5°C. On day 4 and 5 post infection the 39.5°C and 33.5°C plates respectively were removed, washed with 1X phosphate buffered saline (PBS), fixed with 2% formaldehyde in PBS and stained with 1% crystal violet. Permissive and restrictive temperature EOL incubation times were determined such that at each dilution the extent of cell lysis was similar for both unmutagenized ARV 138 and clones known to be non-*ts*. The ability of each virus to lyse cells at both temperatures was compared using an efficiency of lysis (EOL) ratio:

$$\text{EOL value} = \frac{\text{ID}_{\text{NP}}}{\text{ID}_{\text{P}}}$$

Where ID = infectious dose required to lyse the monolayer of cells, NP = non-permissive temperature (39.5°C), and P = permissive temperature (33.5°C). Clones that exhibited reduced levels of cell lysis at the non-permissive temperature in comparison to the permissive temperature, and whose EOL ratio was significantly less than the EOL ratio of unmutagenized parental ARV 138 were considered potentially *ts*. The *ts* status of such clones was then confirmed by the classic EOP assay as described in the previous section.

2.5 Recombination assay. Identified *ts* mutants were subjected to pair-wise mixed infections at an MOI of 5 for each input virus in 24-well tissue culture plates with sub-confluent QM5 monolayers. After adsorption each well was overlaid with 0.48ml completed media and incubated at 33.5°C for 32 hours (~ one cycle of replication). The plates were frozen and thawed twice and then sonicated to disrupt viral aggregates. Samples were immediately titered at 33.5°C and 39.5°C as described in section 2.2.1.

2.5.1 Standard *Reoviridae* recombination formula. Mutant cross results were analyzed by the standard *Reoviridae* recombination formula:

$$\frac{(AB)_{NP} - (A+B)_{NP}}{(AB)_P} \times 100 \quad (\text{Fields and Joklik, 1969})$$

where AB = progeny from a mixed infection of parental viruses A and B, NP = non-permissive temperature (39.5°C), and P = permissive temperature (33.5°C).

2.5.2 Recombination Index (RI) formula. The recombination index (RI) formula used to assess recombination of bovine rotavirus *ts* mutants was also applied to ARV *ts* mutant mixed infection data:

$$\text{Recombination Index (RI)} = \frac{(AB)_{NP}}{(A+B)_{NP}} \quad (\text{Greenberg } et al., 1981)$$

RI values >5 indicate recombination between the *ts* mutants has occurred whereas values <5 suggest recombination has not taken place (Greenberg *et al.*, 1981).

2.5.3 Novel EOP recombination formula. Data was also analyzed by a novel formula that examines changes in the progeny efficiency of plating (EOP) values compared to the parental virus EOP values:

$$\text{EOP Recombination Value} = \frac{\text{EOP}_{AB}}{0.5(\text{EOP}_A + \text{EOP}_B)}$$

EOP recombination values <5 indicate *ts* mutants are members of the same recombination group and values >20 indicate they belong to separate recombination groups. The novel formula, which will be detailed later, was developed to address the inadequacies of the standard *Reoviridae* and RI formulae and to clarify the organization of *ts* mutants into recombination groups.

2.6 Reassortant mapping.

2.6.1 Generation of reassortants. A 24-well tissue culture dish with sub-confluent QM5 monolayers was co-infected with a selected *ts* mutant clone (derived from ARV 138) and unmutagenized ARV 176 with MOI ratios of 5/5, 2/8, 8/2 plaque forming units/cell for the *ts* mutant and ARV 176 respectively. Infections were incubated at 33.5°C for 32 hours. The infections were freeze/thawed twice and the cell lysates were sonicated and serially diluted in gel saline. Aliquots (300µl) of each of the ~1:10⁴⁻⁶ dilutions from each mixed infection were infected into P100 tissue culture dishes with sub-confluent QM5 monolayers. After adsorption the viral inoculum was removed and the cells were overlaid with 15ml 1X Medium199/1% agar and incubated at 33.5°C for 9 days (to allow detection of slow growing reassortants). On day 5 the infections were fed with 12ml 1X Medium199/1% agar, and on day 9 the plates were stained with 12ml 0.02% neutral red. Individually isolated plaques separated by at least 0.75 cm were picked, then amplified twice as described earlier.

2.6.2 Isolation of viral double stranded RNA (dsRNA). The P2 progeny clones (300µl) were used to infect P100 dishes of sub-confluent QM5 monolayers, overlaid with QM5 Media199 and incubated at 33.5°C until 75% CPE was evident. Cells were scraped

off the plate and pelleted at 1100rpm in the IEC floor centrifuge. To lyse cell membranes pellets were resuspended in 500µl NP40 buffer (140mM NaCl, 1.5mM MgCl₂, 10mM Tris-HCl, pH 7.4) with 0.5% NP40 detergent, incubated on ice, and vortexed every 10 minutes for 30 minutes. Cellular nuclei and organelles were pelleted at 1100rpm in the IEC floor centrifuge and supernatants were collected in sterile microfuge tubes. Phenol/chloroform extraction (600µl of phenol/chloroform at a 1:1 ratio) of viral dsRNA segments was performed. RNA was precipitated at -20°C overnight in 0.108mM sodium acetate and 2.5 volumes of ice cold ethanol, then pelleted at 12,500rpm for 30 minutes in a Biofuge microcentrifuge (VWR Scientific, Toronto, ON). Viral dsRNA pellets were lyophilized (SC100 speed-vac, Savant, Holbrook, NY) and resuspended in 30µl 1x electrophoresis sample buffer (0.24M Tris-HCl pH 6.8, 1.5% dithiothreitol, 1% SDS).

2.6.3 Identification of reassortants by SDS-PAGE. Sodium dodecyl sulfate polyacrylamide gel electrophoresis (SDS-PAGE) was used to resolve dsRNA gene segments. 12.5% slab gels (16cm x 16 cm x 0.1 cm) were poured and polymerized overnight. Viral dsRNA samples were heated to 65°C for 5 minutes prior to loading and electrophoresed for 1.5 hours at 18mAmps/gel, 66 hours at 12mAmps/gel and 3-5 hours at 2mAmps/gel. Viral dsRNA bands were stained with ethidium bromide (3 µg/ml) and visualized by ultraviolet irradiation. Photographs were taken with a Gel Doc 2000 (BioRad) apparatus and reassortant progeny clones were identified by comparison of progeny gene segment profiles to that of the two parents involved in the infection.

2.7 Identification of total viral double stranded RNA (dsRNA) production.

2.7.1 Infection and $^{32}\text{PO}_4^{3-}$ labeling of viral dsRNA. Viral clones were used to infect both P60 and 6 well dishes of sub-confluent QM5 monolayers at an MOI of 10 plaque forming units/cell. Dishes were incubated at 39.5°C (P60 dish) or 33.5°C (6-well dish) and 23.7 $\mu\text{Ci/ml}$ ^{32}P (Orthophosphate, Mandel Scientific) was added to the infections at 30 minutes and 45 minutes PI, respectively. The 39.5°C and 33.5°C infections were incubated for a total of 18 and 24 hours post infection (equivalent replication time), respectively. Progeny dsRNA is synthesized prior to completion of assembly, thus the time points chosen represent slightly less than one complete cycle of replication.

2.7.2 Cytoplasmic extraction of radiolabeled viral dsRNA. Immediately after incubation, infections were placed on ice and the cell monolayers were washed with ice cold NP40 buffer to remove unincorporated label. Cytoplasmic extraction of viral dsRNA was performed as described previously. However, prior to phenol/chloroform extraction, crude cell extracts were incubated with 50 $\mu\text{g/ml}$ proteinase K (Sigma Aldrich) at 37°C for 30 minutes to aid in protein removal.

2.7.3 Labeled viral dsRNA resolved by SDS-PAGE. Viral dsRNA profiles were resolved on a 12.5% SDS polyacrylamide gel as described earlier. The gel was dried at 80°C (Slab Gel Dryer, SGD4050, Savant) for 2 hours, then exposed to a Molecular Imager Fx Imaging screen (BioRad) for 18 hours at room temperature. Phosphor images of the dried gel were analyzed by a Personal Molecular Imager[®] Fx (BioRad).

2.8 Electron Microscopy.

2.8.1 Thin section transmission electron microscopy. P100 dishes with sub-confluent QM5 monolayers were infected in duplicate at an MOI of 10 plaque forming units/cell. One plate of the pair was incubated at 39.5°C and the other at 33.5°C for 22 hours and 30 hours respectively (~ one round of replication). Cells were harvested by trypsinization (0.25%) at 37°C, and then fixed with 2% glutaraldehyde at 4°C. All subsequent steps were performed at 4°C. Cells were pelleted and washed 3 times with SC-Mg buffer (100mM sodium cacodylate, 10mM magnesium chloride, pH 7.4) followed by fixation with 1% osmium tetroxide (in SC-Mg buffer) and 2 additional SC-Mg buffer washes. Pellets were mixed with an equal volume of 3% low melting point agarose at 30°C and allowed to cool to create solid cell/agarose blocks. Slivers of the cell/agarose blocks were cut and stained with 2% aqueous uranyl acetate and dehydrated through a series of increased acetone concentrations. The cells were infiltrated with fresh embedding medium (DER 332-732) and polymerized (overnight at 37°C, 24 hours at 48°C, and 36 hours at 60°C). Thin sections were cut (diamond knife: Microstar, Huntsville, Texas) with a LKB Ultratome III ultramicrotome (LKB, Upsalla) and placed on copper grids (Maravac Ltd, Halifax, NS). Sections were stained with saturated ethanolic uranyl acetate and 0.25% lead citrate in 0.1M NaOH. A Philips model 201 electron microscope was used to view sections at 60KeV (acceleration voltage) and magnifications of 4,500-100,000X. Photographs were taken and printed.

2.8.2 Proportions of viral and sub-viral particles. Sub-confluent QM5 cells (24-well tissue culture dish) were infected in duplicate at an MOI of 10 plaque forming units/cell. One plate of the pair was incubated at 39.5°C and the other at 33.5°C for 22 hours and 30 hours respectively. Infections were freeze/thawed twice and cell lysates

(500µl) were pre-cleared at 15,000rpm (Eppendorf Model 5412 centrifuge) for 3 minutes to remove mitochondria, nuclei, and large aggregated macromolecules. The supernatant was centrifuged for 1 hour on a 30% potassium tartrate cushion (pH7.2) in the Airfuge® (Beckman Instruments, Palo Alto, C; A100 rotor) at 26psi to obtain viral and sub-viral pellets. Pellets were resuspended in 1X Medium199 supplemented with 0.1% glutaraldehyde and fixed on ice. The samples were pelleted directly onto formvar coated 400 mesh grids for 30 minutes at 26psi (Airfuge®, EM-90 rotor). The grids were stained with 2.5mM phosphotungsten acid and viewed (magnifications 30,000 – 70,000X). For each prepared sample grid, the viral and sub-viral particles (top component, core, outer shell) produced during the infection were counted in five non-adjacent grid squares (center and the 4 corner grids). The total number of particles/ml was calculated by the formula:

$$\text{Particles/ml} = (\text{average number of particles})(1.79 \times 10^5)(\text{dilution factor})$$

(Hammond *et al.*, 1981)

2.9 Determination of the ARV138 and *tsA12* mutant S2 gene sequence.

2.9.1 Preparation of viral template. ARV 138 or *tsA12* was infected into 4 P100 dishes with sub-confluent QM5 monolayers. When 90% CPE was evident the supernatants were collected and the virus was pelleted at 7,000rpm for 16 hours in the Beckman RC centrifuge (Fullerton, CA) using a JA-20 rotor. The virus was resuspended in 1x PBS and semi-purified through a 30% sucrose cushion as described in section 2.2.3. The pellet was resuspended in dialysis buffer (150mM NaCl, 15mM sodium citrate pH7.0). Phenol/chloroform extraction was carried out twice followed by a single

chloroform extraction. The aqueous phase was precipitated overnight at -20°C in a silanized corex tube (0.108mM sodium acetate, 2.5 volumes of ice cold ethanol) and pelleted in the JA-20 rotor (Beckman RC centrifuge) at 9,000rpm, 5°C for 30 minutes. The RNA pellet was washed with 70% ethanol and resuspended in 20µl 90% DMSO/10% 10mM Tris pH6.8.

2.9.2 Design of primers specific for the S2 gene segment. The ARV strain 138 S2 gene sequence (1324 base pairs) (Duncan, 1999) was used to design terminal primers and a series of internal primers to “walk” along the S2 gene sequence (Figure 5). The *tsA12* mutant was derived from ARV 138, thus the same primers were used on both clones. The terminal upper strand primer (ARV#1) is complementary to bases (5')1-18(3'), where the start codon (ATG) covers bases (5')16-18(3') (Sheng Yin *et al.*, 2000). The terminal lower strand primer (ARV#5) is complementary to bases (5')1303-1288(3'). The S2 gene stop codon (TAG) is located at base (5')1264-1266(3') (Sheng Yin *et al.*, 2000). The sequenced S2 product covered the entire length of the open reading frame and was read in both directions. De-salted primers were purchased from Gibco-BRL (Life Technologies).

2.9.3 Reverse transcription polymerase chain reaction (RT-PCR). 6µl of purified dsRNA was heated for 45 minutes at 50°C to denature the strands. The RNA was “snap cooled” with 63 µl DEPC-ddH₂O (DEPC: diethylpyrocarbonate) on ice. 32U (0.8µl of 40U/µl) Rnasin, 0.1µM (1µl of 10µM) of both terminal primers (upper: ARV#1, lower: ARV#5), 10mM (5µl each) of dATP, dCTP, dGTP, dTTP, 20 µl of 5x 1st

1 5' ARV#1 3'
 gctttttctc ccacgatggc gcgtgcogta taogacttct tttctacgcc tttcgggaat
 61 cgtgggtctag cgacgaatcg tactcaactg tcatcactac taacaagctc gaattcccca
 121 tggcaacgat ttctatcatc actgactcca ttgacggcgc caggtatcgt ctcaacacct
 181 gaagcacctt atccaggttc gttgatgtat caggagtcta tgctccacag tgttactggt
3' ARV#8 5'
 241 ccgggagtac tgggtaatcg tgatgcttgg cgtacattca atgtcctcgg gctttcatgg
 301 actgatgaag gactatcagg actagtggct gctcaagatc ctctcccgcc tgccccgat
 361 cagccagcct ctgctcagtg gtcagatctc ctcaactacc ctagatgggc aacagagcgt
 421 5' ARV#2 3'
 cgtgagctgc aatctaaata ccgcttctg cttagatcca cgctgcttcc cgccatgcga
 481 gctgggtctg ttctttatgt tgagacgtgg cogaatatga tttcaggagc actagccgac
 541 tggttcatgt cccaatatgg taacaatttc gttgacatgt gcgccagggt aacgcagtct
3' ARV#7 5'
 601 tgttcgaaca tgcctgttga acctgatggg aactatgatc agcagatgcg tgctttgatt
 661 agtttgtggc tcctttcata cattggggta gtcaaccaga ccaataccat cagcggcttc
 721 tactttctct cgaagactcg ggtcaagcg ttggacagtt ggaccttatt ctatactaca
 781 aacaccaacc gtgtccaat taccagaga catttogett acgtgtgtgc acggtctccc
 841 gattggaacg tggataagtc atggatcgtc gcggcgaact taaccgctat cgcatggct
 901 5' ARV#3 3'
 tgcogtcaac cgccgatgtt tgccaatcaa ggcgttatta accaggcaca gaaccgacct
 961 ggcttttoca tgaatggggg gacgcccgtc catgagctca acttactaac taccgcgcag
3' ARV#6
 1021 gaatgcatcc ggcagtgggt ggtagctggg ttgggtgacg cagogaaggg gcaagcatta
5'
 1081 acgcaggagg ctaatgactt ttogaacctc atccaggcag atctaggaca gatcaaggcg
 1141 caggatgacg ctctgtacaa tcagcagcca ggatacgcga gaagaataaa acccttctgt
 1201 aacggtgact ggacaccagg tatgaccogc caagctttgg ccgttctage cacttttacc
 1261 gcttaggcgt agggctgtac gctgcccag tccagccctc cggcagcaag tgggtgtatt
3' ARV#5 5'
 1321 catc

Figure 5. The ARV 138 S2 cDNA sequence and designed primers. The plus strand of the double stranded ARV 138 S2 cDNA sequence is shown (1324 nucleotides). Primers were designed to sequence the entire open reading frame of the S2 gene in both directions, as described in the Materials and Methods. Blue arrows represent primers whose sequences are identical to the bases shown, and read in the forward direction. Red arrow primer sequences are complementary to the bases shown and read in the opposite direction. Primer names are indicated and their sequences are oriented in the 5' to 3' direction.

strand buffer (250mM Tris-HCL pH8.3, 375mM KCl, 15mM MgCl₂), 0.1mg/ml (1μl of 10mg/ml) BSA, 1μM (1μl of 100μM) DTT and 160U (0.8μl of 200U/μl) Superscript enzyme (Gibco-BRL) were added to a final reaction volume of 100μL, and then incubated at 42°C for 1.5 hours.

2.9.4 Amplification of S2 gene and cDNA purification. The cDNA produced above was immediately amplified using the Expand™ Long Template PCR System with template PCR buffer I (Boehringer Mannheim). The cycling reaction was performed on a GeneAmp PCR system 9700 (PE Applied Biosystems; Foster City, CA) for 5 cycles (95°C for 1.5' to denature cDNA, 55°C for 1.5' to allow primers to anneal, and 70°C for 3'10" for elongation) and 31 cycles (92°C for 1.5' to denature, 55°C for 1.5' to anneal primers, and 70°C for 3'10" to elongate). The S2 cDNA product was resolved on a 0.9% agarose gel in 0.5x TBE buffer (4.5mM tris, 4.5mM boric acid, 0.9μM EDTA) that contained 0.004μg/ml ethidium bromide, excised from the gel, and the QIAquick™ gel extraction kit (Qiagen, Germany) was used to separate the cDNA from the agarose matrix.

2.9.5 Cycle sequencing. The ABI PRISM® BigDye™ terminator cycle sequencing ready reaction kit (Perkin Elmer {PE} Applied Biosystems; Foster City, CA) was used. Separate sequencing reactions were set up for each primer: 0.16μM ARV primer, 7.5-30ng of cDNA template (optimized reactions), 4.0μl BigDye™ terminator ready reaction mix, and deionized water to a final volume of 20μl. Cycle sequencing was performed on GeneAmp PCR system 9700 for 35 cycles of: 96°C for 30 seconds, 50°C for 30 seconds, and 60°C for 3 minutes 10 seconds. The products were double purified

by isopropanol precipitation, dried, and resuspended in 22 μ l template suppression reagent (ABI PRISM, Perkin Elmer) for 1 hour. The sample was then heated to 95°C for 2 minutes to denature the strands and the ABI PRISM 310 Genetic Analyzer (PE Applied Biosystems; Foster City, CA) was used to read the sequence for each reaction. Sequences were manually analyzed using Chromas version 1.45 (McCarthy, 1998) to ensure accuracy.

3. RESULTS

3.1 Generation and identification of avian reovirus (ARV) temperature sensitive (*ts*) mutants.

3.1.1 Generation of ARV *ts* mutants. Various concentrations of three chemical mutagens; bromodeoxyuridine, nitrosoguanidine, or proflavin were applied to ARV 138 and ARV 176 infections immediately after adsorption. The infections were incubated for 24 hours and then harvested. Cell lysates were analyzed for percent of virus survival by comparison of progeny titers to that of unmutagenized control infections. The optimal mutagen concentration to apply to maximize production of *ts* mutants results in a 1-10% survival of viral progeny (Pringle, 1996). Bromodeoxyuridine, a DNA mutagen (Boccardo *et al.*, 1986) had little effect on avian reovirus survival even at high concentrations of mutagen (Figure 6). Nitrosoguanidine and proflavin are known RNA mutagens and have been used in the chemical mutagenesis of mammalian reovirus (Ikegami and Gomatos, 1968; Fields and Joklik, 1969), rotavirus (Ramig, 1983), and influenza A virus (Simpson and Hirst, 1968). Avian reovirus survival was reduced in the presence of increased concentrations of nitrosoguanidine or proflavin (Figure 6). Conditions for maximum *ts* mutant production were met when 5-8 μ g/ml proflavin or 34 μ g/ml nitrosoguanidine were applied to infections (Figure 6). We chose to continue our analyses of nitrosoguanidine-treated samples because, in the case of mammalian reovirus *ts* mutants, there are fewer proflavin-generated mutants than nitrosoguanidine-generated mutants (Fields and Joklik, 1969). In addition, the best characterized proflavin-generated

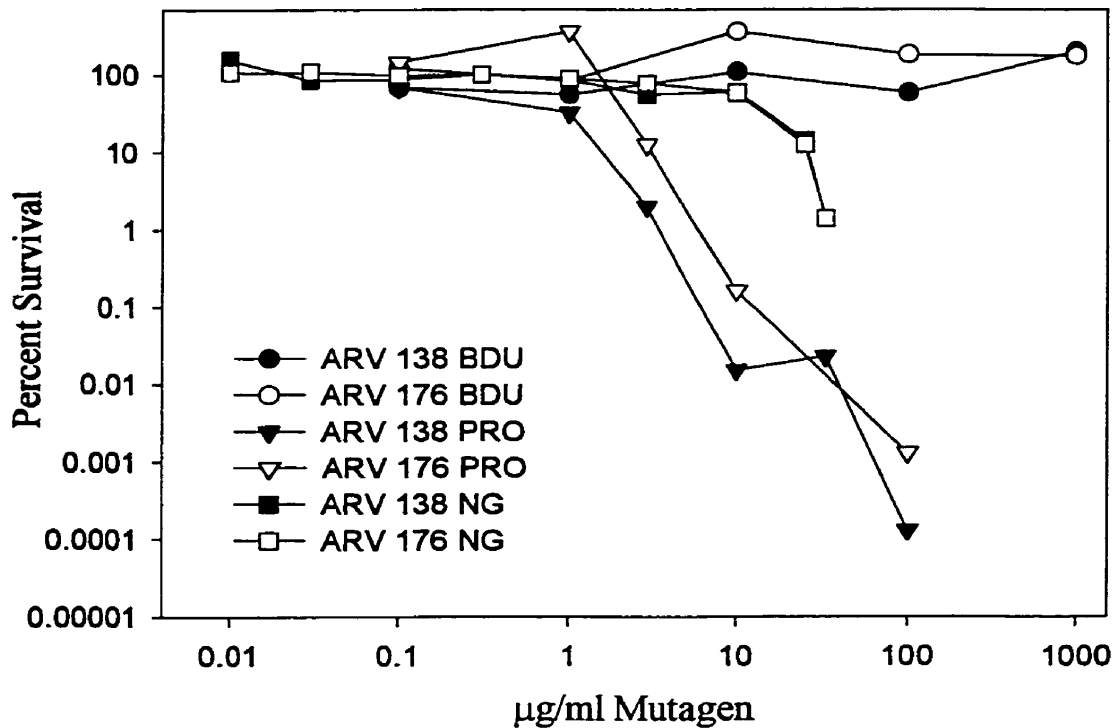


Figure 6: Survival curves of ARV 138 and ARV 176 after chemical mutagenesis. Various concentrations of 5-bromo-2'-deoxyuridine (BDU), proflavin (PRO), and N-methyl-N'-nitro-N-nitrosoguanidine (NG) were used to mutagenize ARV strain 138 and strain 176 infections as described in the Materials and Methods and percent survival determined. The mutagen concentration that maximizes production of *ts* mutants results in a 1-10% survival of progeny virions (Pringle, 1996). ARV 138 infections treated with 34µg/ml NG resulted in a 4% survival of progeny and were chosen for the isolation of *ts* mutants.

MRV *ts* mutants (*tsA201* and *tsA279*) appear to have multiple lesions and EOP values not significantly different than that of wild type (Hazelton and Coombs, 1995; 1999). Conversely, the best characterized nitrosoguanidine-generated MRV mutants (*tsC447* and *tsG453*) clearly have *ts* lesions in a single gene segment and very low EOP values (Coombs *et al.*, 1994; Shing and Coombs, 1996). This study focused on *ts* mutants derived from ARV strain 138 since little has been reported about this strain in comparison to ARV strain 176.

3.1.2 Identification of ARV *ts* mutants.

3.1.2.1. Isolation of ARV *ts* mutants and initial EOP screening. A total of 351 individual plaques that represented potential temperature-sensitive mutants were picked from a culture of ARV 138 infected in the presence of 34µg/ml nitrosoguanidine. Each clone was individually re-plaque purified (= double plaque purified) and then amplified through 2 passages as described in Materials and Methods. The classical efficiency of plating (EOP) assay was used to screen for temperature sensitivity, where viral titer at non-permissive temperature (39.5°C) was mathematically compared to the titer at permissive temperature (33.5°C) (described in Materials and Methods). It is generally accepted for mammalian reovirus and rotavirus that random variation of wild type virus EOP values is within $1.0 \pm \text{Log}_{10}$, whereas *ts* mutant EOP values fall below this lower limit of random variation. Non-*ts* parental virus ARV strain 138 was capable of efficient growth at both temperatures, having an EOP value of $5.16 \times 10^{-1} \pm 1.97 \times 10^{-1}$ standard deviations (sd) (Table 1). Eighty-one of the 351 clones were initially screened by the EOP assay and four stable *ts* mutants were identified. The ARV mutants *ts* 12, *ts*

Table 1**Efficiency of plating (EOP) values of isolated ARV 138 *ts* mutants**

<i>ts</i> Mutant	Efficiency of Plating (EOP) Value ^a	Standard Deviation ^b
<i>ts</i> 12	0.0000206	0.0000161
<i>ts</i> 31	0.00166	0.00172
<i>ts</i> 37	0.000425	0.000483
<i>ts</i> 46	0.0000183	0.0000198
<i>ts</i> 86	0.0108	0.00849
<i>ts</i> 108	0.00250	0.00220
<i>ts</i> 146	0.0000102	0.00000410
<i>ts</i> 158	0.0000144	0.0000134
<i>ts</i> 171	0.01450	0.0103
<i>ts</i> 188	0.0460	0.0194
<i>ts</i> 195	0.0000849	0.0000559
<i>ts</i> 205	0.00477	0.00581
<i>ts</i> 206	0.00135	0.00173
<i>ts</i> 207	0.00327	0.00282
<i>ts</i> 219	0.0000487	0.0000339
<i>ts</i> 247	0.0000940	0.0000916
<i>ts</i> 287	0.000551	0.000469
ARV 138	0.517	0.197

^aEOP values calculated as described in the Material and Methods, where:

$$\text{EOP} = \frac{\text{viral titer at non-permissive temperature}}{\text{viral titer at permissive temperature}}$$

^bStandard deviation (sd) values based on 3-5 trials for each of the *ts* mutants and 9 trials for unmutagenized ARV 138 (non-*ts* control).

31, *ts* 37, and *ts* 46 had EOP values of $2.06 \times 10^{-5} \pm 1.61 \times 10^{-5}$ sd, $1.66 \times 10^{-3} \pm 1.72 \times 10^{-3}$ sd, $4.25 \times 10^{-4} \pm 4.83 \times 10^{-4}$ sd, and $1.83 \times 10^{-5} \pm 1.98 \times 10^{-5}$ sd, respectively (Table 1).

3.1.2.2 Efficiency of lysis assay. To reduce the number of clones to be screened by the standard EOP method we created a new efficiency of lysis (EOL) technique to screen for temperature sensitivity. The four EOP-confirmed *ts* clones (*ts* 12, *ts* 31, *ts* 37, *ts* 46), and some EOP-confirmed non-*ts* clones (Clone 289, Clone 294) were used in the development of the EOL assay. Avian reovirus infections are ultimately lytic to the host cell (Duncan *et al.*, 1996). The EOL assay compares the virus' ability to lyse cells at permissive and non-permissive temperature. Consequently, *ts* mutations that affect any stage prior to release or cell lysis itself at restrictive temperature will be identified by this method. EOL resembles the EOP assay but is less precise as it relies on general cell lysis rather than individual plaque enumeration to measure temperature sensitivity. The EOL assay allowed simultaneous analysis of up to 8 different clones in each plate, using 11 serial 1:3.16 (equivalent to $\sqrt{10}$) dilutions in a 96-well plate as described in the Materials and Methods section 2.4.2. The EOL dilutions used covered a range similar to the EOP assay where 6 serial 1:10 dilutions are examined. EOL incubation times were optimized such that similar amounts of cell lysis were found in comparable dilutions of the unmutagenized ARV 138 parent and the various non-*ts* clones at both 33.5°C and 39.5°C (Figure 7). In contrast, cell lysis by the confirmed *ts* clones was found in much lower dilutions at non-permissive temperature than at the permissive temperature. For example, a 1:316-560 dilution of unmutagenized ARV 138

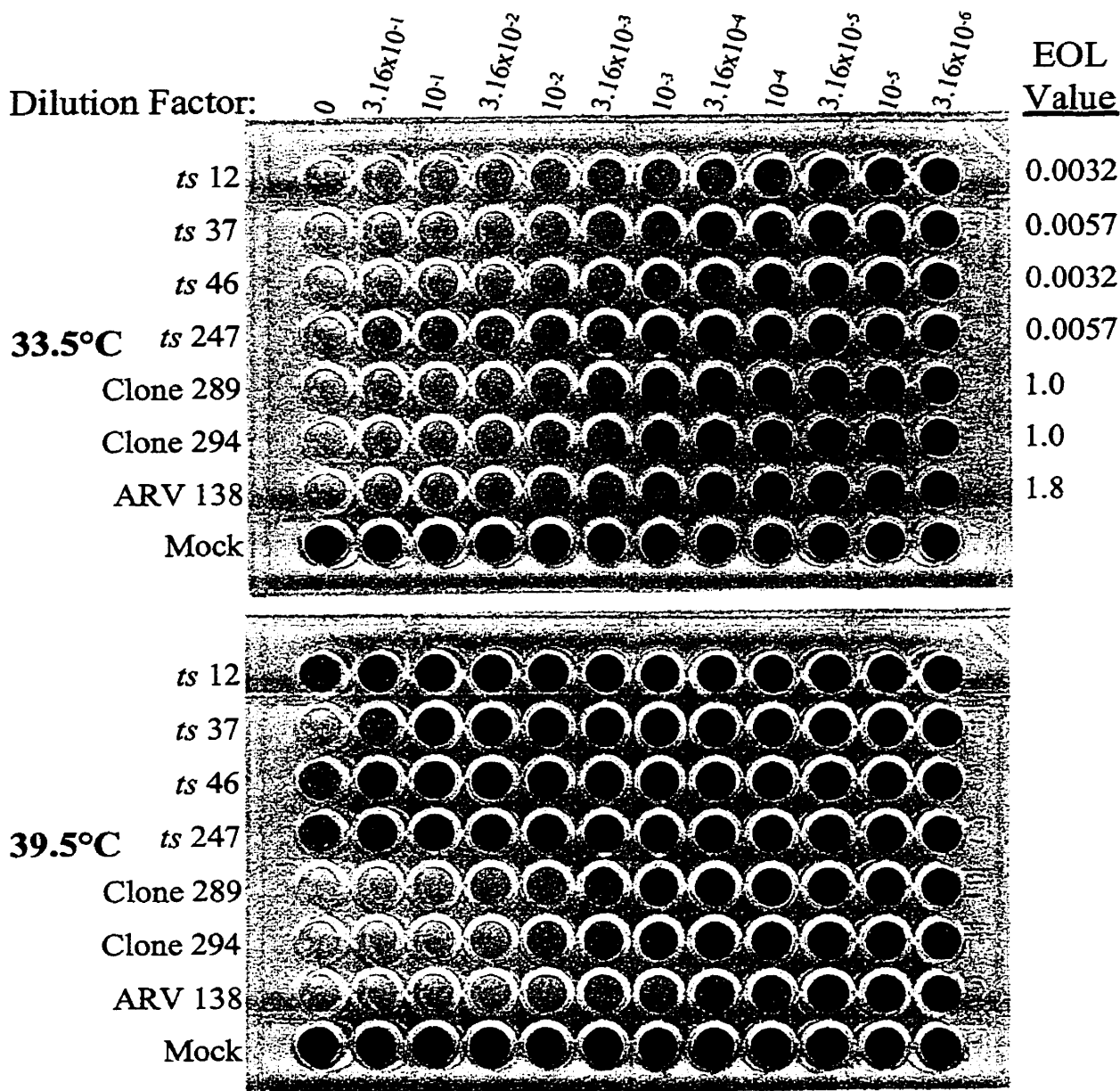


Figure 7: Efficiency of lysis (EOL) plates at permissive and restrictive temperatures. Duplicate 96 well plates of QM5 cells were infected with serial dilutions (indicated above the wells) of various virus clones, incubated at 33.5°C and 39.5°C for 5 and 4 days respectively, fixed, and stained as detailed in Materials and Methods. Lightly colored wells represent areas of cell lysis, while those with stain have intact cell monolayers. The temperature sensitive mutants are *ts* 12, *ts* 37, *ts* 46, and *ts* 247. Clone 289 and clone 294 are chemically mutagenized ARV138 progeny isolated as described in Material and Methods, but which, upon examination by EOL and EOP, were identified as non-*ts*. Mock represents uninfected cells.

resulted in cell lysis at both 39.5°C and 33.5°C, respectively. The ARV 138 EOL ratio of 560/316 (the non-permissive dilution value divided by the permissive dilution value) is 1.78 (Figure 7). Conversely, a 1:316 dilution of *ts* 12 was capable of cell lysis at the permissive temperature while undiluted *ts* 12 stocks were not capable of host cell lysis at non-permissive temperature. Thus, the EOL ratio for *ts* 12 is 1/316 or 0.0032 (Figure 7). Therefore, clones with reduced levels of cell lysis at 39.5°C in comparison to 33.5°C, and whose EOL ratio was less than the EOL ratio of unmutagenized ARV 138 or confirmed non-*ts* clones are considered potentially temperature sensitive.

Application of the new EOL assay to the remaining 271 picked clones indicated that 219 (81%) of the clones could be classified as non-*ts*. The other 52 clones identified as potentially *ts* by the EOL assay, as well as randomly chosen clones identified as non-*ts*, were then examined by the EOP assay. All tested clones that were non-*ts* by EOL were confirmed as non-*ts* by the more accurate EOP assay, while 13 (25%) of the clones identified as *ts* by EOL were also temperature-sensitive by EOP. The efficiency of lysis screening assay consistently identified temperature sensitive negative clones but overestimated the presence of temperature sensitive clones according to the EOP assay. The EOL assay is highly sensitive in the identification of *ts* clones and has negligible false negative rate; however, it is less accurate than the EOP assay due to its high false positive rate. Thus, the novel efficiency of lysis assay is useful to initially screen for temperature sensitivity and the combined EOL/EOP approach serves to rapidly and accurately identify *ts* clones. Seventeen clones representing stable ARV 138 *ts* mutants were confirmed by the combined EOL/EOP approach and had EOP values significantly less than that of unmutagenized ARV 138 (Table 1).

3.2 Genetic recombination analysis of the panel of ARV *ts* mutants.

The segmented nature of the reovirus, rotavirus, and avian reovirus genome permits recombination through random assortment of individual gene segments during mixed infection, rather than the classical means of strand breakage and rejoining (Coombs, 1998; Fields and Joklik, 1969; Ramig, 1982). This property has been exploited in other members of the *Reoviridae* (mammalian reovirus and rotavirus) by screening for the generation of ts^+ progeny from *ts* mutant mixed infections to genetically group *ts* mutants (Coombs, 1998; Fields and Joklik, 1969; Ramig, 1982; 1983). Pair-wise mixed infections (AxA, BxB, AxB where A and B represent two different *ts* mutant clones) of ARV *ts* mutants were performed as described in the Materials and Methods section 2.5. The viral progeny titers (A, B, and AB) were examined by various formulae to organize the mutants into genetic recombination groups.

3.2.1 Recombination analysis: standard *Reoviridae* recombination formula.

The standard *Reoviridae* recombination formula (Materials and Methods section 2.5.1) calculates the percentage of viral progeny capable of growth at non-permissive temperature and accounts for background levels of replication of the two parental clones at 39.5°C. Recombination values of <0%, <0.1%, or <0.2% are reported to indicate the parental *ts* mutations lie on the same gene segments (belong to the same recombination group), whereas values >1%, >2%, or >3% suggest the *ts* mutations exist on different gene segments (belong to different recombination groups) (Coombs, 1998; Fields and Joklik, 1969; Ramig, 1982).

The newly generated ARV *ts* mutants were analyzed by this formula, and most of the mutants examined could be placed in genetic recombination groups. For example, when clone *tsD46* was crossed with *tsD195*, and *tsD219*, the average recombination values obtained from 3 experiments was -0.001, and 0 respectively (Table 2, upper value in corresponding cells), indicating lack of recombination and suggesting the 3 viruses have *ts* lesions in the same gene segment. Conversely, crosses between *tsD46* and each of the other *ts* clones generated recombination values that ranged from 1.7 (*tsD46* X *tsA146*) to 10 (*tsD46* X *tsF206*). These values indicated recombination had occurred and suggested each of these clones have their *ts* lesions in a different gene segment than *tsD46*.

The organization of some ARV 138 *ts* mutants by the standard recombination formula was unclear since the recombination values generated were in the range between the generally accepted limits (Table 2). For example, crosses between *tsB31* and *tsD195* generated an average value of 0.3 (Table 2). This value has been perceived as not representing recombination in some studies (Ramig, 1982). In MRV *ts* mutant studies similar problems have been observed. For example, a cross involving *tsI138* (*ts* mutation in L3; Hazelton and Coombs, unpublished; Ramig *et al.*, 1983) and *tsG453* (*ts* mutation in S4; Mustoe *et al.*, 1978; Shing and Coombs, 1996) resulted in recombination values as low as 0.1 in some cases, and indicated a lack of recombination (Coombs, unpublished). The rationale for ambiguous recombination values is not understood. *ts* mutants that are only mildly temperature sensitive (high EOP values) may interfere with detection of *ts*⁺ reassortant progeny by the standard formula. Alternatively, viral interference has been suggested to prevent production and/or growth of *ts*⁺ reassortants (Chakraborty *et al.*,

Table 2
Organization of ARV 138 *ts* mutants into recombination groups.

Group	Clone	EOL ^a	EOP ^b	Recombination Value ^c						
				A(<i>ts</i> 12)	B(<i>ts</i> 31)	C(<i>ts</i> 37)	D(<i>ts</i> 46)	E(<i>ts</i> 158)	F(<i>ts</i> 206)	G(<i>ts</i> 247)
A	<i>ts</i> 12	0.043	0.000021	-0.001 ^d (0.5) ^e 1.0 ^f	4.9 (89) 263	5.0 (72) 453	3.1 (2710) 2347	2.5 (800) 807	4.5 (20) 22	8.6 (3621) 5676
	<i>ts</i> 146	0.0056	0.000010	-0.002 (0.1) 0.2	1.0 (14.2) 38	1.8 (13.1) 3338	1.7 (880) 1018	1.3 (406) 445	5.0 (14.5) 25	8.1 (3078) 4645
B	<i>ts</i> 31	0.0056	0.0017	4.9 (89) 263	-0.06 (0.5) 1.0	2.5 (13) 142	2.2 (18) 92	2.6 (21) 74	6.3 (12) 26	8.9 (25) 194
	<i>ts</i> 37	0.0056	0.00043	5.0 (72) 453	2.5 (13) 142	-0.1 (0.5) 1.0	3.1 (76) 224	2.6 (11) 107	10.8 (31) 42	8.8 (20) 202
C	<i>ts</i> 287	0.18	0.00055	6.0 (72) 160	12.2 (37) 147	0.2 (1.9) 4.4	7.7 (102) 196	4.2 (14) 110	7.0 (20) 29	9.6 (50) 250
	<i>ts</i> 46	0.0032	0.000018	3.1 (2710) 2347	2.2 (18) 92	3.1 (76) 224	-0.004 (0.5) 1.0	2.0 (3365) 602	10.0 (17) 49	8.7 (1038) 3210
D	<i>ts</i> 195	0.10	0.000085	1.0 (304) 343	0.3 (62) 68	1.8 (552) 545	-0.001 (0.3) 0.3	0.9 (34) 374	6.0 (1.7) 83	6.0 670
	<i>ts</i> 219	0.10	0.000049	7.9 (3800) 3752	19.1 (68) 399	15.4 (50) 339	0 (1.0) 1.9	3.8 (703) 787	11.1 (21) 53	6.4 (1093) 2026
E	<i>ts</i> 158	0.18	0.000014	2.5 (800) 807	2.6 (21) 74	2.6 (11) 107	2.0 (3365) 602	0.002 (0.5) 1.0	6.3 (9.6) 29	4.1 (621) 965
F	<i>ts</i> 206	0.10	0.0013	4.5 (20) 22	6.3 (12) 26	10.8 (31) 42	10.0 (17) 49	6.3 (9.6) 29	-0.4 (0.5) 1.0	9.6 (15) 47
G	<i>ts</i> 247	0.10	0.000094	8.6 (3621) 5676	8.9 (25) 194	8.8 (20) 202	8.7 (1038) 3210	4.1 (621) 965	9.6 (15) 47	-0.003 (0.5) 1.0
ARV138		8.71	0.52							

^a Efficiency of lysis values determined as described in Materials and Methods, using the formula:

$$\text{EOL value} = \frac{\text{ID}_{\text{NP}}}{\text{ID}_{\text{P}}}$$

TsA12 and ARV 138 (unmutagenized control) EOL values represent averages of five trials, all others are single screening trials.

^b Efficiency of plating values as described in the Materials and Methods.

^c Identified prototype *ts* mutants of recombination groups A-G.

^d Recombination values calculated using the classic formula $\frac{(\text{AB})_{\text{NP}} - (\text{A+B})_{\text{NP}}}{(\text{AB})_{\text{P}}} \times 100$ (Fields, 1969; Ramig, 1982; Ramig, 1983; Coombs, 1998). Here A and B are the two infecting *ts* parents, and AB are the resulting progeny. NP represents the titer of the virus at non-permissive temperature and P is the titer at permissive temperature. Values represent averages of at least three trials.

^e In parentheses, recombination index values calculated as described in the Materials and Methods, where

$$\text{RI} = \frac{(\text{AB})_{\text{NP}}}{(\text{A+B})_{\text{NP}}} \quad (\text{Greenberg } et al., 1981)$$

Values represent the averages of three trials.

^f In italics and bold, EOP recombination values calculated using a novel recombination formula as described in Materials and Methods where the progeny (AB) EOP value is compared to that of the average EOP of the two parental *ts* mutant (A, B) EOP values. Values represent averages of at least three trials.

$$\text{EOP Recombination Value} = \frac{\text{EOP}_{\text{AB}}}{0.5(\text{EOP}_{\text{A}} + \text{EOP}_{\text{B}})}$$

1979; Rozinov and Fields, 1994). If the number of ts^+ progeny produced from the mixed infection is only minor (but greater than that produced by parental viruses) compared to the total ts progeny population, these ambiguous low recombination values may be obtained.

3.2.2 Recombination analysis: recombination index (RI) formula. An alternative formula, denoted the recombination index, has been used to assess recombination in ts mutants of bovine rotavirus, a member of the family *Reoviridae* (Greenberg *et al.*, 1981). This formula was used to confirm ARV ts mutant recombination groups assigned by the standard *Reoviridae* recombination formula and to clarify ambiguous standard recombination values. The recombination index mathematically compares the progeny titer (AB) to the sum of the parental titers (A+B) at non-permissive temperature as described in the Materials and Methods (section 2.5.2). RI values greater than 5.0 suggest recombination has occurred and the mutants belong to different recombination groups (Greenberg *et al.*, 1981).

ARV data was analyzed by the RI formula to confirm the genetic organization of mutants assigned by the standard recombination formula. In most cases, RI analysis confirmed the classic *Reoviridae* recombination formula groups. For example, in the cross involving $tsA12$ and $tsA146$ the RI value of 0.1 (Table 2; middle value in corresponding cells) indicated the mutants belong to the same recombination group (standard recombination formula value = -0.002; Table 2). Conversely, when $tsA12$ was crossed with $tsB31$ the RI value of 89.2 suggested the mutants belong to different recombination groups (standard recombination formula value = 4.9; Table 2). The RI index approach clarified some ambiguous standard *Reoviridae* recombination values that

fell between the defined limits. For example, mixed infections of *tsB31* x *tsD195* and *tsE158* x *tsD195* have standard recombination values of 0.3 and 0.9, respectively; whereas RI values of 62 and 34, respectively, clearly assign these mutants to different recombination groups (Table 2).

In some cases, the standard *Reoviridae* recombination formula and recombination index values were inconsistent. For example, *ts86* failed to recombine with *tsD46* and *tsF206* with RI values of 1.1 and 1.4, respectively (Table 3, middle value in corresponding cells). Standard recombination formula analysis of *ts86* indicated a lack of recombination with *tsD46*, *tsE158*, *tsF206* and *tsG247* based on recombination values of -0.001, -0.01, -17.3, and -6.8, respectively (Table 3, upper value in corresponding cells). Despite the discrepancy, both formulas applied suggested an absence of recombination between *ts86* x *tsF206* and *ts86* x *tsD46*, and confirmed the presence of mutations in the same gene segments. Analysis of *tsD195* and *tsF206* mixed infections by the standard recombination and RI formula suggested opposing genetic organization. The standard value of 6.0 (Table 2) indicated mutations resided on different gene segments, while the RI value of 1.7 (Table 2) suggested recombination had not occurred and *ts* lesions were present within the same gene segment. To determine which formula correctly measures recombination in crosses that presented inconsistent results, a third recombination formula was developed.

3.2.3 Recombination analysis: novel EOP recombination formula.

A novel EOP-based recombination formula was created to address the inadequacies of the standard *Reoviridae* and recombination index formulas and to attempt to more clearly determine ARV *ts* mutant genetic recombination groups. This formula

Table 3
ARV 138 *ts* mutants that cannot be placed into defined groups

Group	Clone	EOL ^b	EOP ^c	Recombination Value						
				A(<i>ts</i> 12)	B(<i>ts</i> 31)	C(<i>ts</i> 37)	D(<i>ts</i> 46)	E(<i>ts</i> 158)	F(<i>ts</i> 206)	G(<i>ts</i> 247)
X ^a	<i>ts</i> 86	0.0056	0.011	0.2 ^d	0.3	0.9	-0.001	-0.01	-17.3	-6.8
				(16) ^e	(14)	(47)	(1.1)	(8.9)	(1.4)	(49)
				32^f	41	130	0.2	20	11.0	5.1
	<i>ts</i> 108	0.0178	0.0025	0.4	0.1	0.6	0.9	-0.1	nd ^g	nd
				(3.7)	(2.3)	(14)	(8.1)	(0.3)	nd	nd
				9.9	4.7	12.9	20.6	0.9	nd	nd
	<i>ts</i> 171	0.178	0.015	-0.1	-0.8	1.1	-0.2	0	nd	nd
				(0.6)	(0.06)	(3.1)	(0.4)	(1.1)	nd	nd
				1.2	0.3	11.2	1.0	3.0	nd	nd
	<i>ts</i> 188	0.10	0.046	-15.5	-9.7	-10.3	-8.0	-7.6	nd	nd
				(0.009)	(0.03)	(0.1)	(0.01)	(0.3)	nd	nd
				0.06	0.1	0.4	0.04	0.3	nd	nd
	<i>ts</i> 205	0.18	0.0048	6.4	5.7	8.5	7.8	3.5	-1.9	-7.1
				(2.8)	(2.2)	(2.8)	(2.3)	(0.3)	(0.8)	(0.4)
				2.4	2.5	3.2	3.3	0.8	1.6	0.9
	<i>ts</i> 207	0.056	0.0033	0	-2.9	2.9	0.3	3.6	-0.7	1.0
				(1.0)	(0.4)	(2.3)	(1.1)	(0.6)	(0.9)	(1.2)
				0.9	0.6	1.8	1.4	1.3	1.4	2.0
ARV138		8.71	0.52							

^a Temperature sensitive mutants that were found to fall into more than one recombination group. This indicates that more than one gene segment has *ts* lesions.

^b Efficiency of lysis values determined as described in Materials and Methods, using the formula:

$$\text{EOL value} = \frac{\text{ID}_{\text{NP}}}{\text{ID}_{\text{P}}}$$

tsA12 and ARV 138 (unmutagenized control) EOL values represent averages of five trials, all others are single screening trials.

^c Efficiency of plating values as described in the Materials and Methods.

^d Recombination values calculated using the classic formula $\frac{(\text{AB})_{\text{NP}} - (\text{A+B})_{\text{NP}}}{(\text{AB})_{\text{P}}} \times 100$ (Fields, 1969; Ramig, 1982; Ramig, 1983; Coombs, 1998). Here A and B are the two infecting *ts* parents, and AB are the resulting progeny. NP represents the titer of the virus at non-permissive temperature and P is the titer at permissive temperature. Values represent averages of at least three trials.

^e In parentheses, recombination index values calculated as described in the Materials and Methods, where

$$\text{RI} = \frac{(\text{AB})_{\text{NP}}}{(\text{A+B})_{\text{NP}}} \quad (\text{Greenberg } et al., 1981)$$

Values represent the averages of three trials.

^f In italics and bold, EOP recombination values calculated using a novel recombination formula as described in Materials and Methods where the progeny (AB) EOP value is compared to that of the average EOP of the two parental *ts* mutant (A, B) EOP values. Values represent averages of at least three trials.

$$\text{EOP Recombination Value} = \frac{\text{EOP}_{\text{AB}}}{0.5(\text{EOP}_{\text{A}} + \text{EOP}_{\text{B}})}$$

^g nd; not determined.

compares the temperature sensitivity of the progeny, as defined by their collective EOP value, to that of the average temperature sensitivity of the two *ts* parents involved in the cross. It has been generally accepted that the random variation of wild type virus EOP values is within $1 \pm \text{Log}_{10}$. *Ts* mutants, defined as having EOP values more than an order of magnitude lower than the wild type virus EOP value, can fluctuate randomly within similar limits ($\pm \text{Log}_{10}$). Thus, progeny EOP values that are $\frac{1}{2}$ -1 order of magnitude greater than parental *ts* mutant EOP values would signify wild type (ts^+) reassortants were produced and the parental mutants belong to different recombination groups. Progeny EOP values that fall within the range of random variation of the parental mutant EOP values (within a magnitude of 5) would indicate all progeny are *ts* and the *ts* parents belong to the same recombination group.

ARV *ts* mutants analyzed by this novel formula were clearly sorted into genetic groups. For example, by this new formula, the average EOP recombination value from 3 experiments that involved clones *tsA12* and *tsA146* was 0.2 (Table 2, italicized bold faced lower value in each cell). This value suggested non-*ts* reassortants were not produced and the parental *ts* lesions are within the same gene segment. Conversely, crosses between *tsA12* and all other *ts* clones generated EOP recombination values that ranged from 22 (*tsA12* X *tsF206*) to 5676 (*tsA12* X *tsG247*) (Table 2). These values indicated ts^+ reassortants were produced and that these *ts* clones have their *ts* lesions in different gene segments than *tsA12*. The EOP recombination formula accentuated the differences between recombination groups and clarified the ambiguous results of the standard recombination formula. For example, in the cross involving *tsB31* and *tsD195*, where the classical recombination formula had failed to definitively group these mutants,

the average novel EOP recombination value was 68 (Table 3), clearly placing the mutants into separate recombination groups.

In some cases the novel EOP recombination formula, standard recombination formula, and RI formula results were inconsistent with each other. For example, in the crosses involving *ts86* and *tsD46*, *tsE158*, *tsF206*, *tsG247* the novel EOP recombination formula values of 0.2, 20, 11.0, and 5.1 respectively (Table 3, lower value in corresponding cells) suggested *ts86* fails to recombine only with *tsD46*. The standard recombination formula values of -0.001, -0.01, -17.3, -6.8 (Table 3) suggest that *ts86* is incapable of recombination with each of these mutants, whereas the RI values suggest *ts86* fails to recombine with *tsD46* (RI value = 1.1) and *tsF206* (RI value = 1.4) (Table 3). *ts86* has a mildly temperature sensitive phenotype (EOP value of 0.011, Table 1) and may account for the discrepancy between the recombination results. Two of three recombination formulas applied (standard and RI formula) suggest *ts86* fails to recombine with both *tsD46* and *tsD206*, and confirms the presence of multiple gene segments with *ts* mutations in *ts86*. The average novel EOP recombination value for mixed infections of *tsD195* and *tsF206* was 83 (Table 2), and indicated recombination had occurred between these two clones. This supports standard recombination formula conclusion (recombination value of 6.0; Table 2), and led to the organization of *tsD195* and *tsF206* into separate recombination groups (Table 2).

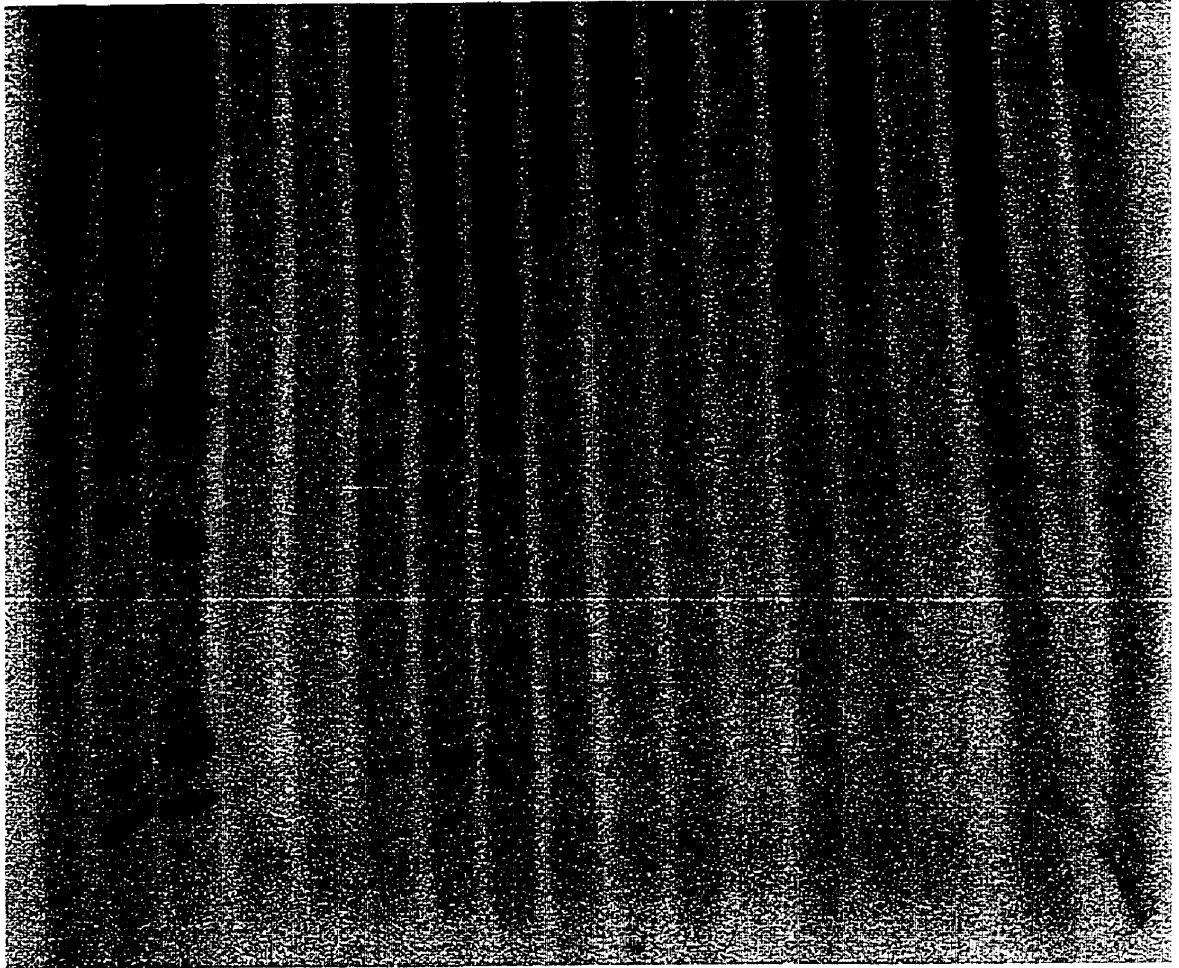
3.2.4. Organization of ARV *ts* mutants into recombination groups. The data was analyzed with the above mentioned formulae and those groups that were confirmed by at least two formulae were considered significant. In most cases, the novel EOP recombination formula organization of mutants was similar to the recombination index

group assignments, but superior to the standard recombination analysis as ambiguities were eliminated. The novel formula measures changes in progeny temperature sensitivity to detect *ts*⁺ clones, thus represents a more powerful evaluation of recombination than RI analysis which focuses only on non-permissive titers. A total of seven recombination groups were clearly identified indicating each had their *ts* mutations in different genes and that 7 of the 10 ARV 138 dsRNA gene segments have representative temperature sensitive mutations. Prototype *ts* mutants were chosen (arbitrarily assigned for those recombination groups that contain more than one clone): *tsA12*, *tsB31*, *tsC37*, *tsD46*, *tsE158*, *tsF206*, *tsG247*. Six *ts* mutants (*ts86*, *ts108*, *ts171*, *ts188*, *ts205*, *ts207*) failed to recombine with numerous mutants in more than one recombination group and suggested that they have multiple gene segments with *ts* lesions (Table 3).

3.3 Total dsRNA synthesis of ARV *ts* mutants. To phenotypically characterize the isolated ARV *ts* mutants, the total dsRNA produced from one cycle of replication was measured at both permissive and non-permissive temperatures. The ability to produce the viral dsRNA genome has been used to characterize mammalian reovirus (Cross and Fields, 1972) and rotavirus *ts* mutants (Chen *et al.*, 1990), where mutants are placed in one of two groups: mutants capable of dsRNA synthesis (+), and those that are not (-). This localizes the effects of the *ts* lesion to a certain stage within the viral lifecycle; either prior to or during replication or at the genome packaging step (dsRNA (-) mutants), or at the later stage of capsid assembly and virus release (dsRNA (+) mutants). Characterization of genome synthesis in the ARV *ts* mutants serves as a preliminary analysis of the biological implications of the *ts* lesions.

The total dsRNA produced from infections incubated at non-permissive and permissive temperature was isolated as described in the Materials and Methods, and served as the criteria for assignment of *ts* mutants to one of two dsRNA groups. The *ts* mutant dsRNA profiles at 33.5°C were similar to that of the controls (ARV 138 and ARV 176). To phenotypically characterize the *ts* lesion, changes in dsRNA expression at 39.5°C were scored. Those mutants capable of dsRNA synthesis at 39.5°C, *ts*B31, *ts*C37, *ts*C287, were labeled dsRNA (+), whereas all other mutants failed to synthesize dsRNA at 39.5°C and were identified as dsRNA (-) (Figure 8). The multifunctional nature of viral proteins allows different mutations to disrupt alternate protein functions. Thus, *ts* lesions within mutants that belong to the same recombination group reside in the same protein but may result in different viral phenotypes. In our analysis of dsRNA production by the ARV *ts* clones, all mutants that belong to the same recombination group were phenotypically similar with respect to genome synthesis (recombination group A, D members: dsRNA (-); group C members: dsRNA (+)) (Figure 8). This indicates similar protein functions may be targeted by the individual *ts* lesions within each recombination group. Some *ts* mutants identified to have multiple mutated gene segments by recombination analysis (*ts*86, *ts*108, *ts*205, *ts*207) were examined for total dsRNA production. *ts*86 and *ts*108 were dsRNA (-) and unable to synthesize or package their viral genomes, while *ts*205 and *ts*207 were capable of dsRNA synthesis (dsRNA(+)) as their *ts* lesions may affect later stages of the viral lifecycle (Figure 8). Due to complications in interpretation of gene and protein function relationships, *ts* mutants that have multiple gene segments with *ts* lesions were not examined further in our study. In all cases, the incorporation of ³²P radioactive label into wild type virus (ARV 138 and ARV 176) dsRNA was greater than that of the

Mock
ARV 138
ARV 176
tsA12
tsA146
tsB37
tsC37
tsC287
tsD46
tsD195
tsD219
tsE158
tsF206
tsG247
ts 86
ts 108
ts 205
ts 207



+ + - - + + + - - - - - - - - + +

Figure 8: Total dsRNA production at non-permissive temperature. Cells infected with unmutagenized ARV 138, unmutagenized ARV 176, ARV 138 *ts* mutants, or mock infected were incubated at non-permissive and permissive temperature for 18 and 24 hour PI, respectively, as described in Materials and Methods. The *ts* mutant dsRNA profiles at permissive temperature were similar to wild type virus and are not shown. This figure represents the ³²P-labeled dsRNA profiles as resolved in 12.5% SDS-polyacrylamide gel and visualized by phosphor-imaging. The ability of each clone to synthesize (+) dsRNA at 39.5°C, or not (-), is scored at the bottom of the gel.

dsRNA (+) *ts* mutants (*tsB31*, *tsC37*, *tsC287*, *ts205*, *ts207*) (Figure 8), and may be attributed to non-*ts* mutations in the mutant clones that confer a poor growth phenotype at both permissive and non-permissive temperatures. Attempts to measure dsRNA production by phosphor-image analysis was only partially successful due to differences in background levels between lanes, where dsRNA (-) and (+) mutants represented approximately 10%, and greater than 25% of the ARV 138 values at 39.5°C, respectively (data not shown). Visual inspection of the dsRNA (-) mutants suggests the phosphor-image measured values overestimate dsRNA synthesis. However, a low level of viral genome synthesis (typically <0.1% for mammalian reovirus dsRNA (-) *ts* mutants; Coombs, 1998) may be identified at restrictive temperature in dsRNA deficient mutants since the *ts* mutation fails to completely inhibit viral growth, also demonstrated by the few viral plaques identified at 39.5°C in EOP analyses. Despite the sub-optimal quantitative analysis, visual examination of mutant dsRNA profiles allowed obvious classification into dsRNA (+) and dsRNA (-) categories and could be duplicated in repeat experiments.

3.4 Efficiency of plating profile of ARV *ts* mutants. To better characterize the *ts* mutants in recombination groups A-G, an efficiency of plating profile for each clone was examined over a series of non-permissive temperatures (Figure 9). Clones *tsA12*, *tsD195* and *tsD219* expressed temperature sensitivity at a non-permissive temperature of 37°C while clones *tsD46* and *tsD158* required a temperature of 38°C to show temperature sensitivity. Clones *tsA146*, *tsB31*, *tsC37*, *tsC287*, *tsF206*, and *tsG247* demonstrated the *ts* phenotype only at restrictive temperatures in excess of 38°C. The EOP profiles of

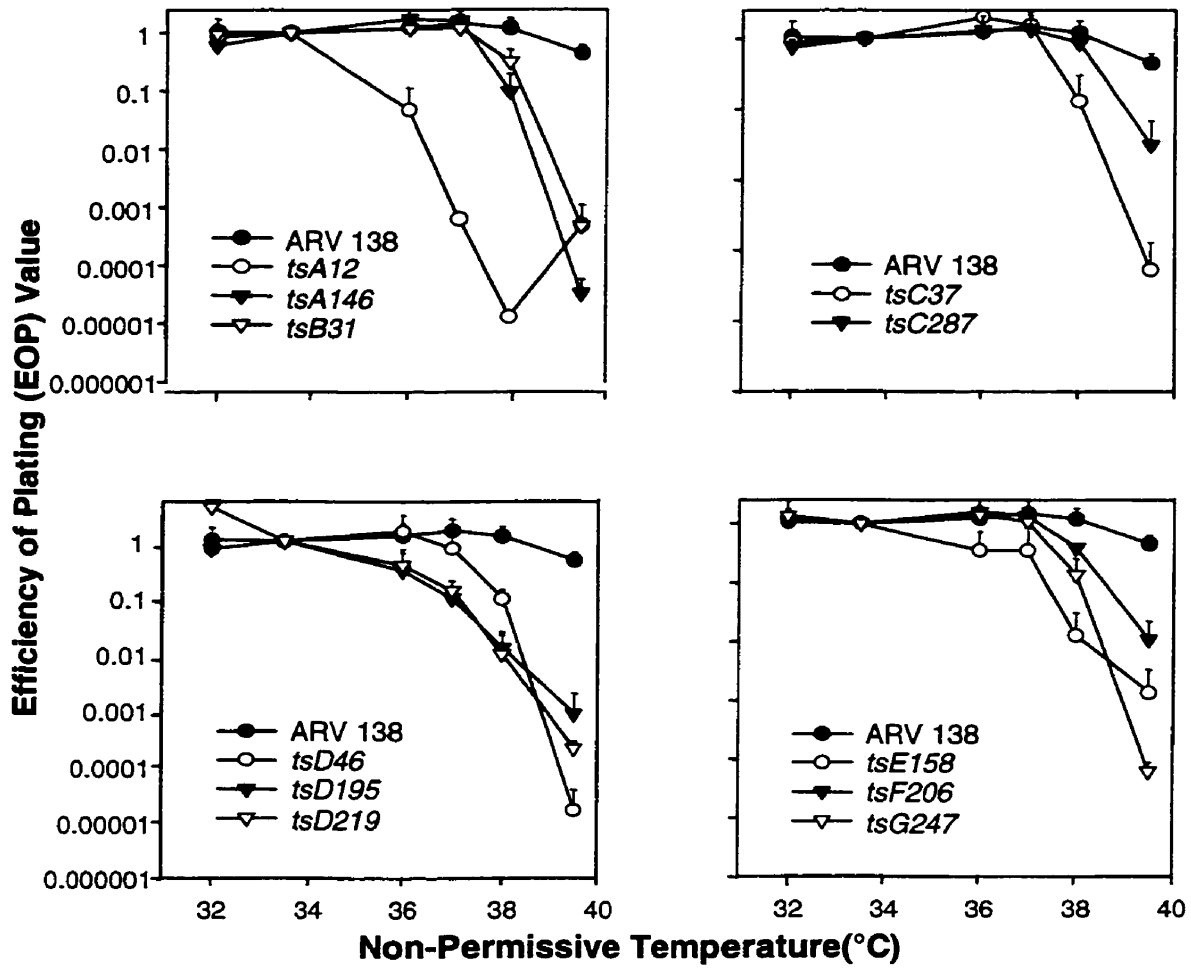


Figure 9: Efficiency of plating profiles for *ts* mutants that belong to recombination groups A-G. In each graph ARV138 represents unmutagenized wild type virus. Efficiency of plating values were calculated as described in Materials and Methods with a permissive temperature of 33.5°C and indicated non-permissive temperatures. Error bars represent standard deviations. Recombination group A: *tsA12* (prototype), *tsA146*. Recombination group B: *tsB31* (prototype). Recombination group C: *tsC37* (prototype), *tsC287*. Recombination group D: *tsD46* (prototype), *tsD195*, *tsD219*. Recombination groups E, F, and G: *tsE158* (prototype), *tsF206* (prototype), *tsG247* (prototype).

individual mutants in recombination groups that contain more than one member (groups A, C, and D) were unique and suggested that the different mutants in each group represent different viral isolates. The majority of mutants showed a continual decline in EOP values with increased temperatures. However, *tsA12* had an increase in its EOP value at 39.5°C compared to 38°C. This increase is insignificant as the mutant remained within the limits of temperature sensitivity and may be attributed to over-estimated 39.5°C titers due to the decreased host cell viability at more extreme temperatures.

3.5 Reassortant mapping of selected ARV *ts* mutant clones.

3.5.1 Reassortant mapping of *tsA12*. To determine the gene segment that harbored the *ts* lesion in recombination group A mutants, reassortant mapping of prototype *tsA12* was performed. A total of 244 progeny clones were picked from a mixed infection of *tsA12* and unmutagenized ARV 176 as described in the Materials and Methods. Reassortants were generated with a 9% efficiency as twenty-two clones were identified with hybrid electropherotypes. When reassortants were examined for temperature sensitivity by the EOP assay, those clones that retained a *ts* phenotype were organized into one panel, while non-*ts* clones were placed into a separate panel. Virtually all identified *ts* clones had their S2 gene segments derived from the *tsA12* parent, whereas the non-*ts* reassortants contained S2 gene segments from the ARV 176 parent (Table 4). The other 9 gene segments were randomly associated with the temperature sensitive phenotype. This indicates the *tsA12* mutation resides within the S2 gene segment. The recombination group data (Table 2) suggests the temperature sensitive

mutation of *tsA146* may also reside in the S2 gene segment; however, reassortment mapping is needed to confirm the location of the *tsA146* mutation.

Analysis of reassortant 125 (R125) genotype by SDS-PAGE suggested an apparent lack of the S1 gene segment (Table 4). A deletion within the S1 gene segment may have occurred and resulted in a smaller dsRNA segment that was lost under our electrophoresis conditions. Truncated ARV S1 gene segments that retain essential coding information have been reported and are replicated to high amounts relative to full length S1 (Ni *et al.*, 1994). The large population of sub-genomic segments out competes the wild type segment during packaging (Ni *et al.*, 1994), and may explain the absence of full length S1 in R125.

Three reassortants (R186, R220, and R222) exhibited anomalous S2 and S3 gene segment migration patterns by SDS-PAGE. The migration of S2 and S3 was slightly retarded compared to *tsA12* and ARV 176 parental genes and prevented identification of gene segment origin in these clones (Table 4). Spontaneous mutations, inherent within RNA viruses, result from the lack of proof-reading ability in the RNA dependent RNA polymerase. Thus, point mutations (single base changes) occur frequently at non-conserved regions and are important in the evolution of RNA viruses. Mutations that increase viral "fitness" or do not disrupt protein function will be retained throughout subsequent passages. Nucleic acid bases have unique molecular weights (MW) and a series of base changes within a gene segment may be detected by SDS-PAGE due its altered MW. For example, MRV S2 gene segments of serotypes T1L, T2J, and T3D are identical in length (1331 nucleotides), and have 72% sequence identity (Dermody *et al.*, 1991) with base counts of 327A, 294C, 335G, 375U for T1L (George *et al.*, 1987) and

Table 4
Reassortant mapping of tsA12

| Clone | Electropherotype | | | | | | | | | | EOP ^b | Standard Deviation ^c |
|--------------------------|------------------|----|----|----|----|----|----|------------------|-----|----|------------------|---------------------------------|
| | L1 | L2 | L3 | M1 | M2 | M3 | S1 | S2 | S3 | S4 | | |
| <u>Cross^a</u> | | | | | | | | | | | | |
| tsA12 | 3 | 3 | 3 | 3 | 3 | 3 | 3 | 3 | 3 | 3 | 0.0000206 | 0.0000161 |
| ARV 176 | 7 | 7 | 7 | 7 | 7 | 7 | 7 | 7 | 7 | 7 | 0.936 | 0.207 |
| <u>Reassortant</u> | | | | | | | | | | | | |
| 125 | 3 | 3 | 7 | 3 | 3 | 7 | X | 3 | 7 | 7 | 0.00000639 | 0.00000281 |
| 64 | 3 | 7 | 7 | 3 | 3 | 3 | 3 | 3 | 3 | 3 | 0.00000958 | 0.00000869 |
| 186 | 3 | 3 | 3 | 7 | 3 | 3 | 7 | 3/7 ^d | 3/7 | 3 | 0.0000197 | 0.00000651 |
| 151 | 3 | 7 | 7 | 7 | 7 | 3 | 7 | 3 | 3 | 7 | 0.0000235 | 0.0000174 |
| 131 | 7 | 7 | 7 | 7 | 3 | 3 | 3 | 3 | 3 | 3 | 0.0000257 | 0.0000194 |
| 187 | 3 | 3 | 3 | 7 | 3 | 3 | 3 | 3 | 3 | 3 | 0.0000275 | 0.0000120 |
| 160 | 7 | 7 | 7 | 3 | 7 | 7 | 7 | 3 | 3 | 7 | 0.0000361 | 0.0000282 |
| 222 | 3 | 3 | 7 | 7 | 7 | 3 | 3 | 3/7 | 3/7 | 3 | 0.0000425 | 0.00000636 |
| 192 | 3 | 3 | 7 | 7 | 3 | 3 | 3 | 3 | 3 | 3 | 0.0000697 | 0.0000400 |
| 26 | 7 | 3 | 7 | 7 | 3 | 7 | 7 | 3 | 3 | 7 | 0.000343 | 0.0000743 |
| 220 | 7 | 3 | 3 | 3 | 3 | 7 | 7 | 3/7 | 3/7 | 3 | 0.000522 | 0.000214 |
| 12 | 3 | 3 | 7 | 3 | 7 | 3 | 7 | 3 | 3 | 3 | 0.00433 | 0.000355 |
| 65 | 7 | 7 | 7 | 7 | 3 | 3 | 7 | 7 | 7 | 7 | 0.229 | 0.174 |
| 169 | 7 | 7 | 7 | 7 | 3 | 7 | 7 | 7 | 7 | 3 | 0.238 | 0.0643 |
| 30 | 7 | 3 | 7 | 7 | 3 | 7 | 7 | 7 | 7 | 3 | 0.398 | 0.0936 |
| 148 | 7 | 3 | 7 | 7 | 3 | 3 | 7 | 7 | 7 | 7 | 0.548 | 0.176 |
| 229 | 3 | 7 | 7 | 7 | 3 | 7 | 3 | 7 | 7 | 3 | 0.596 | 0.000214 |
| 215 | 7 | 7 | 7 | 7 | 7 | 3 | 7 | 7 | 7 | 7 | 0.637 | 0.312 |
| 100 | 7 | 7 | 7 | 7 | 7 | 7 | 7 | 7 | 7 | 7 | 0.685 | 0.120 |
| 243 | 7 | 7 | 7 | 7 | 3 | 7 | 7 | 7 | 7 | 7 | 1.051 | 0.293 |
| 194 | 7 | 7 | 7 | 7 | 7 | 7 | 7 | 7 | 3 | 7 | 1.87 | 1.13 |
| 159 | 7 | 7 | 7 | 7 | 7 | 7 | 3 | 7 | 7 | 7 | 40.89 | 20.00 |
| Exceptions | 6 | 6 | 9 | 8 | 11 | 8 | 9 | 0 | 2 | 9 | | |

^a A mixed infection of tsA12 and unmutagenized ARV 176 produced reassortants listed.

^b Average efficiency of plating (EOP) value from 2 trials. EOP calculated as described in the Material and Methods, where:

$$\text{EOP} = \frac{\text{Titer at non-permissive temperature}}{\text{Titer at permissive temperature}}$$

^c Standard deviation based on 2 trials.

^d 3/7 indicates the parental origin could not be assigned because of an anomalous migration pattern.

313A, 319C, 341G, 358U for T2J (Dermody *et al.*, 1991). These base changes are responsible for differential migration as seen by SDS-PAGE (Sharpe *et al.*, 1978). Reassortants 186, 220 and 222 were randomly isolated from the *tsA12*/ARV 176 mixed infection and may represent spontaneous mutants. These aberrant clones demonstrated similar S2 and S3 migration patterns after 3 serial passages at a high multiplicity of infection and suggests a propensity for certain base changes. However, the changes do not include alteration of the pre-existing *ts* mutation since all three clones retain the temperature sensitive phenotype. Restriction endonuclease digestion and determination of the nucleotide sequence of these aberrant dsRNA gene segments may allow identification of parental origin and potential base changes.

3.5.2 Reassortant mapping of *tsD46*. To determine the gene segment that contains the *ts* lesion in recombination group D, prototype *tsD46*, reassortant mapping was performed as described in Materials and Methods. From mixed infections of *tsD46* and unmutagenized ARV 176, a total of 94 progeny clones were picked, 12 of which were identified as reassortants (indicating a 12.8% efficiency of producing reassortants) (Table 5, Figure 10). Reassortants were analyzed for temperature sensitivity by the EOP assay. Clones that exhibited a *ts* phenotype were placed into one panel, while those that were non-*ts* were organized in a separate panel. The identified temperature sensitive reassortants each had their L2 gene segments from the *tsD46* parent, whereas the non-*ts* reassortants contained L2 genes derived from the ARV 176 parent. All other gene segments were randomly assorted with respect to temperature sensitivity. This mapping suggests the *ts* lesion of the mutant clone *tsD46* resides within its L2 gene segment. The *ts* mutation of the remaining recombination group D clones (*tsD195* and *tsD219*) may

Table 5
Reassortant mapping of tsD46

| Clone | L1 | L2 | L3 | M1 | M2 | M3 | S1 | S2 | S3 | S4 | EOP ^b | Standard Deviation ^c |
|--------------------------|----|----|----|----|----|----|----|----|----|----|------------------|---------------------------------|
| <u>Cross^a</u> | | | | | | | | | | | | |
| tsD46 | 3 | 3 | 3 | 3 | 3 | 3 | 3 | 3 | 3 | 3 | 0.000018 | 0.000020 |
| ARV 176 | 7 | 7 | 7 | 7 | 7 | 7 | 7 | 7 | 7 | 7 | 0.96 | 0.87 |
| <u>Reassortant</u> | | | | | | | | | | | | |
| 43 | 7 | 3 | 7 | 7 | 7 | 7 | 7 | 7 | 7 | 7 | 0.039 | 0.032 |
| 78 | 3 | 3 | 7 | 3 | 3 | 3 | 3 | 3 | 3 | 3 | 0.044 | 0.047 |
| 39 | 7 | 3 | 7 | 7 | 3 | 7 | 7 | 7 | 7 | 7 | 0.066 | 0.0030 |
| 74 | 3 | 3 | 3 | 7 | 3 | 7 | 7 | 3 | 3 | 3 | 0.088 | 0.013 |
| 7 | 7 | 7 | 7 | 7 | 7 | 3 | 7 | 7 | 7 | 7 | 0.57 | 0.41 |
| 16 | 7 | 7 | 7 | 7 | 3 | 7 | 7 | 7 | 7 | 7 | 0.61 | 0.47 |
| 89 | 3 | 7 | 3 | 3 | 3 | 7 | 3 | 3 | 3 | 3 | 0.79 | 0.34 |
| 87 | 3 | 7 | 3 | 3 | 3 | 3 | 3 | 3 | 3 | 3 | 0.97 | 0.13 |
| 81 | 3 | 7 | 7 | 7 | 3 | 3 | 3 | 3 | 3 | 7 | 1.0 | 0.43 |
| 20 | 7 | 7 | 3 | 3 | 3 | 3 | 7 | 3 | 3 | 3 | 1.9 | 1.5 |
| 61 | 3 | 7 | 3 | 7 | 3 | 3 | 3 | 3 | 7 | 7 | 2.2 | 0.31 |
| 1 | 7 | 7 | 3 | 3 | 7 | 3 | 7 | 3 | 3 | 3 | 3.5 | 1.8 |
| Exceptions | 6 | 0 | 8 | 7 | 7 | 9 | 7 | 8 | 7 | 6 | | |

^a A mixed infection of tsD46 and unmutagenized ARV 176 produced reassortants listed.

^b Average efficiency of plating (EOP) value from 2 trials. EOP calculated as described in the Material and Methods, where:

$$\text{EOP} = \frac{\text{Titer at non-permissive temperature}}{\text{Titer at permissive temperature}}$$

^c Standard deviation based on 2 trials

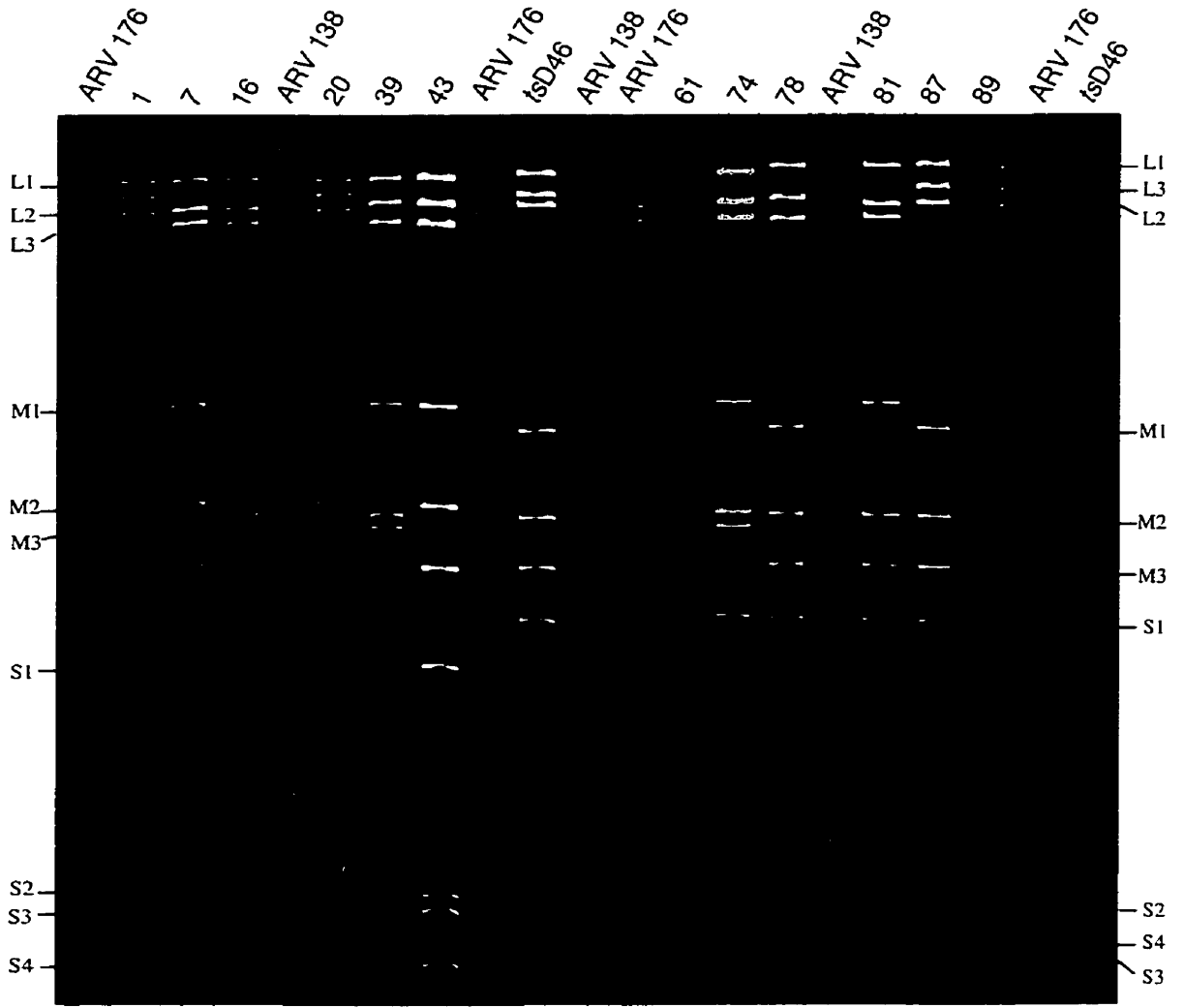


Figure 10: Electropherotypes of ARV 138, ARV 176, *tsD46*, and reassortants produced from a *tsD46* x ARV 176 mixed infection. The double stranded RNA genome segments were isolated from samples as described in Materials and Methods, and resolved in 12.5% SDS-polyacrylamide gels. *TsD46* and ARV 138 have identical electropherotypes (gene segment migration profiles) as *tsD46* was produced from chemical mutagenesis of ARV strain 138. ARV 176 has a unique gene segment profile compared to *tsD46* and allows the parental origin of reassortant (*tsD46* x ARV 176) gene segments to be identified.

reside within the L2 gene segment, however this can be confirmed through reassortant mapping each group D mutant.

3.6 Electron microscopic analysis of *tsA12* and *tsD46*.

3.6.1 Analysis of *tsA12*.

3.6.1.1 Viral and sub-viral particle counts for *tsA12* infections. To characterize potential assembly defects that result from the *ts* mutation in the S2 gene segment of *tsA12*, the proportions of viral and sub-viral particles were counted. QM5 cell cultures were infected with ARV 138 or *tsA12* and incubated at permissive (33.5°C) and restrictive temperatures (39.5°C) for 30 hours and 22 hours respectively. Infections were harvested and examined for viral and sub-viral particles (top component, cores, outer shells) as described in Materials and Methods. *TsA12* exhibited a poor growth phenotype compared to ARV 138 at both permissive and non-permissive temperature with a decreased total number of particles/ml (65% decline at 33.5°C and a 100-fold decline at 39.5°C) (Table 6). Non-*ts* defects that may have resulted from nitrosoguanidine mutagenesis could account for the decreased growth of *tsA12* permissive temperature. Our analysis of *tsA12* focuses on morphological changes seen at 39.5°C compared to 33.5°C. Thus, non-*ts* mutations present at both temperatures are mathematically eliminated and are not examined in our study. Changes in the *tsA12* distribution of viral and sub-viral particles seen at 39.5°C compared to 33.5°C that differ from the distribution of ARV 138 particles seen at 39.5°C were considered significant. Averages from 10 grid sections indicated the proportion of *tsA12* structures was altered from 33.5°C to 39.5°C as top component (72% to 36%) and outer shells (10% to 8%)

Table 6

Viral and sub-viral particle counting of ARV 138, ts A12, and ts D46 at permissive and non-permissive temperature

| Sample | Temperature | Total Particles/ml ^a | Percent of Total Particles (%) ^c | | | |
|---------|-----------------|---------------------------------|---|-------------------|-------|--------------|
| | | | Virion | T.C. ^b | Cores | Outer Shells |
| ARV 138 | P ^d | 6.1 X 10 ⁷ | 57 | 37 | 3 | 3 |
| | NP ^e | 4.9 X 10 ⁸ | 39 | 57 | 1 | 2 |
| ts A12 | P | 2.1 X 10 ⁷ | 13 | 72 | 4 | 10 |
| | NP | 5.3 X 10 ⁶ | 20 | 36 | 35 | 8 |
| ts D46 | P | 9.7 X 10 ⁶ | 21 | 65 | 6 | 8 |
| | NP | 2.1 X 10 ⁶ | 36 | 46 | 10 | 8 |

^a Total particles/ml calculated as described in the Material and Methods, where:
 Particles/ml = (average number of particles)(1.79x10⁵)(dilution factor)
 (Hammond *et al.*, 1981)

^b Top component

^c Percentage of total particles represents the average of 10 sample grids.

^d Permissive temperature (33.5°C)

^e Non-permissive temperature (39.5°C)

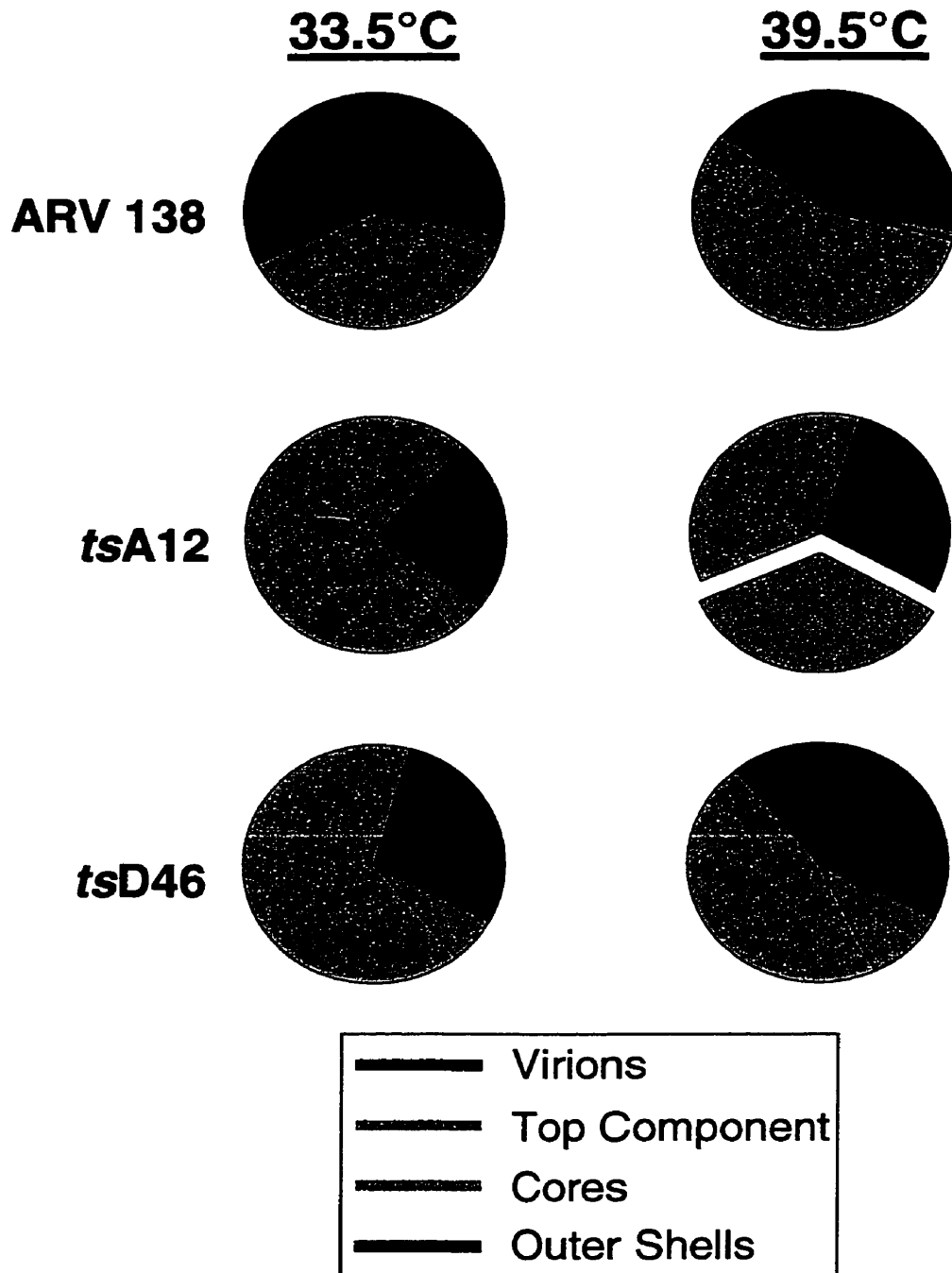


Figure 11: Graphical representation of the proportions of viral and sub-viral particles for ARV 138, *tsA12*, and *tsD46* infections at permissive (33.5°C) and non-permissive (39.5°C) temperature. Sample grids were prepared for ARV 138 (wild type), and ARV *ts* mutants *tsA12* and *tsD46*, as described in the Materials and Methods. Viral (mature virion) and sub-viral (core, outer shell, top component) particles were counted at a magnification of 70,000x using a Philips model 210 electron microscope. The average particle counts from 10 different sample grids are presented in this figure.

declined, virions increased slightly (13% to 20%), and cores increased dramatically (4% to 35%) (Table 6, Figure 11). The accumulation of core particles (35%) at 39.5°C was significantly different from the percentage of cores (1%) seen in ARV 138 infections at the same temperature (Table 6, Figure 11). All other changes in distribution were not as significantly different from the proportions of ARV 138 particles at 39.5°C.

3.6.1.2 Thin section electron microscopy analysis of *tsA12* infected cells. To visualize viral inclusions directly within the infected cells and strengthen our morphological characterization of *tsA12*, thin section electron microscopy was performed. QM5 cell cultures were infected with ARV 138 or *tsA12* and incubated at permissive (33.5°C) and restrictive temperatures (39.5°C) for 30 hours and 22 hours, respectively. Infected cells were processed as described in Materials and Methods section 2.7.1. Viral inclusions in paracrystalline arrays were identified in all ARV 138 infected cells incubated at 33.5°C (total of 44 cells examined: 40 live, 4 dead). A large proportion of top component was identified in the viral inclusions (Figure 12), consistent with particle counting results. ARV 138 infected cells incubated at non-permissive temperature showed similar results. However, viral inclusions were larger (consistent with an increased total particles/ml, Table 6), and an increase in cellular damage was evident (condensation of mitochondria and nucleic acids) at 39.5°C (Figure 12). Consistent with particle counting data, *tsA12* showed a poor growth phenotype at 33.5°C and 39.5°C. The smaller viral inclusions seen at both temperatures may be attributed to non-*ts* defects. *TsA12* infected cells incubated at 33.5°C appeared healthy (18 live cells and 1 dead cell examined), however viral inclusions were significantly smaller and paracrystalline arrays were not as evident as in wild type infections (Figure 12). Similar

A.



B.



C.



D.



Figure 12: Thin section electron micrographs of ARV 138 and *tsA12* infected cells at permissive and non-permissive temperature. Thin sections of ARV 138 or *tsA12* infected QM5 cells, prepared as described in the Materials and Methods, were visualized by the Philips model 201 electron microscope. Micrographs shown are at a final magnification of 50,000x. **A.** Unmutagenized ARV 138 viral inclusion at permissive temperature (33.5°C). **B.** Unmutagenized ARV 138 viral inclusion at non-permissive temperature (39.5°C). **C.** The arrow points to the small viral inclusion of *tsA12* seen at 33.5°C. **D.** *tsA12* viral inclusion at 39.5°C. The arrow points to an incomplete outer shell particle.

to ARV 138, an increased number of unhealthy cells were identified in mutant infections incubated at 39.5°C (28 live, 14 dead). *TsA12* viral inclusions at 39.5°C consisted mainly of top component (similar to particle counting data, Figure 11) and novel incomplete outer shell structures (Figure 11).

3.6.2 Analysis of *tsD46*.

3.6.2.1 Viral and sub-viral particle counts for *tsD46* infections. To examine for possible defects in *tsD46* assembly that result from the *ts* lesion in the L2 gene segment, the proportions of viral and sub-viral particles produced during infection were assessed. Cells infected with ARV 138 or *tsD46* were incubated at 33.5°C and 39.5°C for 30 hours and 22 hours respectively, then processed and analyzed as described in Materials and Methods. *TsD46* displayed a poor growth phenotype at permissive temperature compared to ARV 138, having an 84% decline in total particles/ml (Table 6). This difference may be attributed to the presence of non-*ts* mutations in *tsD46*. At restrictive temperature the total number of *tsD46* particles/ml decreased by 78% compared to its 33.5°C value (Table 6). This temperature sensitive phenotypic change is attributed to the presence of the *ts* lesion. The *tsD46* distribution of virions, top component, cores, and outer shells at 39.5°C resembles its 33.5°C infections and is not significantly different from ARV 138 at 39.5°C (with only a slight increase in top component and cores compared to ARV 138). *TsD46* does not accumulate any particular viral or sub-viral particle but is assembly defective in that the production of all structures is reduced at 39.5°C compared to its growth at 33.5°C.

3.6.2.2 Thin section electron microscopy of *tsD46*. To further characterize the morphological changes in *tsD46* at restrictive temperature, thin section electron microscopy was performed. QM5 cell cultures were infected with ARV 138 or *tsD46* and incubated at permissive (33.5°C) and restrictive temperatures (39.5°C) for 30 hours and 22 hours respectively. Cells were infected at a MOI of 10 plaque forming units/cell and processed as described in Materials and Methods. ARV 138 (control) thin section results are described in section 3.6.1.2. At permissive temperature *tsD46* was present within only 16% of cells examined, indicating a low level of infection (23 live uninfected cells, 2 dead uninfected cells and 4 live infected cells). The proportion of viral particles was similar to ARV 138 infections. At 39.5°C there was no evidence of *tsD46* progeny virion production within the 25 cells examined, and suggests a decline in the total number of viral particles produced, consistent with particle counting data. Cellular damage from incubation at 39.5°C was reduced in *tsD46* infections compared to ARV 138 (20 live cells, 5 dead cells).

3.7 The S2 gene sequence as determined for ARV138 and *tsA12*.

3.7.1 Identification of the *tsA12* mutation.

To relate morphological changes observed at non-permissive temperature to the alteration present within the protein, the mutated gene segment was sequenced and the protein coding assignment was determined. The S2 gene segment, found to harbor the *ts* lesion in *tsA12*, was sequenced for this clone and unmutagenized ARV strain 138 as described in Materials and Methods. The laboratory strain of ARV 138 that was used to create the panel of ARV *ts* mutants had no S2 gene sequence changes compared to the

ARV strain 138 S2 sequence reported in GenBank (accession number GI"3170620"; Duncan, 1999). The *tsA12* mutant S2 gene was found to have one nucleotide transition at base number 488, where cytosine (ARV 138 sequence; Figure 5) was replaced with uracil in the *tsA12* mutant. This alteration exists at the 2nd position of codon number 158 and results in an amino acid change of proline₁₅₈ (ARV138) (Figure 13) to leucine₁₅₈ (*tsA12*). This ARV 138 σ A proline residue is highly conserved within the orthoreovirus genus, and upon sequence alignment is identified in ARV strain 176, Nelson Bay Virus, Baboon Reovirus, and within the MRV equivalent σ 2 protein of all 3 serotypes (Type 1 Lang, Type 2 Jones, Type 3 Dearing) (Duncan, 1999). This suggests Pro₁₅₈ has a critical role in ARV 138 σ A structure and/or function.

3.7.2 Secondary structure prediction. To determine potential morphological changes in the protein that are induced by this mutation, secondary structure analysis was carried out. The PHD Predict version 1.96 (Burkhard, 1996), PSIPredict version 2.0 (McGuffin *et al.*, 2000), and nnpredict (Kneller, 1991) secondary structure prediction programs were used and results were compared. The PHD predict output (72% accuracy overall) quotes a reliability index (Rel) for each amino acid to account for the strength of each prediction (0=low and 9=high). For residues with Rel<4 a prediction is not made. Similarly, PSIPredict states a confidence (Conf) value for each prediction, where 0=low, 9=high. The results were compiled to deduce the predicted secondary structure of the σ A protein encoded by the S2 gene. In order to improve the accuracy of prediction only those secondary structure predictions that were conserved between 2/3 of the programs were considered (Figure 13). According to PHD predict, and evident in the composite diagram

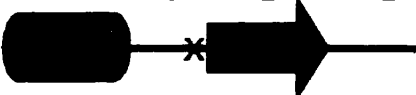




Figure 13: Predicted secondary structure of the ARV 138 σ A protein. The sequence of the unmutagenized ARV 138 S2 gene segment was determined and translated into its corresponding amino acids (σ A protein). The amino acid sequence and proposed secondary structure (β -sheet, α -helix, loop) of σ A is shown. PHD predict (Burkhard, 1996), PSI predict (McGuffin *et al.*, 2000) and nnpredict (Kneller, 1991) programs were used to deduce σ A secondary structure. To improve accuracy, predictions that were conserved in 2/3 of the programs were considered significant and compiled in this figure. The proline (p) residue at position 158 is highlighted in this figure to indicate that this is the amino acid that is mutated in the *tsA12* σ A sequence.

(Figure 13), the predicted σ A structure does not fit into the defined alpha, beta, or alpha/beta categories commonly used to describe protein secondary structures. Thus σ A is considered a mixed class protein. The unmutagenized ARV 138 σ A proline₁₅₈ residue is within a predicted loop structure (PHDpredict Rel=7, PSIPred Conf=7). The npredict program confirmed Pro₁₅₈ was not involved in an α -helix or β -strand. The secondary structure prediction for *tsA12* σ A leucine₁₅₈ residue was not as well defined. PHDpredict made no prediction for Leu₁₅₈ (Rel=2), while PSIPredict suggested Leu₁₅₈ was still involved in a loop structure (Conf=7). The npredict program stated the presence of leucine at position 158 extends the adjacent β -strand (Table 7). The secondary structure changes that occur in response to the Pro₁₅₈ to Leu₁₅₈ mutation are ambiguous. Crystallization of mutant and parental σ A proteins should be carried out to more accurately define the structural changes.

Table 7

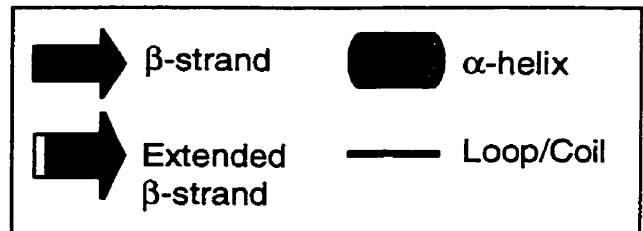
Predicted secondary structure changes in the *tsA12* σ A protein

| Program | <i>tsA12</i> σ A ₁₅₁₋₁₆₇ Secondary Structure | Prediction |
|---|---|--|
| PHD predict^a
Reliability Index | 151 lsamraglvlyvetwpm

<i>tsA12</i> : 99973982789975265
ARV 138: 99972697699972255 | <ul style="list-style-type: none"> • No prediction • (loop) |
| PSI predict^b
Confidence | 151 lsamraglvlyvetwpm

<i>tsA12</i> : 73532797338614720
ARV 138: 73533797338614720 | <ul style="list-style-type: none"> • Same as ARV138 • (loop) |
| nnpredict^c | 151 lsamraglvlyvetwpm
 | <ul style="list-style-type: none"> • Extended β-strand |

^a Burkhard, 1996

^b McGuffin *et al.*, 2000

^c Kneller, 1991



4. DISCUSSION

4.1 Chemical mutagenesis.

ARV strain 138 was chemically mutagenized and 17 stable *ts* mutants were isolated. The mutagenesis strategy, comparable to that reported for other members of the *Reoviridae* (Ikegami and Gomatos, 1968; Ramig, 1983), incubates actively replicating cultures with a chemical mutagen. The mutagen interacts with progeny RNA as it is replicated and produces genetic mutations. Alternate methods that rely on spontaneous mutagenesis events have been used to generate *ts* mutants in the *Reoviridae*. For example, serial passages at high multiplicity of infection or rescue of pseudorevertant clones from persistent *ts* mutant infections are responsible for 3% and 36% of the MRV *ts* mutants, respectively (Coombs, 1998). The majority of MRV *ts* mutants (61%) are the products of chemical mutagenesis (Coombs, 1998); therefore, this approach was chosen to create ARV *ts* mutants. Unmutagenized, wild type mammalian reovirus clones generate *ts* mutants with a 0.1-0.3% frequency (Fields and Joklik, 1969); however, the application of chemical mutagen significantly increases this value. Nitrosoguanidine mutagenesis creates *ts* mutants with a reported 5% frequency (Fields and Joklik, 1969), and has been used in mammalian reovirus (Ikegami and Gomatos, 1968; Ramig, 1983), influenza A virus (Simpson and Hirst, 1968), and tobacco mosaic virus systems (Singer, 1967). A total of 17 *ts* mutants were isolated from a total of 351 potentially *ts* mutants. This 4.84% frequency of *ts* mutants is comparable to the expected 5% frequency (Fields, 1969). Although proflavin generates *ts* mutants with a 10% frequency (Fields and Joklik,

1969), its best characterized mammalian reovirus mutants are mildly temperature sensitive and have multiple lesions (Hazelton and Coombs, 1995; 1999). Nitrosoguanidine induces unidirectional transitions in viral RNA, such as cytosine to uracil or adenine to guanine changes (Schuerch and Joklik, 1973). The *tsA12* mutant S2 gene had an amino acid change of proline₁₅₈ to leucine₁₅₈ (Table 7) where codon CCU (nucleotides 487-489) (Figure 5) was mutated to CUU, respectively.

4.2 Efficiency of lysis assay and efficiency of plating assay.

Although avian reoviruses infections induce syncytia formation, they are ultimately lytic to the host cell (Duncan, 1996). The novel efficiency of lysis assay screens for temperature sensitivity as it compares the virus' ability to induce host cell lysis at non-permissive and permissive temperature. *Ts* mutations that affect any stage of the viral life cycle prior to release will be identified by the EOL assay. The high sensitivity of the EOL assay is demonstrated in the lack of falsely identified non-*ts* clones; however, many inaccurately identified false positives (*ts*) were recorded. Thus, confirmation of temperature sensitive status of EOL-identified *ts* clones by the classical EOP assay is essential.

The novel EOL technique has many advantages over the standard EOP temperature sensitivity assay for initial screening of temperature sensitivity. The permissive host for avian reovirus infections, QM5 quail cells, require 10% fetal calf serum (FCS) and are attachment dependent. Thus, the general maintenance of large numbers of stock cells is a costly and cumbersome task. The EOL method alleviates this since 8 samples can be screened with each plate as compared to 1 sample per plate by

EOP. The novel EOL screening approach also involves less handling and requires only 5 days to complete, in contrast to the labor-intensive efficiency of plating assay that requires a minimum of 8 days to complete. Thus, the EOL assay is a useful means to screen the often hundreds of potentially *ts* clones isolated to reduce the number that need to be confirmed by the “gold standard” method of EOP.

4.3 Organization of ARV *ts* mutants through genetic recombination analysis.

To begin the characterization of the panel of ARV *ts* mutants, they were organized into genetic groups to identify those mutants with *ts* lesions located in similar gene segments. Genetic recombination in viruses with segmented genomes occurs through reassortment of individual gene segments rather than the classical means of strand breakage and rejoining. Classically, mathematical recombination analysis of reovirus *ts* mutants organizes the mutants into groups based on the presence of *ts* lesions in the same or different gene segments. Pair-wise mixed infections of mutants whose lesions reside on different gene segments will result in the production of some reassortant progeny whose genotype contains no *ts* mutation and acts wild-type-like (ts^+). All progeny arising from mixed infections of mutants whose *ts* lesions are within the same gene segment will have a *ts* phenotype. Recombination in the *Reoviridae* is described as an “all or none event”, either producing ts^+ progeny or not. Thus, a continuum of recombination values is not found (Coombs, 1998; Ramig, 1983). This principle is reflected in the defined limits of recombination in each of the formulae applied: standard recombination formula, recombination index formula, and the novel EOP recombination formula.

Organization of ARV *ts* mutants into recombination groups by the standard *Reoviridae* recombination and recombination index formulae was problematic. Various limits of recombination have been reported for the standard recombination formula, where values of <0%, <0.1%, or <0.2% indicate that mutants belong to the same group and values of >1%, >2%, or >3% suggest mutants belong to different groups (Coombs, 1998; Fields and Joklik, 1969; Ramig, 1982). The lack of defined limits resulted in uncertainty in the assignment of ARV recombination groups. Furthermore, some ARV *ts* mutants fell within the undefined range of recombination and were unclassifiable, a common problem in the analysis of *Reoviridae* recombination with this formula (Table 2) (Fields, 1969; Coombs, 1998). To clarify the organization of ARV *ts* mutants, the recombination index (RI) formula developed to analyze recombination in bovine rotavirus *ts* mutants was applied to ARV recombination data. In most cases the RI formula more clearly defined the ARV recombination groups compared to the standard formula. However, some inconsistencies between the results of the two formulae were present (Table 2 and 3). The RI analysis examines only viral titers at non-permissive temperature and does not account for viral growth at permissive temperature. Thus, the RI may inaccurately assess recombination in viral clones that are mildly temperature sensitive as small increases in the number of *ts*⁺ progeny may go undetected.

A novel recombination formula was designed to overcome the inadequacies of the standard *Reoviridae* recombination and RI formulae, and to attempt to more clearly identify *ts*⁺ recombinants. This new formula compares the temperature sensitivity of the progeny, as defined by their collective EOP value, to that of the average temperature sensitivity of the two *ts* parents involved in the cross. If reassortment of gene segments

results in the production of ts^+ recombinants the progeny EOP value would be more wild-type-like than the parental EOP values. The accepted random variation of wild type virus EOP values is within an order of magnitude of one. EOP values of ts mutants may also vary randomly within similar limits and progeny EOP values outside these limits are significantly different. It was noted that recombination values within the same group did not exceed a value of 5 (Table 2 and 3); however, the significance of the consistency is not known and will require further examination. This formula examines parental and progeny virus titers at both non-permissive and permissive temperature in the calculation of their EOP values, thus is a more powerful approach than the recombination index. Mixed infections that involve mutants from different groups resulted in a large diversity of recombination values from 21.7 to 5676.1. Underestimation of the progeny non-permissive titer would result in a lower recombination value overall, and several explanations for this are possible. First, chemical mutagenesis may result in the production of non- ts mutations. The combination of non- ts mutations in ts^+ reassortants may not be favored and prevent their detection. Secondly, mixed infections with some ts mutant combinations may interfere with the growth and detection of non- ts reassortants, as has been suggested for rotavirus (Ramig and Ward, 1991). Finally, a physical separation of inclusion bodies within the mixedly infected cell may inhibit the process of reassortment (Nibert *et al.*, 1996).

Genetic organization of ARV ts mutants was improved by use of the novel recombination formula compared to the standard formula; however it was not perfect. For example, in the mixed infection of $ts86$ and $tsF206$ the recombination index analysis confirmed the standard formula value and not the novel formula results. The EOP

recombination formula eliminated many ambiguities present in the standard formula results. Various assigned limits of recombination have been reported in standard recombination analyses where values of <0%, <0.1%, or <0.2% suggest lesions lie on the same gene segment and values of >1%, >2%, or >3% indicate different gene segments (Fields, 1969; Ramig, 1982; Coombs, 1998). Exceptions are often present within the undefined range of the standard formula (Fields, 1969; Coombs, 1998) and in some cases the organization of ARV *ts* mutants was unclear. For example, the standard formula limits of either <0%, <0.1%, or <0.2% had 2, 1, or 0 exceptions outside the range, respectively. Similarly, limits of >1%, >2%, or >3% had 2, 8, or 20 exceptions, respectively (Table 2). Although the novel EOP analysis of recombination is superior in the present ARV *ts* mutant system, it is not flawless, and should be used for clarification in conjunction with other formulae.

A total of 11 ARV *ts* mutants were organized into 7 recombination groups and indicates that 7 of the 10 ARV gene segments have representative *ts* mutations. Failure to identify all possible recombination groups from a large panel of *ts* mutants is not unprecedented. For example, the 58 MRV *ts* mutants were organized into only eight of the ten available recombination groups (Coombs, 1998; unpublished). It is possible that mutations within certain gene segments may result in non-viable clones at any temperature, and may account for their absence. Expansion of the panel of ARV *ts* mutants is needed to attempt to isolate clones that belong to the three unidentified recombination groups and to eliminate the possibility that some grouped mutants may contain multiple gene segments with *ts* lesions. To date, six *ts* mutants isolated have numerous gene segments with *ts* mutations. *Ts*188 failed to recombine with 5

recombination groups (Table 3) and suggests 50% of its genome harbors *ts* mutations. Due to the limited size of the viral capsid, viruses carry only essential genetic information. A virus such as *ts188* (with ½ of its genome carrying *ts* mutations) would likely fail to thrive even at permissive temperature. *ts188* exhibits a mildly temperature sensitive phenotype (EOP=0.046; Table 3) and is capable of marginal growth at non-permissive temperature. This feature may not allow adequate analysis of *ts188* by these recombination formulae.

4.4 The *tsA12* mutant and recombination group A summary

The temperature sensitive lesion of *tsA12*, and presumably *tsA146* (another member of recombination group A), resides within the S2 gene segment that encodes the σ A protein. σ A is a 45.5 kDa major core protein (Sheng Yin *et al.*, 2000) 416 amino acids in length (Duncan, 1999) that attaches to the outer face of the core structure (Duncan, 1996; Sheng Yin *et al.*, 2000). Recent crystallization of the MRV core particle revealed that the equivalent mammalian reovirus protein σ 2 (S2 gene) binds to the outer face of the viral core and acts as a “clamp” to hold the structure together (Reinisch *et al.*, 2000). However, prior to our analysis of ARV *tsA12*, the viral assembly process and the structural role of ARV σ A had not yet been studied. The ARV σ A protein binds dsRNA in a non-sequence specific manner (Sheng Yin *et al.*, 2000) and prevents activation of host dsRNA dependent enzymes that induce an antiviral state (Martinez-Costas *et al.*, 2000); however, whether σ A has a role in the replication process is unknown. Although the protein sequence similarity between ARV σ A and 3 serotypes of MRV σ 2 is low

(33% compared to MRV type1, 32.8% compared to MRV type2, and 34.3% compared to MRV type3), σA and $\sigma 2$ share similar predicted secondary structure (Sheng Yin *et al.*, 2000). Thus, we were interested to examine this group of mutants to enhance our structural and biological understanding of σA function.

Reassortant mapping concluded the *tsA12* temperature sensitive lesion is localized within the S2 gene segment; however, the parental origin of the S2 and S3 gene segments in some reassortant clones (R186, R220, R222) was unidentifiable by SDS-PAGE. Polyacrylamide gel electrophoresis in the presence of SDS allows band separation based on size differences, however other factors may affect mobility. For nucleic acid sequences identical in length, the specific base content (A, C, G, U) influences the molecular weight of the strand and thus it's migration profile. This phenomenon is demonstrated in the MRV S2 gene segments (1331 base pair in length) of T1L, T2J, and T3D. Thus, point mutations may account for the aberrant migration of the S2 and S3 gene segments in R186, R220, and R222. In mammalian reovirus, the presence of hybrid dsRNA secondary structure is reported to inhibit migration through the gel matrix (Ito and Joklik, 1972). Reassortant dsRNA was not completely denatured prior to loading, however the presence of secondary structure in non-engineered viral dsRNA is an unlikely scenario.

4.4.1 Morphology of *tsA12*

Structural analysis of *tsA12* yielded inconsistent results that may enhance our understanding of ARV assembly. Particle counting data indicated an accumulation of core particles at non-permissive temperature compared to ARV 138 infections. At least

two scenarios for mutant σA could account for the temperature sensitive phenotype identified. First, σA may add onto the core structure incorrectly at restrictive temperature and prevent the addition of outer shell proteins. Alternatively, σA may add onto the core properly but the *ts* mutation lies on the outward face of the protein and inhibits the addition of the outer shell proteins. If the mutation exists on the outward face of the σA protein, a conformational change at the surface would be expected, and may expose alternate protease cleavage sites. For example, α -chymotrypsin, a protease that processes the mature virion into the core particle, may identify such changes on the core surface. To test this hypothesis, mass spectrometry could be performed on *tsA12* core particles produced at permissive and restrictive temperature to attempt to detect differences in the peptide profiles and indicate a potential conformational change. The *ts* phenotype identified by thin section electron microscopy was inconsistent with particle count results. An accumulation of cores was not identified at 39.5°C, instead novel incomplete outer shell structures were evident. To date, identification of incomplete outer shells is unprecedented and implies a second structural role for σA , where outer shell structures require an association with the σA protein to complete their assembly. This interaction may be disrupted at 39.5°C due to the *ts* lesion within σA . These open outer shell structures could have been disrupted and lost during particle counting sample preparation and may account for their absence. In contrast, the *ts* mutant equivalent in the MRV system, *tsC447* (mutated $\sigma 2$ protein), lacks core structures and accumulates complete outer shells at non-permissive temperatures (Fields *et al.*, 1971; Ramig *et al.*, 1978). The MRV $\sigma 2$ *ts* mutation resides within a different region of the core protein than the ARV

σ A *ts* mutation. Thus, the σ 2 lesion may not inhibit the completion of outer shell structures in *tsC447* but prevent the addition of “clamp” protein (σ 2) to the core, resulting in its instability and loss. Alternatively, the ARV and MRV assembly process may occur by different mechanisms. The discrepancy between particle counting and thin section electron microscopy data has been identified in MRV *ts* mutants. For example, MRV *tsA279* particle counting data suggests an accumulation of spikeless cores at restrictive temperature, whereas outer shells are identified by thin section electron microscopy (Hazelton and Coombs, 1995; 1999).

4.4.2 Secondary structure predictions for the *tsA12* σ A protein.

To interpret morphological changes seen in *tsA12* at non-permissive temperature, the amino acid alteration within the mutant σ A protein was identified. The *tsA12* temperature sensitive mutation resides in the S2 gene segment (σ A) and corresponds to an amino acid change at codon₁₅₈ where a highly conserved proline residue (Duncan, 1999) is replaced by leucine. Amino acid residues that are evolutionarily conserved within a genus imply their importance in the structure and/or function of the protein. σ A, a major core protein, likely plays a critical role in ARV structure. Proline is a rigid non-polar cyclic amino acid recognized for its “helix breaking” ability, whereas leucine is non-polar and less rigid. The amino acid change within *tsA12* may result in increased flexibility of the protein or may alter critical tertiary structure amino acid interactions. The conformational change induced is detrimental to the virus at non-permissive temperature (39.5°C) whereas at permissive temperature (33.5°C) the change is either not

evident or not lethal. Secondary structure predictions for the mutated σA protein codon₁₅₈ were not consistent from the 3 programs used (PHD predict, PSI predict, nnPredict). The lack of consensus suggests that a structural change from wild type σA at this position is possible. Crystallization or nuclear magnetic resonance image analysis of the mutant and wild type σA protein is required to determine the precise morphological change. Comparison to the MRV core particle crystal structure (Reinisch *et al.*, 2000) using the RasMol 2.7.1 graphics visualization tool (Berstein, 1999), suggests the mutated amino acid (at position 158) lies directly below the outer face of the σA protein. Perturbation at this location may skew the arrangement of amino acids on the outer face, leading to non-viable core particle at non-permissive temperatures (Figure 14). Electron microscopic particle counting data suggested *tsA12* accumulated core particles at non-permissive temperatures. It is speculated that the altered σA secondary structure may destabilize the protein at the non-permissive temperature and prevent the addition of the outer shell onto the core. Further structural investigations of *tsA12*, such as crystallization, nuclear magnetic resonance imaging, or mass spectrometry as outlined earlier, is required to definitively assess the mutant protein changes.

4.4.3 Biological role of σA in dsRNA production. To assess the biological implications of the altered σA structure, the production of progeny dsRNA was examined in recombination group A mutants. *TsA12* and *tsA146* both failed to synthesize dsRNA at non-permissive temperature and were classified as dsRNA (-) (Figure 8). This suggests a role for σA in the replication strategy and implies the protein is involved in either the

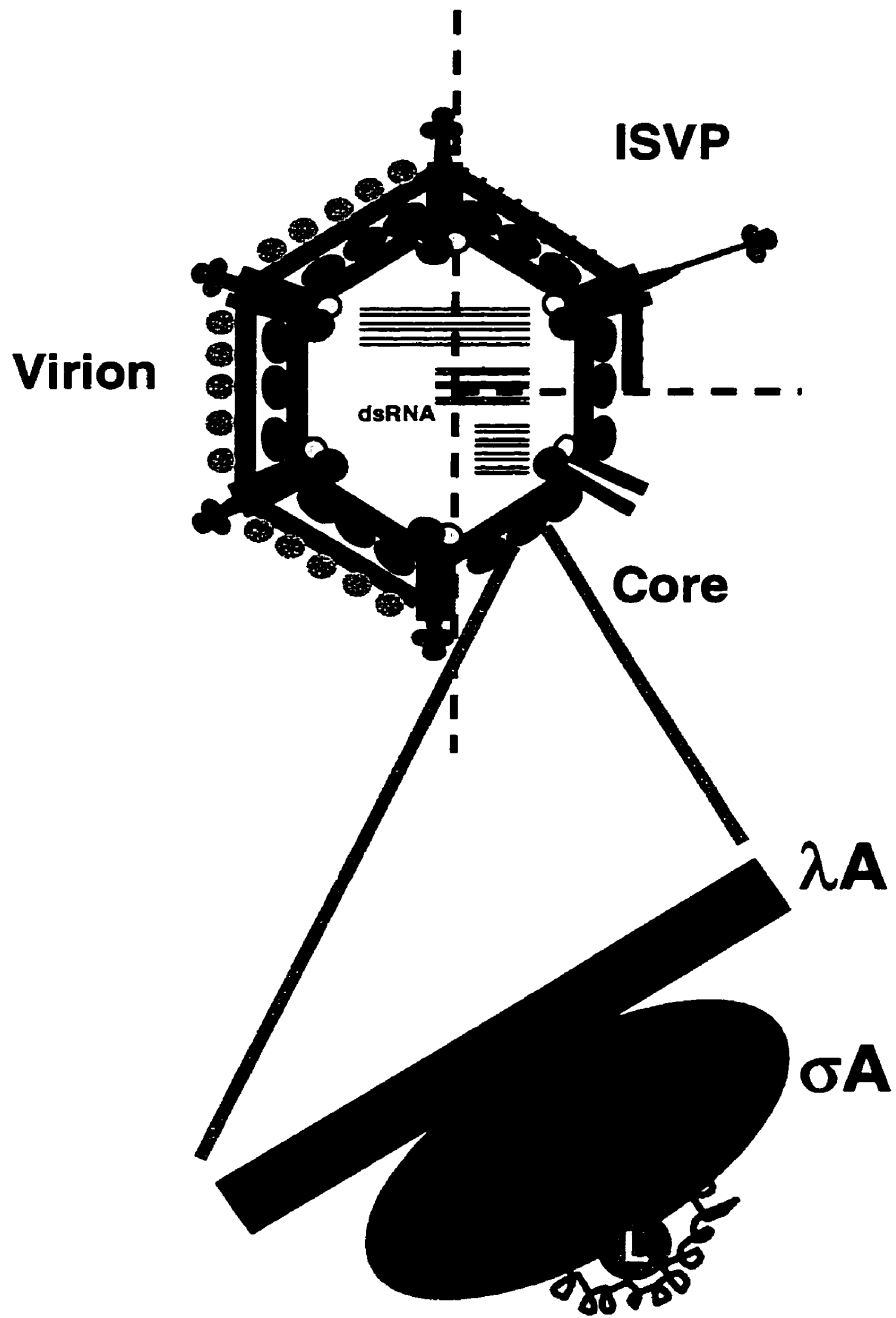


Figure 14: Proposed conformational change in the *tsA12* σA protein. The temperature sensitive mutation of *tsA12* resides within the σA protein. A section of the core particle (σA , λA) is enlarged and the σA amino acid change shown in red (L: leucine residue at codon 158). For the names of the other proteins present within the virion, core, or ISVP, refer to Figure 1. A conserved proline (rigid, non-polar amino acid) residue that lies just beneath the protein surface (based on MRV crystal structure, Reinisch *et al.*, 2000) is replaced by leucine in this *ts* mutant. Leucine is a non-polar amino acid with less inherent structural constraints than proline, and may result in increased protein flexibility at this region. A conformational change may be induced at the surface of σA , explaining the accumulation of cores as the addition of the outer shell is prevented. This type of alteration may be detrimental to the virus at non-permissive temperature and cause the *ts* phenotype; however, the model must be confirmed by protein crystallization, NMR imaging, or mass spectrometry.

production of the (+) ssRNA (template for (-)RNA), assortment of plus sense strand into the assortment complex, or directly in the synthesis of the (-) strand. Evidence that the σ A protein binds dsRNA in a sequence non-specific manner (Sheng Yin *et al.*, 2000) supports the involvement of σ A in the replication process. Similarly, the MRV equivalent protein σ 2 binds dsRNA (Dermody *et al.*, 1991) and its representative *ts* mutant, *tsC447*, fails to synthesize dsRNA (Ito and Joklik, 1972b). The biological correlation between ARV recombination group A mutants (*tsA12*, *tsA146*) and the MRV group C mutant (*tsC447*) confirms a role for this major core protein in the replication cycle. However, the mechanism in which σ A is involved is not yet understood and further investigations are required. One possible explanation for this dsRNA (-) phenotype is that an interaction between σ A and the newly synthesized dsRNA stabilizes and promotes continued elongation of the progeny genome. Perhaps a conformational change in the mutant σ A protein at non-permissive temperature inhibits this interaction and prevents the production of dsRNA.

4.5 The *tsD46* mutant and recombination group D

The temperature sensitive mutation in *tsD46* was identified in the L2 gene segment known to encode the λ B protein. The *ts* lesion in other members of recombination group D, *tsD195* and *tsD219*, may also reside in the L2 gene, however confirmation by reassortant mapping is required. The 130 kDa ARV λ B protein is present within core particles (Martinez-Costas *et al.*, 1997) and is predicted to function as the RNA dependent RNA polymerase (RdRp) based on its location in the virion,

stoichiometry, and correlation to MRV (Van Regenmortel *et al.*, 2000). To date, the avian reovirus RdRp has not been studied and little is known in comparison to the MRV equivalent protein, $\lambda 3$. MRV $\lambda 3$, a minor internal core protein, is associated at the 12 vertices of the icosahedron and requires the $\mu 2$ protein as a cofactor for activity. Together the MRV $\lambda 3$ and $\mu 2$ function as the RdRp, helicase, and RNA triphosphatase within the core particle (transcription) and in progeny assortment complexes (transcription and replication) (Van Regenmortel *et al.*, 2000). To broaden our understanding of the avian reovirus counterpart (λB protein) and to correlate it to MRV $\lambda 3$, ARV recombination group D was characterized structurally and biologically.

4.5.1 Electron microscopic analysis of *tsD46*.

To morphologically characterize the temperature sensitive phenotype of *tsD46*, electron microscopic analysis was performed. *TsD46* exhibited a poor growth phenotype at both permissive and non-permissive temperature by particle counting analysis and thin section electron microscopy. The growth of *tsD46* at 39.5°C was further reduced compared to 33.5°C infections, as seen by decreased total particles/ml in the particle counting analysis, and the absence of *tsD46* infected cells at 39.5°C by thin section electron microscopy. Particle count preparations indicated the distribution of *tsD46* viral and sub-viral particles was similar for both temperatures and resembled ARV 138 39.5°C infections. The temperature sensitive phenotype of *tsD46* is characterized at 39.5°C by a decline in the total number of viral and sub-viral particles while maintaining proportions similar to permissive temperature infections and suggests that the λB mutation disrupts an early stage of viral replication and/or assembly. This evidence supports the predicted

λ B replicase (RdRp) function as mutations here would interfere with viral replication and transcription and result in a general decline in dsRNA genome, protein synthesis and total viral progeny.

4.5.2 Biological role of λ B in dsRNA production. To examine the biological effects of the λ B *ts* mutation within members of recombination group D, the ability to synthesize dsRNA at 33.5°C and 39.5°C was assessed. *TsD46*, *tsD195*, and *tsD219* failed to synthesize dsRNA at the restrictive temperature (Figure 8), while at permissive temperature dsRNA production was similar to that of the controls. This common recombination group D dsRNA(-) phenotype suggests the *ts* lesion in all members affects similar λ B protein function. These results support the predicted RdRp function of λ B as disruption in this protein would result in decreased transcription and replication and thus an overall decline in total dsRNA production. Similarly, the representative MRV RdRp (λ 3) temperature sensitive mutant, *tsD357*, fails to synthesize dsRNA (Cross and Fields, 1972) and further supports the proposed function of λ B.

4.6 Recombination group B, C, E, F, G, and ungrouped mutants dsRNA production. To biologically characterize *ts* lesions in mutants that belong to recombination groups B, C, E, F, G, and those mutants with multiple mutated gene segments (*ts* 86, *ts* 108, *ts* 205, *ts* 207), the ability to produce dsRNA at 33.5°C and 39.5°C was examined. The recombination group B mutant (*tsB31*), group C mutants (*tsC37*, *tsC287*), and the ungrouped mutants *ts* 205 and *ts* 207 retained the ability to synthesize dsRNA at restrictive temperature and were classified as dsRNA (+) (Figure 8).

The protein(s) that harbors their *ts* lesions has not yet been identified by reassortant mapping; however, the disrupted function is not related to progeny genome production. Mutants that belong to recombination group E (*tsE158*), F (*tsF206*), G (*tsG247*), and the unclassified mutants *ts* 86 and *ts* 108 failed to produce dsRNA (dsRNA (-)) at 39.5°C. This suggests the mutated proteins represented by these mutants disrupt transcription, replication, and/or genome packaging at some stage of the viral life cycle at the non-permissive temperature. To meaningfully interpret these results, identification of the mutant protein by reassortant mapping is required.

4.7 Future Directions.

This research has introduced the first panel of ARV *ts* mutants and initiated their characterization; however, many aspects (biological and morphological) of their *ts* phenotypes have yet to be explored. Expansion of the panel of *ts* mutants is required to isolate the three missing recombination groups and eliminate the possibility that mutants from groups A-G carry multiple mutated (*ts*) gene segments. Furthermore, a panel of ARV *ts* mutants with representative *ts* mutations in all 10 gene segments would allow thorough characterization of ARV protein function. To date, the gene segment that harbors the *ts* lesion has been identified in only two of the seven recombination groups. Reassortant mapping of the other groups is required to allow meaningful interpretation of phenotypic characterization studies. Little is known about the ARV assembly process, and morphological analysis (thin section electron microscopy, particle counting) of other prototype mutants may increase our knowledge in this area. Our analysis of ARV σA suggests this protein attaches to the outer face of the core, similar to MRV $\sigma 2$, and may

be involved in the assembly of complete outer shell structures, unlike MRV $\sigma 2$. This difference may reflect a unique ARV assembly pathway, or an association not yet identified in the MRV *ts* mutant system. To confirm the location of σA , crystallization, NMR imaging, or mass spectrometry of the core particle should be performed. The replication cycle of avian reovirus has not been previously characterized. Preliminary biological studies (dsRNA synthesis) implicated the proteins represented by recombination groups A (σA), D (λB), E, F, and G as being involved in replication cycle prior to virion assembly, while the *ts* mutant proteins of groups B and C are not involved in dsRNA synthesis. The predicted RdRp function of λB was confirmed by our phenotypic investigation of recombination group D and by correlation with the MRV RdRp *ts* mutant, *tsD357*. More detailed studies, such as synthesis of plus sense ssRNA template, may further elucidate protein function in the viral lifecycle. Mixed infection of *tsA12* and ARV 176 generated a series of clones with potential S1 gene segment deletions. Characterization of these deletion mutants by S1 sequence analysis may identify essential coding sequences and/or sequences that promote this deletion. Analysis of protein production at restrictive temperature would also enhance our characterization of the panel of ARV *ts* mutants, and are currently underway. Avian reovirus is an atypical member of the orthoreovirus genus; however, it possesses unique features not identified in the prototypic mammalian reovirus. Recently, studies in the avian reovirus field have increased. This panel of ARV *ts* mutants may serve as an important tool to uncover the molecular mechanisms of ARV and enhance our understanding of the *Reoviridae* as a whole.

5. REFERENCES

- Bernstein, H.J. (1999) RasMol 2.7.1[®] molecular graphics visualization tool. Bernstein and Sons, Bellport, NY, USA.
- Black, L.W., Showe, M.K., and Steven, A.C. (1994) Morphogenesis of the T4 Head. In: Karam J.D., Drake, J.W., Kreuzer, K.N., Mosig, G, Hall, D., Eiserling, F.A., Black, L.W., Kutter, D., Spicer, E., Carlson, K., and Miller, E.S. (eds) *Molecular Biology of Bacteriophage T4*. American Society for Microbiology, Washington, DC, pp218-258.
- Boccadoro, M., Redoglio-V, Gavarotti, P, and Pileri, A. (1986) Multiple myeloma plasma cell kinetics: rapid and reliable evaluation using 5-bromo-2-deoxyuridine (BrdUrd) DNA incorporation detected by an anti-BrdUrd monoclonal antibody. *Tumor* 72, 135.
- Calnek, B.W., Barnes, J.H, Beard, C.W., McDougald, L.R., and Saif, Y.M., Eds. (1997) *Diseases of Poultry*. 10th Edition, Iowa State University Press, Ames, Iowa, USA.
- Carleton, M., and Brown, D.T. (1996) Events in the endoplasmic reticulum abrogate the temperature sensitivity of Sindbis virus mutant *ts23*. *J. Virol.* 70, 952-959.
- Chakraborty, P.R., Ahmed, R., and Fields, B.N. (1979). Genetics of reovirus: the relationship of interference to complementation and reassortment of temperature-sensitive mutants at non-permissive temperatures. *Virology* 94, 119-127.
- Chen, D., Gombold, J.L., and Ramig, R.F. (1990) Intracellular RNA synthesis directed by temperature-sensitive mutants of simian rotavirus SA11. *Virology* 178, 143-151.

- Chen, H., Ranachandra, M., and Padmanabhan, R. (1994) Biochemical characterization of a temperature-sensitive adenovirus DNA polymerase. *Virology* **205**, 364-370.
- Chiu, C.J., and Lee, L.H. (1997). Cloning and nucleotide sequencing of the S4 genome segment of avian reovirus S1133. *Arch. Virol.* **142**, 2515-2520.
- Compton, S.R., Nelsen, B., and Kirkegaard, K. (1990) Temperature-sensitive poliovirus mutant fails to cleave VP0 and accumulates provirions. *J. Virol.* **64**, 4067-4075.
- Coombs, K.M. (1998) Temperature sensitive mutants of reovirus. *Curr. Top. Microb. Immunol.* **223/I**, 69-107.
- Coombs, K.M., Mak, S.C., and Petrycky-Cox, L.D. (1994) Studies of the major reovirus core protein $\sigma 2$: reversion of the assembly-defective mutant tsC447 is an intragenic process and involves back mutation of Asp-383 to Asn. *J. Virol.* **68**, 177-186.
- Cross, R.K., and Fields, B.N. (1972) Temperature-sensitive mutants of reovirus type 3: studies on the synthesis of viral RNA. *Virology* **50**, 799-809.
- DeMasi, J., and Traktman, P. (2000) Clustered charge-to-alanine mutagenesis of the vaccinia virus H5 gene: isolation of a dominant, temperature-sensitive mutant with a profound defect in morphogenesis. *J. Virol.* **74**, 2393-2405.
- Dermody, T.S., Schiff, L.A., Nibert M.L., Coombs, K.M., and Fields, B.N. (1991) The S2 gene nucleotide sequences of prototype strains of the three reovirus serotypes: Characterization of reovirus core protein sigma-2. *J. Virol.* **65**, 5721-5731.
- Duncan, R. (1996) The low pH-dependent entry of avian reovirus is accompanied by two specific cleavages of the major outer capsid protein $\mu 2C$. *Virology* **219**, 179-189.

- Duncan, R. (1999) Extensive sequence divergence and phylogenetic relationships between the fusogenic and nonfusogenic orthoreoviruses: a species proposal. *Virology* **260**, 316-328.
- Duncan, R., and Sullivan, K. (1998) Characterization of two avian reoviruses that exhibit strain-specific quantitative differences in their syncytium-inducing and pathogenic capabilities. *Virology* **250**, 263-272.
- Duncan, R., Chen, Z., Walsh, S., and Wu, S. (1996) Avian reovirus-induced syncytium formation is independent of infectious progeny virus production and enhances the rate, but is not essential for virus-induced cytopathology and virus egress. *Virology* **224**, 453-464.
- Ericsson, M., Cudmore, S., Shuman, S., Condit, R.C., Griffiths, G., and Krijnes Locker, J. (1995) Characterization of ts16, a temperature-sensitive mutant of vaccinia virus. *J. Virol.* **69**, 7072-7086.
- Fields, B.N., and Joklik, W.K. (1969) Isolation and preliminary genetic and biochemical characterization of temperature-sensitive mutants of reovirus. *Virology* **37**, 335-342.
- Fields, B.N., Raine, C.S., and Baum, S.G. (1971) Temperature-sensitive mutants of reovirus type 3: defects in viral maturation as studied by immunofluorescence and electron microscopy. *Virology* **37**, 335-342.
- George, C.X., Crowe, A., Munemitsu, S.M., Atwater, J.A., and Samuel, C.E. (1987) Biosynthesis of reovirus-specified polypeptides: molecular cDNA cloning and nucleotide sequence of the reovirus serotype 1 lang strain s2 mRNA which encodes the virion core polypeptide sigma-2. *Biochem. Biophys. Res. Commun.* **147**, 1153-1161.

- Gombold, J.L., and Ramig, R.F. (1987) Assignment of simian rotavirus SA11 temperature sensitive mutant groups A, C, F, and G to genome segments. *Virology* 161, 463-473.
- Greenberg, H.B., Kalica, A.,R, Wyatt, R.G., Jones, R.W., Kapikian A.Z., and Chanock, R.M. (1981) Rescue of noncultivable human rotavirus by gene reassortment during mixed infection with *ts* mutants of a cultivatable bovine rotavirus. *Proc. Natl. Acad. Sci. USA* 78, 420-424.
- Hammond, G.W., Hazelton, P.R., Cheung, I., and Klisko, B. (1981). Improved detection of viruses by electron microscopy after direct ultracentrifuge preparation of specimens. *J Clin Microbiol.* 14, 210-221.
- Hazelton, P.R. (1998). Morphogenesis of reovirus as defined by the Fields panel of temperature sensitive mutants. Ph.D. thesis. University of Manitoba, Winnipeg, Manitoba, Canada.
- Hazelton, P.R., and Coombs, K.M. (1995) The reovirus mutants *tsA279* has temperature-sensitive lesions in the M2 and L2 Genes: the M2 Gene is associated with decreased viral protein production and blockade in transmembrane transport. *Virology* 207, 46-58.
- Hazelton, P.R., and Coombs, K.M. (1999) The reovirus mutant *tsA279* L2 gene is associated with generation of a spikeless core particle: implications for capsid assembly. *J. Virol.* 73(3), 2298-2308.
- Herenda, D.C., and Franco, D.A., Eds. (1996) Poultry Diseases and Meat Hygiene first edition, pp 120-135. Iowa State University Press: Ames.

- Hieronimus, D.R.K., Villegas, P., and Kleven, S.H. (1983) Characteristics and pathogenicity of two avian reoviruses isolated from chickens with leg problems. *Avian Dis.* 27, 255-259.
- Ikegami, N., and Gomatos, P.J. (1968) Temperature-sensitive conditional lethal mutants of reovirus 3. I. isolation and characterization. *Virology* 36, 447-458.
- Imani, F., and Jacobs, B.L. (1988) Inhibitory activity for the interferon-induced protein kinase is associated with the reovirus serotype 1 sigma 3 protein. *Pro. Natl. Acad. Sci. USA* 85, 7887-7891.
- Ito, Y., and Joklik, W.K. (1972) Temperature-sensitive mutants of reovirus II. Anomalous electrophoretic migration of certain hybrid RNA molecules composed of mutant plus strands and wild-type minus strands. *Virology* 50, 202-208.
- Ito, Y., and Joklik, W.K. (1972b) Temperature-sensitive mutants of reovirus I. Patterns of gene expression by mutants of group C, D, and E. *Virology* 50, 189-201.
- Jordan, F.T.W, and Pattison, M., Eds. (1996) Reoviridae. In "Poultry Diseases Fourth Edition", pp 218-225. W.B. Saunders Company: London.
- Kneller, D. (1991) nnpredict[®], Regents of the University of California.
- Martinez-Costas, J., Gonzalez-Lopez, C., Vakltaria, V.N., and Benavente, J. (2000) Possible involvement of the double-stranded RNA binding core protein σ A in the resistance of avian reovirus to interferon. *J. Virol.* 74(3), 1124-1131.
- Martinez-Costas, J., Grande, A., Varela, R., Garcia-Martinez, C., and Benavente, J. (1997) Protein architecture of avian reovirus S1133 and identification of the cell attachment protein. *J. Virol.* 71(1), 59-64.

- Martinez-Costas, J., Varlea, R., and Benavente, J. (1995). Endogenous enzymatic activities of the avian reovirus S1133: identification of the viral capping enzyme. *Virology* **206**, 1017-1026.
- Matsuhisz, T., and Joklik, W.K. (1974) Temperature-sensitive mutants of reovirus. V. Studies on the nature of the temperature-sensitive lesion of the group C mutant ts447. *Virology* **60**, 380-389.
- McCarthy, C. (1998) Chromas^o version 1.45. School of Health Science, Griffith University, Gold Coast Campus, Southport, Queensland, Australia.
- McGuffin, L.J., Bryson, K., and Jones, D.T.(2000) The PSIPred version 2.0 protein structure prediction server. Brunel Bioinformatics Group, Department of Biological Sciences, Brunel University, Uxbridge, UK
- Millns, A.K., Carpenter, M.S., and Delange, A.M. (1994) The vaccinia virus-encoded uracil DNA glycosylase has an essential role in viral DNA replication. *Virology* **198**, 504-513.
- Mitraki, A., and King, J. (1992) Amino acid substitutions influencing intracellular protein folding pathways. *FEBS Lett.* **307**, 20-25.
- Mustoe, T.A., Ramig, R.F., Sharpe, A.H., and Fields, B.N. (1978). A genetic map of reovirus III. Assignment of the double-stranded RNA mutant groups A, B, and G to genome segments. *Virology.* **85**, 545-556.
- Nagy, P.D., Dzianott, A., Ahlquist, P., and Bujarski, J.J. (1995) Mutations in the helicase-like domain of protein 1a alter the sites of RNA-RNA recombination in brome mosaic virus. *J. Virol.* **69**, 2547-2556.

- Ni, Y., and Kemp, M.C. (1994) Subgenomic S1 segments are packaged by avian reovirus defective interfering particles having an S1 segment deletion. *Virus Res.* **32**, 329-342.
- Nibert, M.L., Margraf, R.L., and Coombs, K.M. (1996) Nonrandom segregation of parental alleles in reovirus reassortants. *J. Virol.* **70**(10), 7295-7300.
- O'Hara, D., Patrick, M., Cepica, D., Coombs, K.M, and Duncan, R. The avian reovirus major μ -class outer capsid protein influences the efficiency of macrophage infection in a virus strain-specific manner. *J. Virol.* Submitted.
- Pringle, C.R. (1996) Temperature-sensitive mutant vaccines. In: Robinson, A, Graham, G.H., Wiblin, C.N. (eds.) *Methods in molecular medicine: vaccine protocols.* Humana, Totowa, pp 17-32.
- Ramig, R., and Fields, B.N. (1983) Genetics of reovirus. In "The Reoviridae" (W. Joklik, Ed.), pp. 197-228. Plenum: New York.
- Ramig, R.F. (1982) Isolation and genetic characterization of temperature-sensitive mutants of simian rotavirus SA11. *Virology* **120**, 93-105.
- Ramig, R.F. (1983) Isolation and genetic characterization of temperature-sensitive mutants that define five additional recombination groups in simian rotavirus SA11. *Virology* **130**, 464-473.
- Ramig, R.F., Ahmed, R., and Fields, B.N. (1983) A genetic map of reovirus: assignment of the newly defined mutant groups H, I, and J to genome segments. *Virology* **125**, 299-313.
- Ramig, R.F., and Ward, R.L. (1991) Genomic segment reassortment in rotavirus and other Reoviridae. *Adv. Virus Res.* **39**, 164-207.

- Ramig, R.F., Mustoe, T.A, Sharpe, A.H., and Fields, B.N. (1978) A genetic map of reovirus. II. Assignment of the double-stranded RNA-negative mutant groups C, D, and E genome segments. *Virology* **85**, 531-544.
- Reinisch, K.M., Nibert, M.L., and Harrison, M.L. (2000) Structure of the reovirus core at 3.6Å resolution. *Nature* **404**, 960-967.
- Rixon, F.J., Addison, C., and McLaughlan, J. (1992) Assembly of enveloped tegument structures (L particles) can occur independently of virion maturation in herpes simplex virus type 1-infected cells. *J. Gen. Virol.* **73**, 277-284.
- Rost, B. (1996) PHD predict version 1.96, CUBIC, Columbia University, New York, USA.
- Rozinov, M.N., and Fields, B.N. (1994). Interference following mixed infection of reovirus isolates is linked to the M2 gene. *J. Virol.* **68**, 6667-6671.
- Schuerch, A.R., and Joklik, W.K. (1973) Temperature-sensitive mutants of reovirus. IV. Evidence that anomalous electrophoretic migration behavior of certain double-stranded RNA hybrid species is mutant group specific. *Virology* **56**, 218-229.
- Schwartzberg P.L., Roth, M.J., Tanese, N., and Goff, D.P. (1993) Analysis of temperature-sensitive mutation affecting the integration protein of moloney murine leukemia virus. *Virology* **192**, 673-678.
- Sharpe, A.H., Ramig, R.F., Mustoe, T.A., and Fields, B.N. (1978). A genetic map of reovirus.I. Correlation of genome RNAs between serotypes 1, 2, and 3. *Virology* **84**, 63-74.

- Sheng Yin, H., and Lee, L.H. (1998). Identification and characterization of RNA-binding activities of avian reovirus non-structural protein σ NS. *J Gen Virol.* **79**,1411-1413.
- Sheng Yin, H., Shien, J.H., and Huw Lee, L. (2000) Synthesis in *Escherichia coli* of avian reovirus core protein σ A and its dsRNA-binding activity. *Virology* **266**, 33-41.
- Shikova, E., Lin, Y.C., Saha, K., Brooks, B.R., and Wong, P.K. (1993) Correlation of specific virus-astrocyte interactions and cytopathic effects induced by ts1, a neuovirulent mutant of moloney murine leukemia virus. *J. Virol.* **67**, 1137-1147.
- Shing, M., and Coombs, K.M. (1996) Assembly of the reovirus outer capsid requires μ 1/ σ 3 interactions which are prevented by misfolded σ 3 protein in temperature-sensitive mutant *tsG453*. *Virus Res.* **46**, 19-29.
- Shmulevitz, M., and Duncan, R.(2000) A new class of fusion-associated small transmembrane (FAST) proteins encoded by the non-enveloped fusogenic reoviruses. *EMBO J.* **19**, 902-912.
- Simpson, R.W., and Hirst, G.K. (1968) Temperature-sensitive mutants of influenza A virus: isolation of mutants and preliminary observations on genetic recombination and complementation. *Virology* **35**, 41-49.
- Singer, B., and Fraenkel Conrat, H. (1967) Chemical modification of viral RNA, VI. The action of N-Methyl-N'-Nitro-N-Nitrosoguanidine. *Proc. Natl. Acad. Sci. USA* **58**, 234-239.
- Theophilos, M.B., Huang, J-A., Holmes, I.H. (1995). Avian reovirus σ C protein contains a putative fusion sequence and induces fusion when expressed in mammalian cells. *Virology* **208**, 678-684.

Van Regenmortel, M.H.V., Fauquet, C.M., Bishop, D.H.L, Carstens, E.B., Estes, M.K., Lemon, S.M., Maniloff, J., Mayo, M.A., McGeoch, D.J., Pringle, C.R., and Wickner, C.R, Eds. (2000) Family Reoviridae. *In* "Virus Taxonomy, Classification and Nomenclature of Viruses 1st edition. pp395-480. Academic Press: London.

Varela, R., and Benavente, J. (1994) Protein coding assignment of avian reovirus strain 1133. *J. Virol.* **68**(10), 6775-6777.

Wiskerchen, M., and Muesing, M.A. (1995) Human immunodeficiency virus type 1 integrase: effects of mutations on viral ability to integrate, direct viral gene expression from unintegrated viral DNA templates, and sustain viral propagation in primary cells. *J. Virol.* **69**, 376-386.